1984

Tertiary alkalic igneous activity, potassic fenitization, carbonatitic magmatism, and hydrothermal activity in the central and southeastern Bear Lodge Mountains, Crook County, Wyoming

Gordon A. Jenner
University of North Dakota

TERTIARY ALKALIC IGNEOUS ACTIVITY, POTASSIC FENITIZATION, CARBONATITIC MAGMATISM, AND HYDROTHERMAL ACTIVITY IN THE CENTRAL AND SOUTHEASTERN BEAR LODGE MOUNTAINS, CROOK COUNTY, WYOMING

by

Gordon A. Jenner Jr.

Bachelor of Science, St. Lawrence University, 1978

A Thesis

Submitted to the Graduate Faculty

of the

University of North Dakota

in partial fulfillment of the requirements

for the degree of

Master of Science

Grand Forks, North Dakota

December
1984

This thesis submitted by Gordon A. Jenner Jr. in partial fulfillment of the requirements for the degree of Master of Science from the University of North Dakota is hereby approved by the Faculty Advisory Committee under whom the work has been done.

_____
(Chairman)

Chair:
Frank
Karner

_____

_____

This thesis meets the standards for appearance and conforms to the style and format requirements of the Graduate School of the University of North Dakota, and is hereby approved.

_____
Dean of the Graduate School

Permission

Title Tertiary Alkalic Igneous Activity, Potassic Fenitization, Carbonatitic Magmatism, and Hydrothermal Alteration in the Central and Southeastern Bear Lodge Mountains, Crook County, Wyoming

Department Geology

Degree Master of Science

In presenting this thesis in partial fulfillment of the requirements for a graduate degree from the University of North Dakota, I agree that the Library of this University shall make it freely available for inspection. I further agree that permission for extensive copying for scholarly purposes may be granted by the professor who supervised my thesis work or, in his absence, by the Chairman of the Department or the Dean of the Graduate School. It is understood that any copying or publication or other use of this thesis or part thereof for financial gain shall not be allowed without my written permission. It is also understood that due recognition shall be given to me and the University of North Dakota in any scholarly use which may be made of any material in my thesis.

Signature _____

Date _____

TABLE OF CONTENTS

LIST OF ILLUSTRATIONS

Figure

LIST OF TABLES

Table

ACKNOWLEDGEMENTS

With respect and gratitude I acknowledge the assistance of my advisory committee, Dr. Frank Karner, Dr. Dexter Perkins III, and Dr. Don Halvorson, for their advice and assistance throughout the research and their critical review of the manuscript. A special thanks is extended to Dr. Karner who introduced me to the Bear Lodge Mountains and whose enthusiasm, guidance, and patience were invaluable.

I am grateful for the financial support provided by the Mining and Mineral Resources Research Institute of North Dakota, the Department of Geology of the University of North Dakota, Sigma Xi, and the Beta Zeta chapter of Sigma Gamma Epsilon. I am especially indebted to Fred Reisbick of Duval Corporation for providing drill cores used in the study and for helping to offset reproduction costs.

The laboratory assistance of Dr. Robert Stevenson of the Natural Materials Analytical Laboratory at the University of North Dakota and Dr. Nels Forsman is greatly appreciated. I also thank Dr. John Bowman at the Isotope Laboratory of the University of Utah for the use of facilities and Ray Lambert for his help in the acquisition of isotope data.

Finally, I cannot express enough thanks to my parents and sisters for their encouragement and support and to Leigh Lucht, whose love, patience and understanding will forever be cherished.

ABSTRACT

The Bear Lodge Mountains are located in Crook County in northeastern Wyoming. The core of the uplift consists of alkalic igneous rocks that range from Early to Late Eocene in age. A petrologic and geochemical study of surface and subsurface samples from the southeastern and central portions of the core reveals a complex history of multiple alkalic igneous events, potassic metasomatism, carbonatitic magmatism, and hydrothermal alteration.

An early episode of alkalic igneous activity is represented by latite and trachyte porphyries, phonolite and trachyte porphyries, and natrolite-garnet syenites and malignites. Throughout much of the complex, the composition of these older alkalic intrusions has been changed by the metasomatic development of potassium feldspar. This process, termed potassic fenitization, occurred prior to emplacement of carbonatitic dikes and veins. It appears to have involved a volatile-rich aqueous fluid that contained potassium, iron, sulfur, carbon dioxide, and fluorine. Rocks associated with potassic fenitization contain significant deposits of copper, lead, zinc, thorium, cerium, lanthanum, and gold.

Two types of carbonatites may be distinguished in the Bear Lodge Mountains, I-type and S-type. I-type carbonatites occur in the central portions of the core and are enriched in strontium, cerium, and lanthanum. The isotopic compositions of carbon and oxygen in calcites from I-type carbonatites indicate a mantle source for carbon dioxide. S-type carbonatites occur in the southeastern portions of the core and have lower concentrations of strontium, cerium, and lanthanum. It is postulated that I-type carbonatites resulted from differentiation of an

alkali-rich parent magma, while S-type carbonatites formed by local fusion of Paleozoic sedimentary limestone. Significant deposits of thorium, cerium, lanthanum, copper, lead, and zinc are associated with I-type carbonatites.

Hydrothermal alteration accompanied the episode of early igneous activity and continued through the intrusion of I-type carbonatites. The alteration is especially pervasive in the central portions of the core where it typically extends to depths of several tens of meters in the subsurface. Sodalite-bearing and haüyne-bearing analcime phonolite porphyries crosscut hydrothermally altered rocks and represent the last igneous activity in the region.

The igneous rocks of the Bear Lodge Mountains were probably derived from an alkalic parent magma that formed by partial melting of upper mantle material enriched in potassium, rubidium, iron, titanium, cerium, lanthanum, fluorine, carbon dioxide, and water. Fractional crystallization in a crustal resovoir generated latitic, trachytic, and phonolitic differentiates, while immiscible separation resulted in the formation of an alkali-rich carbonatitic magma. Loss of alkalis accompanied the ascent of the carbonatitic magma from the resovoir, resulting in the potassium-rich fluids responsible for fenitization.

INTRODUCTION

General Statement

The following study examines the petrology and geochemistry of an alkalic-carbonatitic complex in the Bear Lodge Mountains of northeastern Wyoming. The area, located in the northern Black Hills, has been extensively explored for copper, gold, thorium, and rare-earth elements since the early nineteen-fifties. The primary goal of the investigation is to unravel the complex sequence of igneous, metasomatic, and hydrothermal events that occurred in this region during Early Tertiary time.

Regional Geologic Setting

The Bear Lodge Mountains represent a northwest extension of the Black Hills, a Laramide uplift whose axis trends in a northwesterly direction from the Nebraska-South Dakota border through northeastern Wyoming into southeastern Montana (Fig. 1). Structural studies suggest regional uplift of the Black Hills began during Late Cretaceous or Early Tertiary time and involved upthrusting of two major basement blocks (Noble, 1952; Lisenbee, 1978). The common boundary between these blocks, termed the Fanny Peak linement by Shapiro (1971a), consists of an overlapping series of small faults and monoclinal folds that runs along the Wyoming-South Dakota state line. The block to the east of the linement is uplifted higher than the block to the west, exposing a large crystalline core of Precambrian igneous and metamorphic rocks (Fig. 1). The Precambrian rocks include granites, schists, and gneisses that range from 1.6 to 2.5 billion years in age (Zartman and Stern, 1967; Peterman and Hedge, 1972).

Figure 1. Generalized geologic map of the Black Hills region showing the location of the Bear Lodge Mountains and outcrop patterns of Precambrian igneous and metamorphic rocks, the Lower Cretaceous Inyan Kara Group, and Tertiary igneous rocks. Modified from Gries and Tullis (1955, p.32).

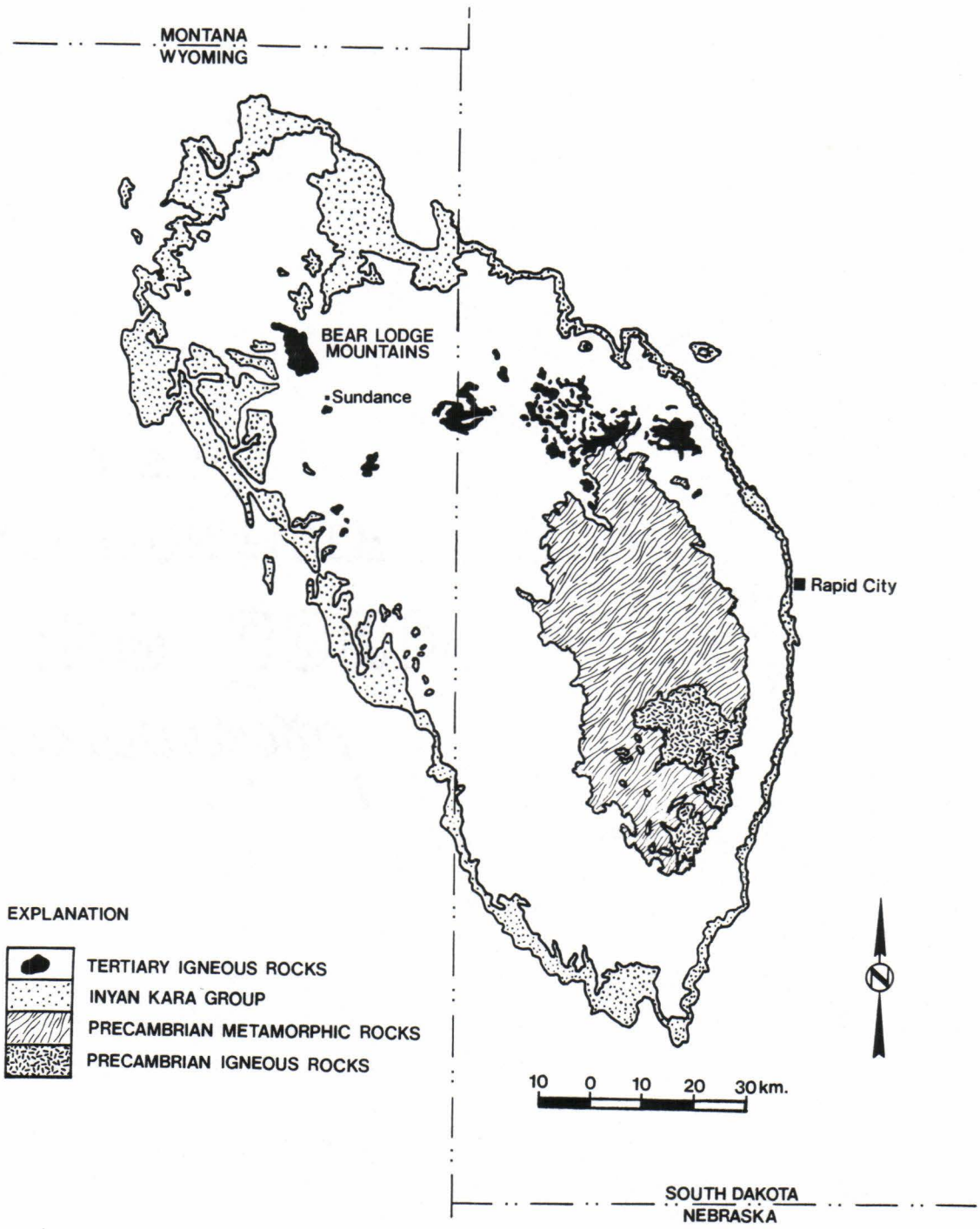
MONTANA
WYOMING
BEAR LODGE
MOUNTAINS
Sundance
Rapid City
EXPLANATION
TERTIARY IGNEOUS ROCKS
INYAN KARA GROUP
PRECAMBRIAN METAMORPHIC ROCKS
PRECAMBRIAN IGNEOUS ROCKS
10 0 10 20 30 km.
SOUTH DAKOTA
NEBRASKA

Phanerozoic sedimentary rocks in the Black Hills region vary between 2,220 and 3,000 meters in thickness (Lisenbee, 1978). Lithostratigraphic units range from the Cambrian-Ordovician Deadwood Formation to the Pliocene Ogallala Group (Fig. 2). Paleozoic and Mesozoic strata are draped over the major bounding faults of the uplift and form a series of large-scale monoclinal folds that encircle the Black Hills. Oligocene, Miocene, and Pliocene strata postdate uplift and lie with angular unconformity on older rocks of the region.

A series of Tertiary alkalic igneous intrusions crosses the northern Black Hills along a well-defined belt that trends in a N.75°W. direction from Bear Butte in South Dakota to Devils Tower and Missouri Buttes in Wyoming (Fig. 1). These small Late Paleocene and Eocene plutons crosscut the other regional structures of the Black Hills and hence, postdate the major episodes of regional uplift (Shapiro, 1971b; Lisenbee, 1978). Potassium-argon dates from several intrusions range from 38 to 59 million years (McDowell, 1971; Hill and others, 1975).

Local Geology

The Bear Lodge Mountains are located near the western terminus of the belt of Tertiary igneous intrusions. The core of the uplift consists of a central dome of alkalic igneous rocks that measures approximately 9 kilometers in length and 4 kilometers in width. Smaller igneous plugs, dikes, and sills occur within upturned Paleozoic and Mesozoic strata around the flanks of the uplift.

The oldest rock exposed in the Bear Lodge Mountains is Precambrian granite with a uranium-thorium-lead date of 2.6 billion years (Staatz, 1983). The granite occurs as large, irregular-shaped xenoliths within the central igneous dome. The largest of these xenoliths is elliptical

Figure 2. Stratigraphic section of the Black Hills region (from Wyoming Geological Society Guidebook, 1968, p.6).

GENERAL OUTCROP SECTION OF THE BLACK HILLS AREA

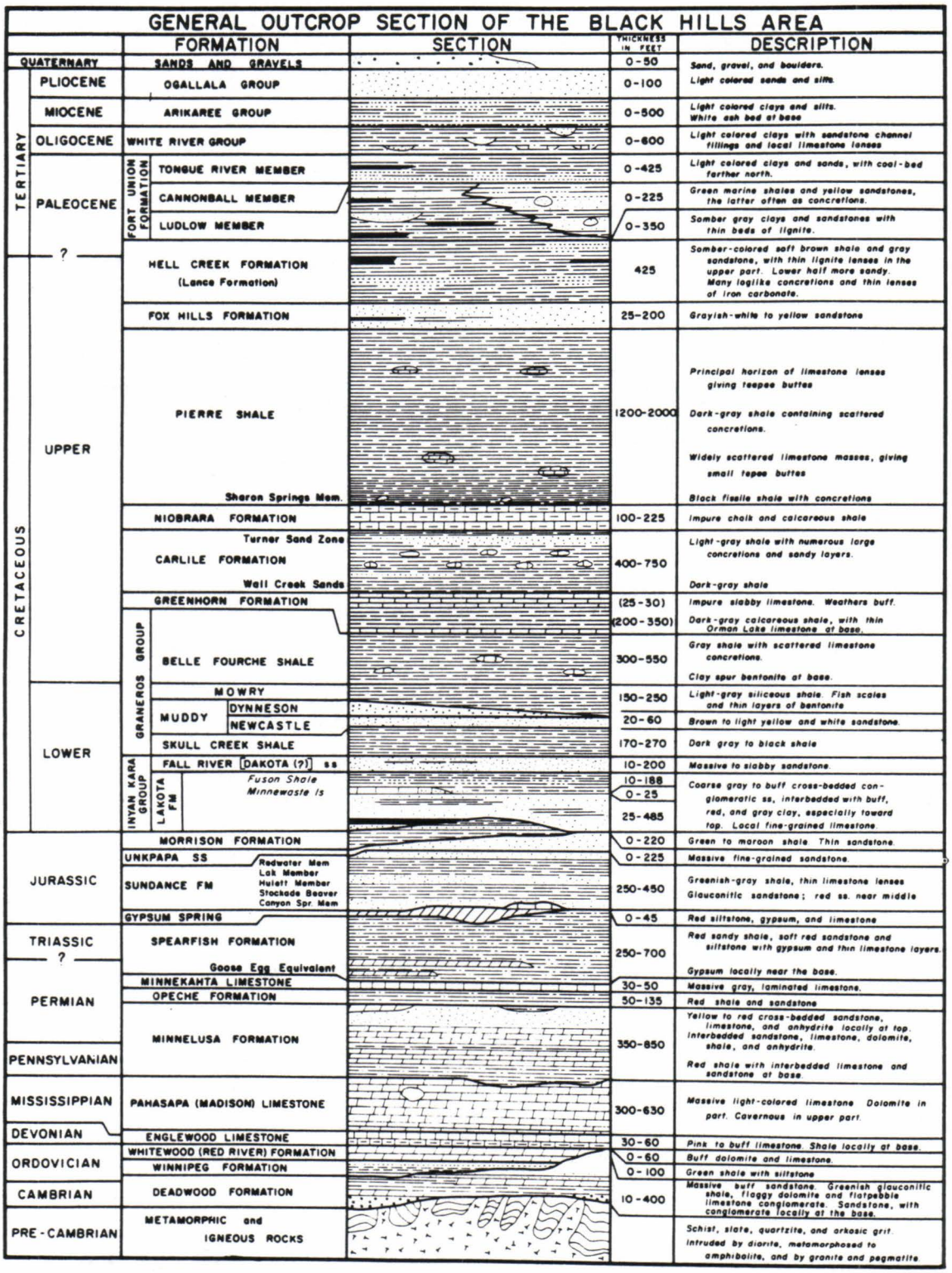

in shape and measures approximately 1200 meters in length and 300 meters in width.

Paleozoic and Mesozoic strata dip radially from the core of the uplift and have a combined thickness of approximately 1,070 meters (Staatz, 1983). Rock stratigraphic units and their geologic ages are: (1) the Deadwood Formation of Late Cambrian and Early Ordovician age, (2) the Whitewood Limestone of Late Ordovician age, (3) the Pahasapa Limestone of Early Mississippian age, (4) the Minnelusa Sandstone of Pennsylvanian and Early Permian age, (5) the Opeche Formation of Permian age, (6) the Minnekata Limestone of Permian age, (7) the Spearfish Formation of Permian and Triassic age, (8) the Sundance Formation of Middle and Late Jurassic age, (9) the Morrison Formation of Late Jurassic age, and (10) the Lakota Formation of Early Cretaceous age. The Devonian and Early Mississippian Englewood Formation, which occurs in other areas of the Black Hills, is absent in the Bear Lodge Mountains (Fig. 2).

The Tertiary igneous rocks exposed at the surface in the Bear Lodge Mountains include latite, trachyte, phonolite, syenite, carbonatite, lamprophyre, and intrusive breccia. Although Staatz (1983) has reported the occurrence of extrusive flows and pyroclastic deposits, the majority of the rocks are subvolcanic in origin. Shallow emplacement occurred during Eocene time with potassium-argon dates ranging from 38 to 50 million years (McDowell, 1971; Staatz, 1983).

Younger Tertiary sedimentary rocks occur on the northern, eastern, and western flanks of the uplift. They consist of the poorly bedded siltstones of the White River Formation and the coarse conglomerates, sandstones, and siltstones of the Ogallala Group (Fig. 2). Both of

these units postdate the structural deformation of the Bear Lodge Mountains and unconformably overlie the Paleozoic and Mesozoic strata and Eocene igneous rocks.

Previous Work

The earliest geologic descriptions of the Bear Lodge Mountains were made during nineteenth-century reconnaisance expeditions undertaken to assess the economic potential of the Black Hills. The most notable of these reports can be found in government publications by Warren (1859), Jenney (1876), and Newton and Jenney (1880).

The first study to examine the structure of the Bear Lodge Mountains was made by Jagger (1901) who published a comprehensive monograph on the geometries and modes of emplacements of the Black Hills igneous bodies. He proposed that the Bear Lodge Mountains represent a laccolith with the upward migration of magma controled by eastward dipping fissures in the Precambrian basement. The lateral migration of magma, he concluded, accompanied doming of the overlying sedimentary rocks and occurred along zones of stratigraphic weakness within the Paleozoic section.

Shortly after the work of Jagger, the first detailed geologic map of the Bear Lodge Mountains was published by Darton and associates (1905a,b) as part of the United States Geological Survey's Geologic Atlas of the United States folio series. Darton accompanied the map with general discussions of the structure, stratigraphy, hydrology, and economic geology of the region. The first petrographic descriptions of the Tertiary igneous rocks were also presented. The rocks were classified as syenite porphyry, trachyte porphyry, and pseudoleucite porphyry.

Following the publication of Darton's map, no major geologic studies were conducted in the Bear Lodge Mountains until the early nineteen-fifties. Brown (1952) studied the southern portions of the uplift and concluded, like Jagger, that the structure of the main igneous intrusion is a laccolith. He further hypothesized that emplacement occurred in two discrete pulses. The first consisted of a relatively fluid magma of trachytic composition that formed the main laccolith chamber. The second consisted of a more viscous phonolitic magma which shattered and mineralized the trachyte core during intrusion.

Two major episodes of igneous activity were also recognized by Chenowith (1955). The two igneous events, he proposed, were separated in time by a period of hydrothermal alteration and mineralization. The older event resulted in the emplacement of syenite porphyry, trachyte porphyry, and pseudoleucite porphyry. The younger event resulted in the intrusion of feldspathoidal trachyte, feldspathoidal latite, and feldspathoidal andesite. The types of mineral deposits described by Chenowith include barite, copper, fluorite, manganese, and rare-earth elements.

The rare-earth deposits reported by Chenowith occur in association with thorium. The deposits were examined in detail by Staatz (1983) who also mapped the complex and described in detail the local structure and stratigraphy. Both disseminated and vein deposits were recognized by Staatz. The disseminated deposits occur in a manner comparable to copper porphyry deposits and consist of altered trachyte and phonolite crosscut by numerous crisscrossing veinlets. The vein deposits also occur in altered igneous rocks and were arbitrarily defined to include

all tabular bodies greater than 5 centimeters in thickness. Although the disseminated deposits are relatively low grade, they encompass a large portion of the central igneous core. According to Staatz (p. 1), they constitute "one of the largest resources of both total rare-earths and thorium in the United States". The principle thorium and rare-earth minerals in both types of deposits are monazite, brockite, and bastnaesite. Chief gangue minerals include potassium feldspar, quartz, cristobalite, limonite, hematite, and various manganese oxides.

Researchers from the Department of Geology at the University of North Dakota began a detailed series of investigations into the structure, igneous petrology, and economic geology of the Bear Lodge Mountains in the late nineteen-seventies. The results of the studies were summarized by Karner (1981) and are briefly discussed below.

Fashbaugh (1979) investigated the geology of the extrusive and intrusive igneous rocks that occur in the Sundance Mountain-Sugarloaf Mountain area (Fig. 3). Two major types of igneous rocks were recognized, older foyaites associated with Bear Lodge Mountains complex and younger quartz latites related to Sundance and Sugarloaf Mountains. According to Fashbaugh, the foyaites were passively emplaced as dikes and sills while field and petrographic evidence indicate the quartz latites were explosively extruded as interstratified breccias, tuffs, and flows.

The petrology of the igneous rocks exposed in the Lytle Creek area in the northern Bear Lodge Mountains (Fig. 3) was examined by White (1980). Calc-alkali trachyte and phonolite, ferrohastingsite trachyte and latite, and pseudoleucite trachyte porphyry are the major igneous rock types. Most intrusions were emplaced as sills or small laccoliths

Figure 3. Map of the Bear Lodge Mountains showing the locations of the area of study, the Sundance-Sugarloaf Mountains area (Fashbaugh, 1979), the Lytle Creek area (White, 1980), the Houston Creek area (O'Toole, 1981), and the Warren Peaks area (Wilkinson, 1982).

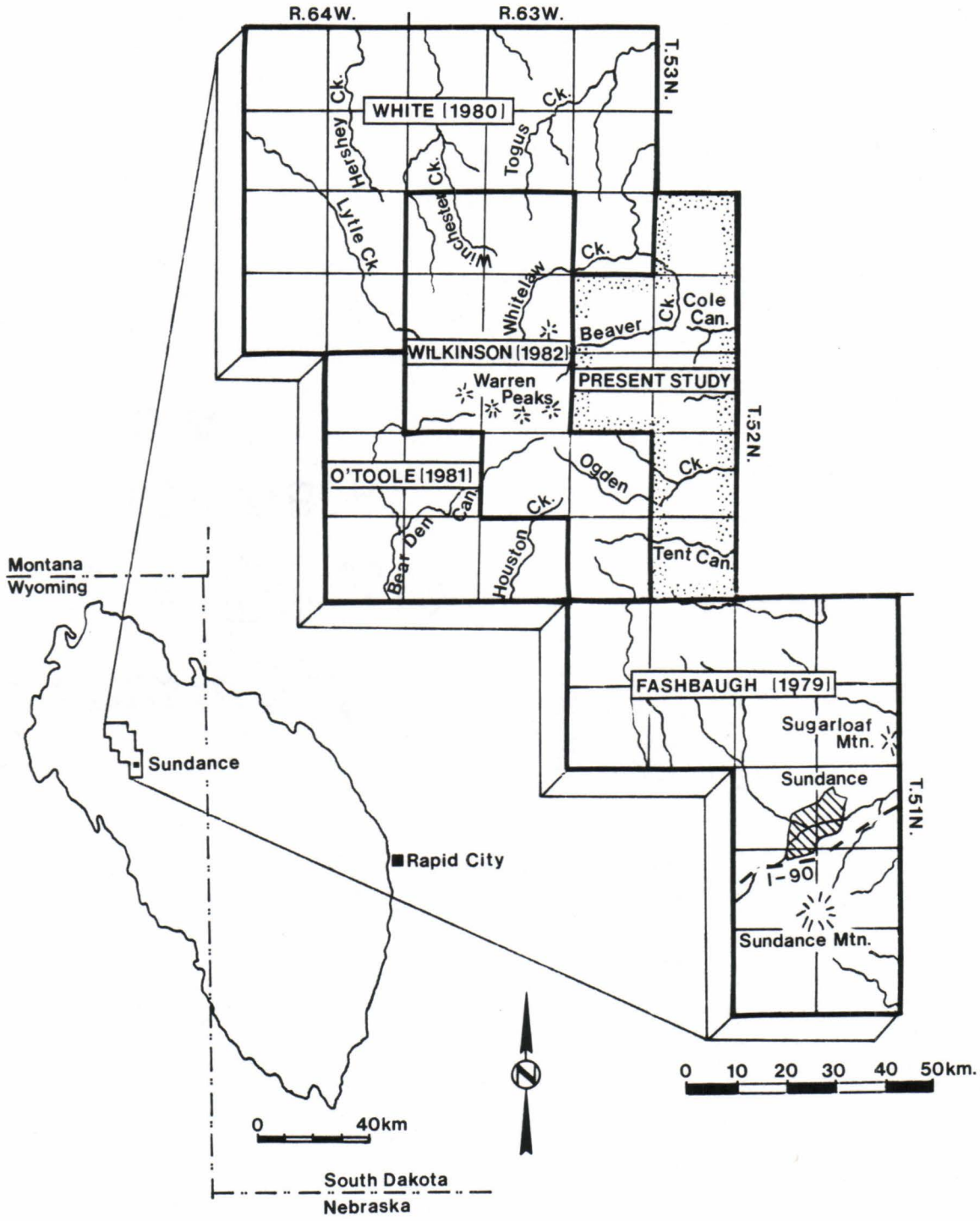
R.64W.
R.63W.
T.53N.
T.52N.
T.51N.
WHITE (1980)
WILKINSON (1982)
PRESENT STUDY
O'TOOLE (1981)
FASHBAUGH (1979)
Hershey Ck.
Lytle Ck.
Ck.
Togus Ck.
Ck.
Whitelaw Ck.
Ck.
Beaver Ck.
Cole Can.
Warren Peaks
Ogden Ck.
Ck.
Bear Den Can.
Houston Ck.
Tent Can.
Sugarloaf Mtn.
Sundance
I-90
Sundance Mtn.
Montana
Wyoming
Sundance
Rapid City
South Dakota
Nebraska
0 40km
0 10 20 30 40 50km.

at or near the Pahasapa Limestone-Minnelusa contact or at the Spearfish Formation-Sundance Formation contact. Chemical data indicate the observed igneous variations are related to the differentiation of an alkali olivine basalt parent magma with enrichments in SiO_2, Al_2O_3, and K_2O attributable to contamination by granitic crustal material.

O'Toole (1981) studied the petrography and petrology of phonolite intrusions occurring in the Houston Creek area of the southwestern Bear Lodge Mountains (Fig. 3). The rocks in this portion of the uplift occur as dikes and sills within Lower and Middle Paleozoic strata and consist of phonolite, phonolite porphyry, sodalite-bearing phonolite porphyry, and trachyte porphyry. Altered felsite of the central igneous core is also present. The chemical trends reported by O'Toole are similar to those of White (1980) and suggest affinities with alkali olivine basalt series rocks. Evidence for crustal contamination includes partially resorbed xenoliths of Precambrian granite in SiO_2-enriched phonolitic rocks.

The petrology and alteration of the igneous rocks exposed in the Warren Peaks area in the central Bear Lodge Mountains (Fig. 3) were investigated by Wilkinson (1982). Alkali trachyte porphyry, latite porphyry, phonolite porphyry, microsyenite porphyry, and carbonatite are the principle rock types. According to Wilkinson, the alteration and ultrapotassic nature of alkali trachyte porphyry and variations of SiO_2 within latite porphyry resulted from an episode of potassic metasomatism which occurred prior to the emplacement of carbonatite dikes. Rare-earth mineralization associated with the carbonatite dikes, in Wilkinson's opinion, is economically significant.

Present Study

The present study investigates the petrology and geochemistry of the igneous rocks exposed along the southeastern flank of the Bear Lodge Mountains in an area that includes Tent, Ogden, and Cole Canyons (Fig. 3). It also examines subsurface specimens collected from drill cores from the central portions of the main igneous dome in an area located north of Whitelaw Creek. The drill cores are the property of the Duval Corporation, a minerals company whose geologists conducted an extensive exploration program in the Bear Lodge Mountains during the early nineteen-seventies.

The major goals of the study are as follows: (1) to construct a detailed geologic map of the southeastern flank of the uplift, (2) to characterize and classify the major types of igneous and metasomatic rocks, (3) to determine the source region of carbonatitic CO_2 using carbon and oxygen isotopes, and (4) to propose a petrogenetic model that relates the igneous history of the Bear Lodge Mountains with episodes of metasomatism, hydrothermal activity, and mineralization.

Methods

Field mapping for this study was conducted at a scale of 1:10,000 using standard pace and compass techniques. The mapped area consists of sections 10, 15, 16, 21, 22, 27, and 34, T.52N. R.63W. (Plate 1). Surface and subsurface samples of the various types of igneous and metasomatic rocks were characterized chemically and mineralogically by means of optical microscopy, x-ray diffraction, scanning electron microscopy, electron microprobe analysis, and x-ray fluorescence. Classification of the specimens is based upon a modified version of the IUGS classification of Streckeisen (1967) that has been proposed by

Sörensen (1974). The isotopic compositions of carbon and oxygen in carbonatitic calcites were determined at the University of Utah under the supervision of Dr. John Bowman. More complete discussions of the analytical procedures mentioned above are presented in Appendix I.

TERTIARY IGNEOUS AND METASOMATIC EVENTS AND ASSOCIATED ROCK TYPES

Sequence of Events

The field, petrographic, and geochemical results of the study can be used to determine the age relationships of the rock types and mineral deposits occurring in the Bear Lodge Mountains (Fig. 4). Four major petrologic events are recognized. They are termed, from oldest to youngest: (1) early igneous activity, (2) potassic fenitization, (3) carbonatitic magmatism, and (4) late igneous activity. A related event, hydrothermal alteration, began during the episode of early igneous activity and continued through the episode of carbonatitic magmatism.

Early Igneous Activity

The oldest petrologic event in the Bear Lodge Mountains is termed "early igneous activity". It is represented by a compositionally and texturally diverse suite of subvolcanic and plutonic igneous rocks which form the bulk of the main igneous dome and which also compose many of the satellitic plugs, dikes and sills that are exposed around the flanks of the uplift. Potassic fenitization and hydrothermal alteration has changed the original compositions and textures of these rocks in many areas of the complex. This is especially true in the central portions of the main igneous dome where the effects of these later events are most pronounced.

The early igneous rocks are alkalic in character and can be classified into three major groups on the basis of texture, mineralogy, and chemical composition: (1) latite and trachyte porphyries, (2) phonolite and trachyte porphyries, and (3) natrolite-garnet syenites and malignites.

Figure 4. Simplified paragenesis diagram of the major petrologic events and associated rock types and mineral deposits of the southeastern and central Bear Lodge Mountains. Uncertainty of relationships indicated by dashed lines.

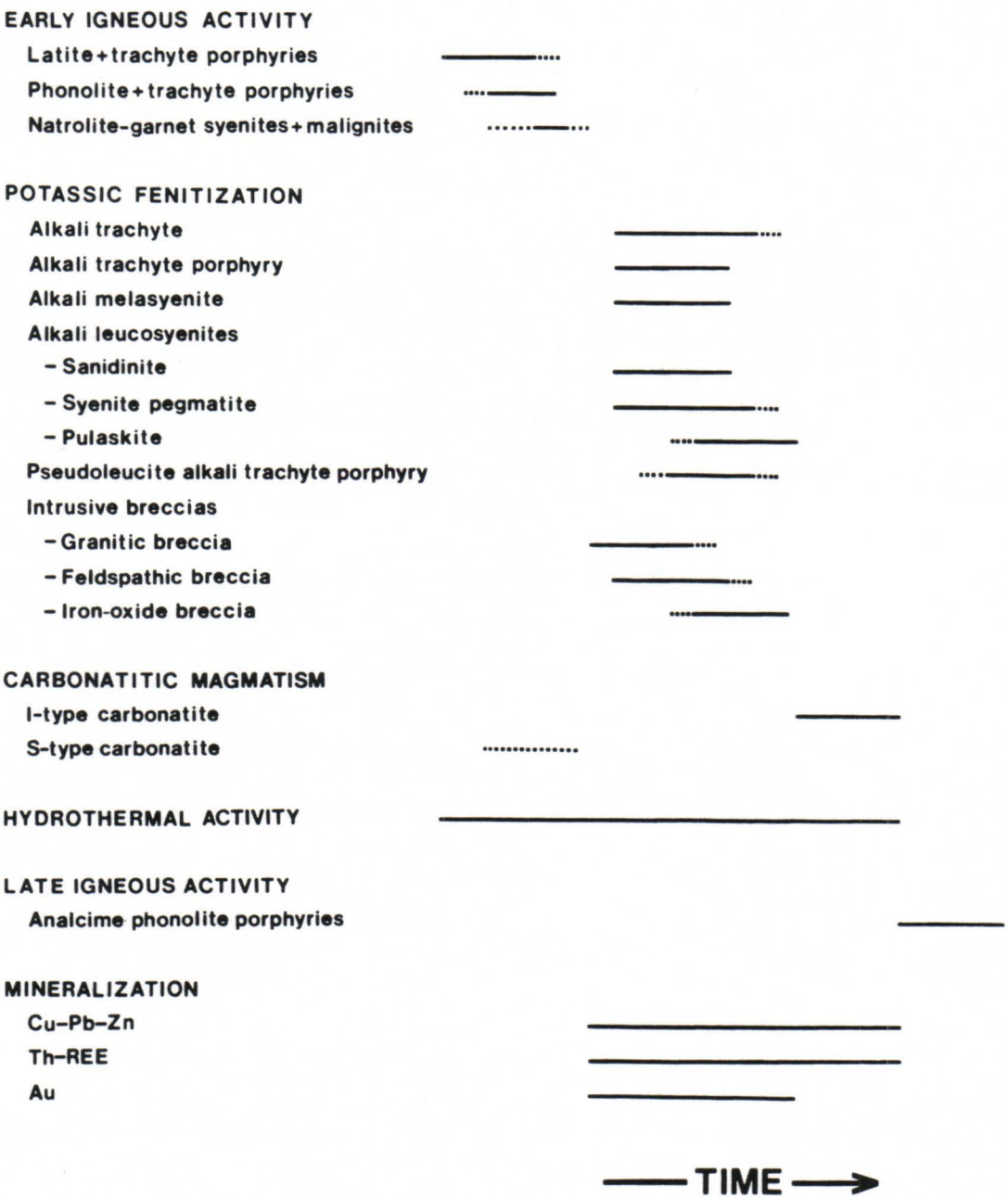
EARLY IGNEOUS ACTIVITY
Latite+trachyte porphyries
Phonolite+trachyte porphyries
Natrolite-garnet syenites+malignites
POTASSIC FENITIZATION
Alkali trachyte
Alkali trachyte porphyry
Alkali melasyenite
Alkali leucosyenites
- Sanidinite
- Syenite pegmatite
- Pulaskite
Pseudoleucite alkali trachyte porphyry
Intrusive breccias
- Granitic breccia
- Feldspathic breccia
- Iron-oxide breccia
CARBONATITIC MAGMATISM
I-type carbonatite
S-type carbonatite
HYDROTHERMAL ACTIVITY
LATE IGNEOUS ACTIVITY
Analcime phonolite porphyries
MINERALIZATION
Cu-Pb-Zn
Th-REE
Au
TIME

Latite and Trachyte Porphyries

General

The most common igneous rocks outcropping along the southeastern flank of the Bear Lodge Mountains are porphyritic varieties of latite, trachyte, analcime-bearing latite, and analcime-bearing trachyte (Table 1). They are often hydrothermally altered and it is frequently difficult or impossible to distinguish one rock type from the others solely on the basis of macroscopic properties. The rocks are collectively termed "latite and trachyte porphyries".

Crosscutting relationships indicate the latite and trachyte porphyries are the oldest rocks exposed in the area of study. They occur as crisscrossing plugs and dikes within the main igneous dome and as sills and dikes within Paleozoic and Mesozoic strata. Compositionally and texturally they are analogous to many of the rock types described in other areas of the uplift by earlier workers, including (1) ferrohastingsite latite and trachyte porphyries reported by White (1980) in the Lytle Creek area, (2) many of the samples of altered felsite reported by O'Toole (1981) in the Houston Creek area, (3) latite porphyry reported by Wilkinson (1982) in the Warren Peaks area, and (4) many of the samples of "older" phonolite, trachyte, and latite reported by Staatz (1983) throughout the main igneous dome and along the flanks of the uplift.

Petrography

Latite and trachyte porphyries are holocrystalline and variably porphyritic (Fig. 5). Colors range from light gray to dark gray to olive-gray for fresh samples and from light brown to yellow-brown to

TABLE 1

MODAL ANALYSES OF LATITE AND TRACHYTE PORPHYRIES

SAMPLE	A	B	C	D	E	F
Primary						
Groundmass						
Sanidine	54.5	42.8	32.2	47.8	43.2	35.3
Oligoclase	9.2	11.6	21.5	10.0	10.1	14.7
Albite	0.0	9.5	0.0	0.0	0.0	6.0
Anorthoclase	10.0	5.4	5.3	8.6	13.7	4.0
Analcime	0.0	0.0	0.0	4.3	3.6	3.3
Calcite	3.1	2.7	0.6	0.7	1.4	3.3
Sanidine	1.2	1.2	8.8	7.4	0.8	2.2
Oligoclase/andesine	3.2	1.8	20.2	1.2	6.2	15.4
Anorthoclase	1.0	0.0	0.8	0.8	0.8	5.8
Salite	4.2	3.2	7.0	8.2	11.0	4.0
Hastingsite	6.2	12.8	0.0	0.6	0.0	0.0
Biotite	tr.	0.0	tr.	0.0	0.0	tr.
Apatite	0.8	0.2	0.6	1.2	0.8	0.4
Sphene	0.8	0.2	0.4	1.4	1.4	0.6
Titanian magnetite	2.4	3.0	1.6	2.0	2.4	1.4
Pyrite	0.0	0.0	0.0	0.0	tr.	tr.
Secondary						
Calcite	1.2	3.8	tr.	0.6	tr.	0.8
Sericite/clays	tr.	1.6	0.6	1.6	tr.	1.4
Iron/titanium oxides	1.2	0.2	0.4	0.6	0.4	0.4
Analcime	0.0	0.0	0.0	3.0	4.2	1.0
Uralite	1.0	tr.	tr.	0.0	tr.	tr.
Chlorite	tr.	0.0	0.0	0.0	0.0	tr.

tr.=trace, less than 0.2% detected

Sample key: A=Sample 21-56B=Trachyte porphyry
B=Sample 21-103=Trachyte porphyry
C=Sample 21-109=Latite porphyry
D=Sample 27-187=Analcime-bearing trachyte porphyry
E=Sample 27-217=Analcime-bearing trachyte porphyry
F=Sample 34-261=Analcime-bearing latite porphyry

Figure 5. Slab photograph of latite porphyry (sample 21-105). Subparallel feldspar phenocrysts, mostly plagioclase (oligoclase-andesine), in a darker, aphanitic groundmass rich in sanidine.

Figure 6. Photomicrograph of trachyte porphyry (sample 21-56B). Phenocrysts of plagioclase (P), hastingsite (H), salite (Sa), apatite (Ap), and titanian magnetite (Tm) enclosed within a microcrystalline groundmass rich in sanidine. Bar scale represents 0.25 mm. Plane-polarized light.

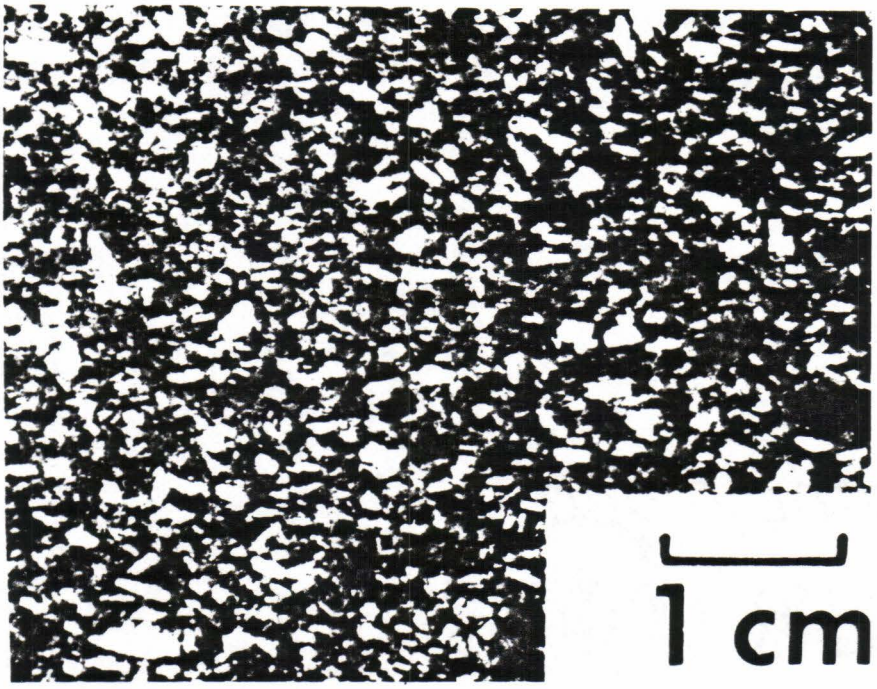
1 cm


H
H
Sa
Sa
Ap
P
Sa
Sa
Sa
Im

rust-brown for altered samples. The major phenocryst minerals are plagioclase, sanidine, salite, and hastingsite (Fig. 6). Accessory minerals include apatite, sphene, and titanian magnetite (Fig. 7). Microprobe analyses of the principle minerals of the rock are presented in Table 2.

The groundmasses of latite and trachyte porphyries are aphanitic to very fine-grained and compose from 50 to 95 percent of the rocks. Textures range from felty to strongly trachytic. The principle groundmass mineral is sanidine which occurs as Carlsbad twinned microlites that range from 0.1 to 0.5 mm in length. Surrounding the microlites is an aphanitic matrix composed of cryptocrystalline albite, oligoclase, anorthoclase, and analcime.

Plagioclase phenocrysts range in composition from oligoclase to andesine. They are highly variable in abundance, ranging from less than 2 percent in some trachytes to more than 20 percent in some latites. The majority of crystals are between 1 and 10 mm in size. They are characterized by both albite and Carlsbad twinning and frequently have corroded and embayed mantles of untwinned anorthoclase (Fig. 8). Most crystals show oscillatory, normal zoning with the more calcic cores altered to a cryptocrystalline mixture of calcite and sericite. Microprobe traverses for calcium, sodium, and potassium across a typical zoned plagioclase phenocryst reveal complex sawtoothed profiles (Fig. 9a and b).

Sanidine phenocrysts are less abundant than plagioclase phenocrysts, composing about 1 to 10 percent of the rocks. The majority of crystals are less than 5 mm in size and display subhedral to anhedral shapes. Although Carlsbad twinning is common in several samples, it is

Figure 7. Photomicrograph of trachyte porphyry (sample 27-11). Phenocryst of euhedral sphene (Sp), hastingsite (H), salite (Sa), apatite (Ap), and titanian magnetite (Tm) enclosed within a microcrystalline groundmass rich in sanidine. Bar scale represents 0.25 mm. Plane-polarized light.

Figure 8. Photomicrograph of trachyte porphyry (sample 27-11). Phenocryst of plagioclase (P) with mantles of anorthoclase (A). Bar scale represents 0.25 mm. Crossed polars.

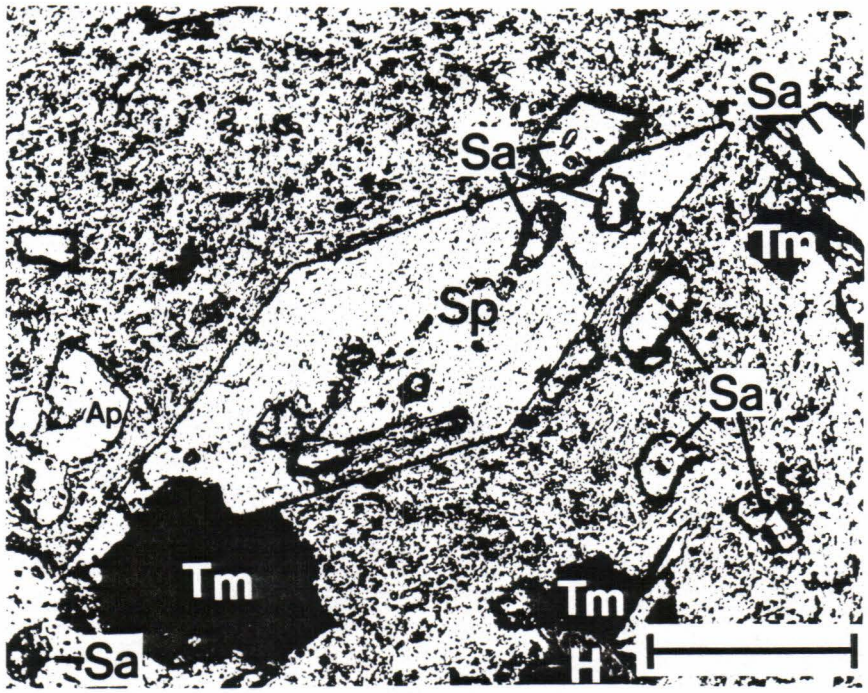
Sa
Sa
Tm
Sp
Sa
Ap
Tm
Tm
Sa
H

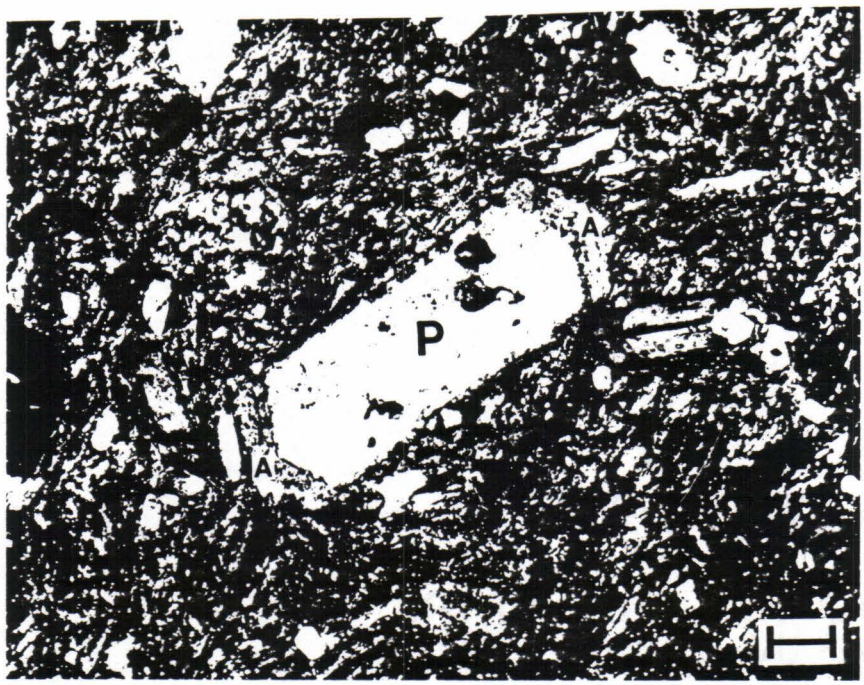
A
P
A

TABLE 2

MICROPROBE ANALYSES OF MINERALS IN LATITE AND TRACHYTE PORPHYRIES

SAMPLE	A	B	C	D	E	F	G	H
SiO2	66.81	69.00	66.09	55.14	63.80	60.16	64.34	66.51
Al2O3	18.46	20.25	19.41	24.54	22.74	25.66	21.42	19.28
FeO*	0.00	0.00	0.69	0.15	0.00	0.22	0.00	0.31
MgO	0.00	0.00	0.00	0.00	0.00	0.00	0.00	0.00
CaO	0.00	0.44	0.39	0.50	3.83	6.19	1.06	0.36
Na2O	0.86	11.65	7.59	11.92	8.70	6.86	6.49	4.66
K2O	14.86	0.17	5.33	0.83	0.87	1.17	5.34	8.96
TiO2	0.00	0.00	0.20	0.00	0.00	0.00	0.52	0.00
P2O5	0.00	0.00	0.00	0.00	0.00	0.00	0.00	0.00
MnO	0.00	0.00	0.00	0.00	0.00	0.00	0.00	0.23
Cl	0.00	0.00	0.00	0.08	0.00	0.00	0.13	0.05
SO3	0.00	0.00	0.00	0.00	0.00	0.00	0.00	0.00
Total	100.99	101.51	99.70	93.16	99.94	100.26	99.30	100.36
	Number of cations on the basis of X oxygens							
	X=32	X=32	X=32	X=7	X=32	X=32	X=32	X=32
Si	12.11	11.89	11.84	2.32	11.29	10.70	11.56	11.95
Al	3.94	4.11	4.10	1.22	4.73	5.38	4.53	4.08
Fe	0.00	0.00	0.10	0.01	0.00	0.03	0.00	0.05
Mg	0.00	0.00	0.00	0.00	0.00	0.00	0.00	0.00
Ca	0.00	0.08	0.07	0.02	0.73	1.18	0.20	0.07
Na	0.30	3.89	2.63	0.97	2.98	2.37	2.26	1.62
K	3.43	0.04	1.22	0.04	0.20	0.26	1.22	2.05
Ti	0.00	0.00	0.03	0.00	0.00	0.00	0.07	0.00
P	0.00	0.00	0.00	0.00	0.00	0.00	0.00	0.00
Mn	0.00	0.00	0.00	0.00	0.00	0.00	0.00	0.03
Cl	0.00	0.00	0.00	0.01	0.00	0.00	0.04	0.02
S	0.00	0.00	0.00	0.00	0.00	0.00	0.00	0.00

* Total Fe as FeO

Sample key: A=Sample 34-261=Sanidine (groundmass); B=Sample 21-103=Albite (groundmass); C=Sample 21-56B=Anorthoclase (groundmass); D=Sample 34-261=Analcime (groundmass); E=Sample 21-109=Oligoclase (phenocryst); F=Sample 27-217=Andesine (phenocryst); G=Sample 34-261=Anorthoclase (rim of plagioclase phenocryst); H=Sample 27-187=Sanidine (phenocryst).

TABLE 2

(continued)

SAMPLE	I	J	K	L	M	N	O	P
SiO2	54.42	50.36	40.82	39.58	38.44	0.00	31.08	0.00
Al2O3	0.86	3.53	11.50	12.24	13.68	0.15	1.49	1.77
FeO*	5.07	9.13	15.06	15.85	11.77	0.00	1.36	83.68
MgO	16.49	12.46	11.36	9.81	17.27	0.13	0.00	0.34
CaO	23.72	22.70	11.13	11.27	0.00	55.07	28.52	0.00
Na2O	0.30	0.78	2.35	2.39	0.78	0.00	0.00	0.60
K2O	0.00	0.00	1.70	1.70	8.94	0.17	0.09	0.00
TiO2	0.44	0.80	3.13	3.30	4.36	0.19	36.07	6.18
P2O5	0.26	0.00	0.00	0.00	0.00	41.61	0.20	0.00
MnO	0.00	0.43	0.18	0.47	0.27	0.00	0.00	0.97
Cl	0.05	0.00	0.08	0.00	0.08	0.15	0.00	0.00
SO3	0.00	0.13	0.17	0.00	0.00	0.00	0.00	0.00
Total	101.61	100.32	97.48	96.61	95.59	97.47	98.81	93.54
	Number of cations on the basis of X oxygens							
	X=6	X=6	X=24	X=24	X=24	X=26	X=20	X=32
Si	1.97	1.89	6.44	6.35	6.15	0.00	4.11	0.00
Al	0.04	0.15	2.14	2.31	2.58	0.03	0.23	0.79
Fe	0.15	0.29	1.99	2.13	1.57	0.00	0.15	26.56
Mg	0.89	0.70	2.67	2.35	4.12	0.03	0.00	0.19
Ca	0.92	0.91	1.88	1.94	0.00	10.37	4.04	0.00
Na	0.02	0.06	0.72	0.74	0.24	0.00	0.00	0.44
K	0.00	0.00	0.34	0.35	1.83	0.04	0.01	0.00
Ti	0.01	0.02	0.37	0.40	0.53	0.02	3.59	1.76
P	0.01	0.00	0.00	0.00	0.00	6.19	0.02	0.00
Mn	0.00	0.01	0.02	0.06	0.04	0.00	0.00	0.31
Cl	0.00	0.00	0.02	0.00	0.02	0.05	0.00	0.00
S	0.00	0.00	0.02	0.00	0.00	0.00	0.00	0.00

* Total Fe as FeO

Sample key: I=Sample 21-56B=Salite (phenocryst-core); J=Sample 21-56B=Salite (phenocryst-rim); K=Sample 21-56B=Hastingsite (phenocryst); L=Sample 21-103=Hastingsite (phenocryst); M=Sample 21-103=Biotite; N=Sample 21-56B=Apatite; O=Sample 27-217=Sphene; P=Sample 21-56B=Titanian magnetite.

Figure 9. Electron microprobe traverse across a zoned plagioclase phenocryst in latite porphyry (sample 21-109).

(a.) Photomicrograph of zoned plagioclase phenocryst showing location of electron microprobe traverse (X-X'). Bar scale represents 0.25 mm. Crossed Polars.

(b.) Electron microprobe traverse (X-X') showing variations in the concentrations of Ca, Na, and K across zoned plagioclase phenocryst shown above.

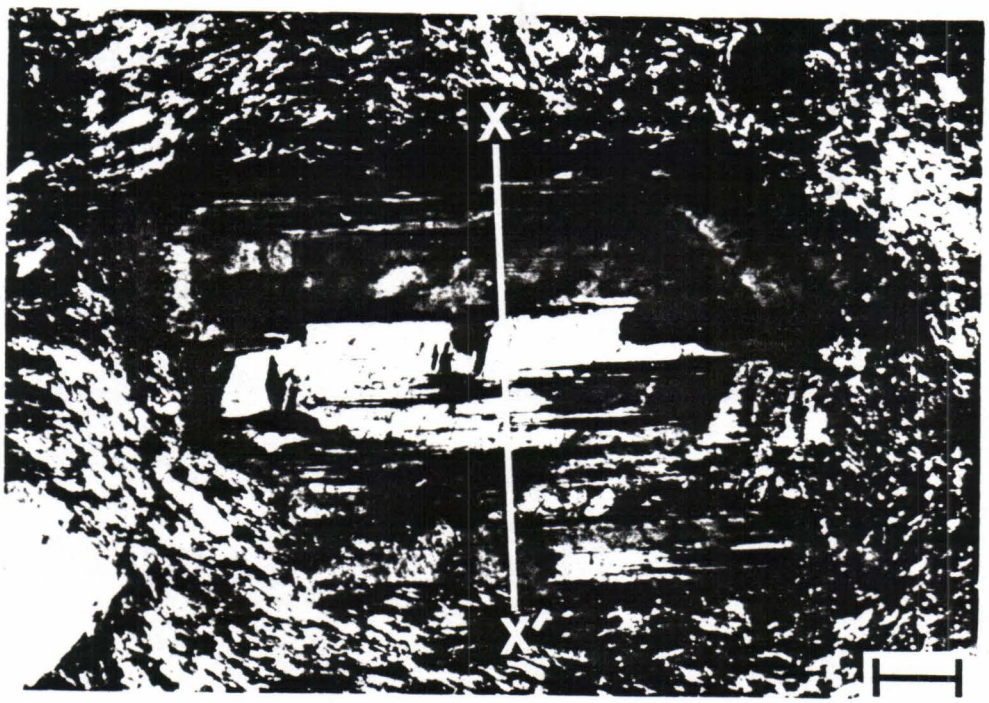
X
X'

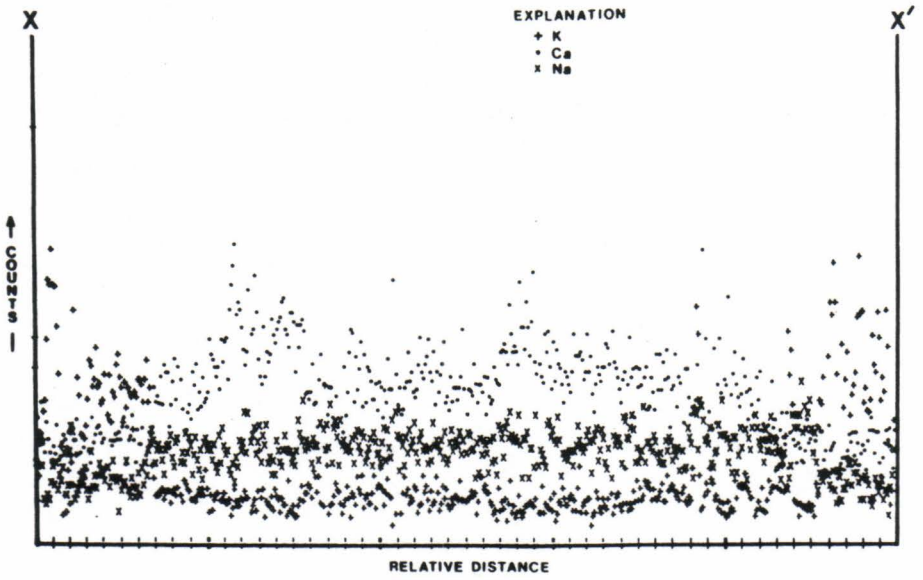
X
X'
EXPLANATION
+ K
· Ca
x Na
GRAIN SIZE
RELATIVE DISTANCE

absent in most. A microprobe analysis of a typical untwinned phenocryst indicates a sodium-rich composition (Table 2, column H).

Salite phenocrysts are ubiquitous in the rocks. They have euhedral to subhedral crystal shapes with stubby, rectangular, prismatic sections and square to octagonal basal sections. Sizes range between 0.5 and 3.0 mm. Normal zoning is common with pale green, iron-poor, magnesium-rich cores and darker green, iron-rich, magnesium-poor rims. Sodium contents also increase from core to rim (Table 2, columns I and J). Inclusions of apatite, sphene, and titanian magnetite are frequent. Alteration products include uralite, chlorite, calcite, and iron oxides.

Hastingsite phenocrysts are abundant in many samples of latite and trachyte porphyries but lacking in others. They occur as slender prismatic crystals up to 10 mm in length. Basal sections show typical diamond-shaped amphibole crystal form with prismatic cleavages intersecting at 54 and 126 degrees. Twinning on (100) is common. Crystals are strongly pleochroic with X=yellowish brown, Y=brown, and Z=greenish brown. Biotite, chlorite, calcite, and iron oxides are common alteration products.

Occurring in accessory amounts in the rocks are apatite, sphene, and titanian magnetite. Apatite crystals are generally euhedral and display hexagonal and prismatic cross-sections up to 1.0 mm in size. Sphene crystals are also less than 1.0 mm in size and typically show euhedral diamond-shaped or wedge-shaped forms. Titanian magnetite, which ranges up to 3 percent in abundance, imparts a distinct magnetic character to the rocks. Crystals are generally less than 0.2 mm in size and commonly possess alteration halos composed of iron and titanium oxides.

Chemistry

Major element chemical analyses and CIPW normative mineralogies of six unaltered samples of latite and trachyte porphyries are presented in Table 3. The samples are peraluminous and range from slightly oversaturated to moderately undersaturated with respect to SiO_2. Differentiation indexes vary between 63 and 84. The values of most of the major oxides are intermediate between the average values for latites and trachytes (Nockolds, 1954, p. 1016-1017). All of the samples fall in the alkaline field proposed by Irving and Baragar (1971) for volcanic igneous rocks (Fig. 10).

Phonolite and Trachyte Porphyries

General

The second group of rocks resulting from the episode of early igneous activity in the Bear Lodge Mountains consists of analcime phonolite porphyry, analcime-bearing alkali trachyte porphyry, and alkali trachyte porphyry (Table 4). They appear similar in hand sample and are termed "phonolite and trachyte porphyries" to avoid confusion with younger and megascopically similar alkali trachyte porphyries associated with later episodes of potassic metasomatism.

Phonolite and trachyte porphyries occur within the southeastern portions of the main igneous dome as dikes crosscutting older latite and trachyte porphyries and as sills and dikes within Lower and Middle Paleozoic strata. The chemistry, mineralogy, and macroscopic appearance of the rocks are comparable to specimens from adjacent areas of the uplift that have been classified as calc-alkali phonolites and trachytes

TABLE 3

MAJOR ELEMENT CHEMICAL ANALYSES AND CIPW NORMATIVE MINERALOGIES OF LATITE AND TRACHYTE PORPHYRIES

SAMPLE	A	B	C	D	E	F
SiO_2	56.03	54.97	56.57	59.32	54.47	60.19
Al_2O_3	16.37	15.39	17.22	19.28	18.04	19.02
Fe_2O_3*	4.91	6.96	3.42	3.88	3.84	2.04
MgO	1.60	3.07	0.79	0.66	0.67	0.38
CaO	4.51	6.23	3.62	3.25	3.83	2.20
Na_2O	4.34	4.02	5.41	5.91	5.67	5.57
K_2O	5.85	4.57	4.57	6.17	5.73	5.61
TiO_2	0.78	1.02	0.54	0.60	0.65	0.23
P_2O_5	0.34	0.56	0.18	0.16	0.18	0.05
MnO	0.13	0.16	0.14	0.13	0.13	0.09
Total	94.86	96.95	92.46	99.36	93.21	95.38
Qz	0.00	0.00	0.78	0.00	0.00	1.29
Or	36.44	27.86	29.21	36.70	36.32	34.76
Ab	37.29	35.04	49.51	39.42	35.09	49.42
An	8.33	10.78	9.95	7.90	7.35	10.82
Ne	0.77	0.00	0.00	5.91	8.88	0.00
Wo	0.00	0.00	0.75	0.43	2.38	0.00
Di	10.44	14.12	5.03	5.05	4.86	0.22
Hy	0.00	2.96	0.00	0.00	0.00	0.00
Ol	0.84	2.10	0.00	0.00	0.00	0.89
Mt	3.48	3.77	3.20	3.06	3.34	0.66
Hm	0.00	0.00	0.00	0.00	0.00	1.36
Il	1.56	2.00	1.11	1.15	1.32	0.46
Ap	0.85	1.37	0.46	0.38	0.46	0.12

* Total Fe as Fe_2O_3

Sample key: A=Sample 21-56B; B=Sample 21-103; C=Sample 21-109; D=Sample 27-187; E=Sample 27-217; F=Sample 34-261

Figure 10. Plot of (Na_2O+K_2O) versus SiO_2 showing Irving and Baragar's (1971) dividing line for making a general distinction between alkaline and subalkaline volcanic igneous rocks. Samples of latite and trachyte porphyries from the southeastern and central Bear Lodge Mountains (open circles) plot in the alkaline field.

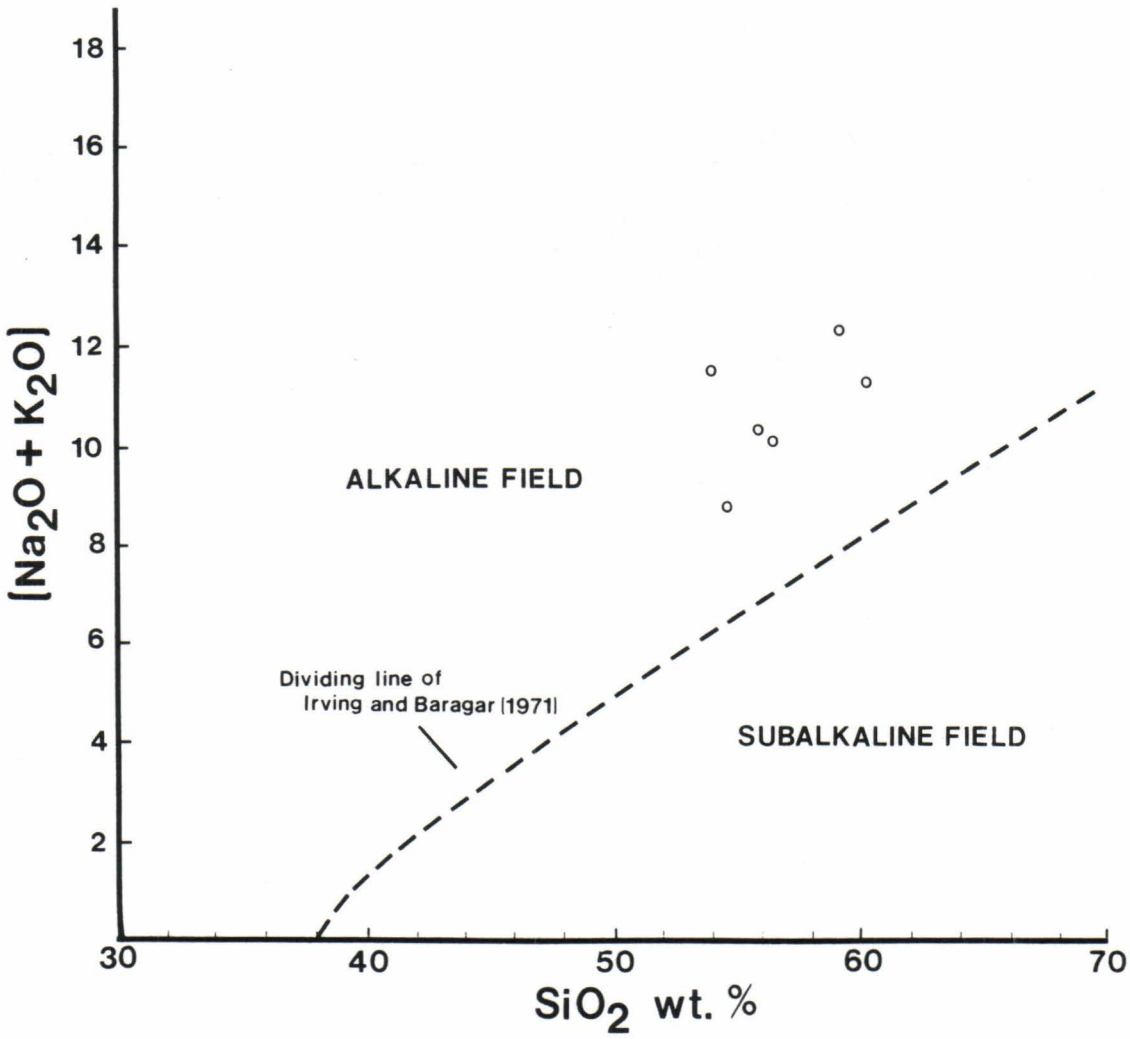
18
16
14
12
10
8
6
4
2
[Na2O + K2O]
ALKALINE FIELD
Dividing line of
Irving and Baragar (1971)
SUBALKALINE FIELD
30
40
50
60
70
SiO2 wt. %

TABLE 4

MODAL ANALYSES OF PHONOLITE AND TRACHYTE PORPHYRIES

SAMPLE	A	B	C	D	E	F
Primary						
Groundmass						
Sanidine	19.9	56.8	21.5	49.3	34.0	23.4
Albite	2.2	2.1	16.4	7.2	7.1	20.1
Anorthoclase	3.7	2.1	8.0	15.9	9.7	9.5
Analcime	4.3	6.2	0.0	0.0	0.0	0.0
Calcite	0.9	1.4	0.9	0.0	0.0	0.0
Sanidine	37.6	3.8	42.4	7.0	30.2	21.4
Salite	3.0	0.0	0.0	0.0	0.0	0.0
Apatite	0.4	0.4	0.2	0.2	tr.	0.0
Sphene	0.2	tr.	0.0	0.0	tr.	0.0
Titanian magnetite	1.4	0.0	0.0	0.0	0.0	0.0
Pyrite	0.0	3.0	0.0	0.0	0.0	0.0
Secondary						
Strontian calcite	4.4	11.4	0.0	0.0	0.0	0.0
Sericite/clays	7.0	5.6	4.2	8.8	7.4	12.2
Iron/titanium oxides	0.6	1.6	5.8	5.8	5.4	13.4
Analcime	10.8	3.0	0.0	0.0	0.0	0.0
Natrolite	1.2	2.6	0.0	0.0	0.0	0.0
Chlorite	2.4	0.0	0.6	0.6	tr.	0.0
Muscovite	0.0	0.0	0.0	5.2	6.2	0.0

tr.=trace, less than 0.2% detected

Sample key: A=Sample 21-85B=Analcime phonolite porphyry
B=Sample 21-73A=Analcime-bearing alkali trachyte porphyry
C=Sample 21-24B=Alkali trachyte porphyry
D=Sample 27-220=Alkali trachyte porphyry
E=Sample 27-233=Alkali trachyte porphyry
F=Sample 34-316=Alkali trachyte porphyry

(White, 1980) and sanidine trachyte porphyry (Wilkinson, 1982). They also are analogous to some of the samples of "older" phonolites and trachytes reported by Staatz (1983) in several areas of the main igneous dome.

Petrography

Phonolite and trachyte porphyries are holocrystalline and distinctly porphyritic (Fig. 11). Fresh exposures of the rocks are rare, the majority showing varying degrees of hydrothermal alteration. Fresh samples range from light to medium gray in color while altered samples occur in various shades of brown, orange-brown, and rust-brown. Microprobe analyses of the major minerals of the rocks are presented in Table 5.

Groundmass usually constitutes between 30 and 70 percent of phonolite and trachyte porphyries. Textures are typically aphanitic and strongly trachytic. Sanidine, which is the major constituent of the groundmass, occurs as small microlites within an aphanitic matrix composed of cryptocrystalline albite, anorthoclase, and analcime. The microlites vary between 0.1 and 0.5 mm in length and display both sodium-rich and sodium-poor compositions (Table 5, columns A and B).

Large tabular phenocrysts of sanidine up to 30 mm in length are a distinctive feature of phonolite and trachyte porphyries (Fig. 12). They comprise between 5 and 40 percent of the rock and often exhibit well-developed trachytoid textures. Crystals are typically euhedral to subhedral and frequently Carlsbad twinned. Alteration to clay minerals and replacement by analcime and strontian calcite along crystal margins and microfractures are common (Fig. 13). Microprobe analyses show a considerable range in sodium contents similar to the range displayed by

Figure 11. Slab photograph of alkali trachyte porphyry (sample 21-24B). Large tabular phenocrysts of sanidine enclosed within an oxidized, aphanitic groundmass rich in sanidine. Zoned appearance of sanidine phenocrysts due to preferential alteration along margins and fractures of crystals.

Figure 12. Photomicrograph of phonolite porphyry (sample 34-335). Phenocrysts of Carlsbad twinned sanidine (S) and an altered, rounded to hexagonal feldspathoid mineral (F) enclosed within a microcrystalline groundmass rich in sanidine. Bar scale represents 0.25 mm. Crossed polars.


1 cm

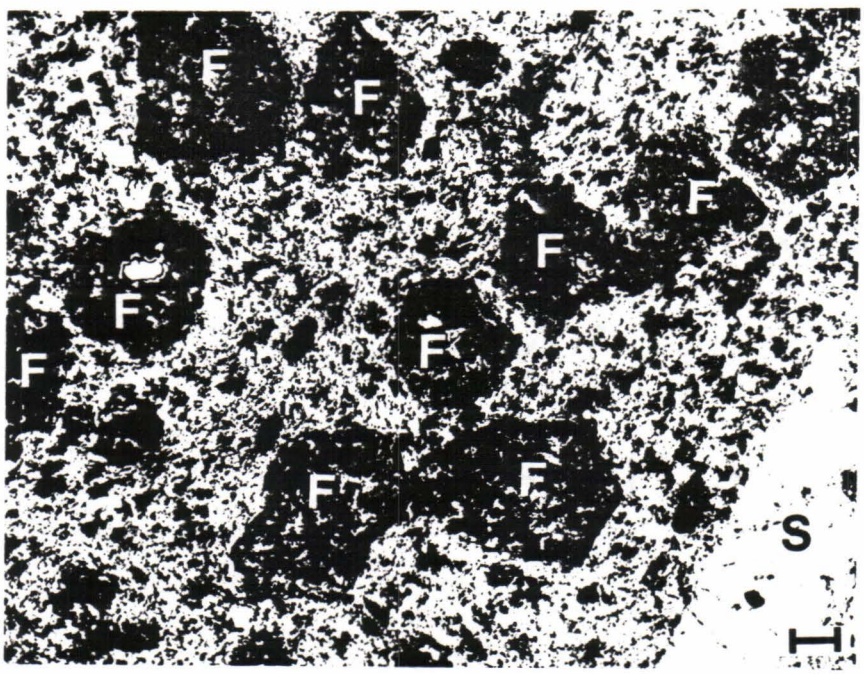
F
F
F
F
F
F
F
F
F
S
T

TABLE 5

MICROPROBE ANALYSES OF MINERALS IN PHONOLITE AND TRACHYTE PORPHYRIES

SAMPLE	A	B	C	D	E	F	G	H
SiO2	66.36	65.73	68.65	68.06	54.89	53.96	66.60	65.48
Al2O3	19.19	18.86	20.25	20.05	24.29	24.81	19.75	19.11
FeO*	0.16	0.00	0.00	0.00	0.00	0.26	0.23	0.00
MgO	0.00	0.00	0.00	0.00	0.00	0.00	0.00	0.15
CaO	0.00	0.00	0.26	0.14	0.00	0.00	0.00	0.00
Na2O	4.03	0.28	11.81	8.71	14.10	13.05	4.14	0.65
K2O	11.08	15.62	0.25	2.16	0.07	0.11	10.28	14.97
TiO2	0.00	0.20	0.00	0.09	0.00	0.00	0.00	0.00
P2O5	0.00	0.00	0.00	0.00	0.00	0.00	0.00	0.00
MnO	0.00	0.00	0.00	0.00	0.32	0.00	0.00	0.00
Cl	0.00	0.08	0.16	0.00	0.00	0.00	0.00	0.10
SO3	0.12	0.00	0.00	0.00	0.00	0.00	0.00	0.00
Total	100.94	100.77	101.38	99.21	93.67	92.19	101.00	100.46
	Number of cations on the basis of X oxygens							
	X=32	X=32	X=32	X=32	X=7	X=7	X=32	X=32
Si	11.93	11.99	11.88	11.99	2.30	2.29	11.91	11.96
Al	4.07	4.05	4.13	4.16	1.20	1.24	4.16	4.11
Fe	0.02	0.00	0.00	0.00	0.00	0.01	0.03	0.00
Mg	0.00	0.00	0.00	0.00	0.00	0.00	0.00	0.04
Ca	0.00	0.00	0.05	0.03	0.00	0.00	0.00	0.00
Na	1.41	0.10	3.96	2.97	1.15	1.07	1.44	1.56
K	2.54	3.63	0.05	0.49	0.00	0.01	2.35	3.49
Ti	0.00	0.03	0.00	0.01	0.00	0.00	0.00	0.00
P	0.00	0.00	0.00	0.00	0.00	0.00	0.00	0.00
Mn	0.00	0.00	0.00	0.00	0.01	0.00	0.00	0.00
Cl	0.00	0.02	0.05	0.00	0.00	0.00	0.00	0.03
S	0.02	0.00	0.00	0.00	0.00	0.00	0.00	0.00

* Total Fe as FeO

Sample key: A=Sample 21-85B=Sanidine (groundmass); B=Sample 34-233= Sanidine (groundmass); C=Sample 21-24B=Albite (groundmass); D= Sample 27-220=Anorthoclase (groundmass); E=Sample 21-85B=Analcime (groundmass); F=Sample 21-73A=Analcime (groundmass); G=Sample 21-24B=Sanidine (phenocryst); H=Sample 34-316=Sanidine (phenocryst).

TABLE 5

(continued)

SAMPLE	I	J	K	L	M	N	O	P
SiO2	45.78	51.23	48.67	55.04	50.29	0.98	30.00	0.00
Al2O3	35.68	2.43	3.18	0.70	2.84	0.17	1.47	0.95
FeO*	2.82	11.34	17.09	4.70	14.70	0.00	2.63	84.95
MgO	0.45	11.65	7.53	17.13	8.44	0.00	0.00	0.42
CaO	0.00	22.45	21.34	23.72	20.71	54.25	27.69	0.00
Na2O	0.00	1.49	1.64	0.00	2.17	0.28	0.00	0.00
K2O	10.91	0.09	0.00	0.13	0.19	0.00	0.08	0.00
TiO2	0.25	0.54	0.79	0.53	0.62	0.11	34.31	4.20
P2O5	0.00	0.00	0.26	0.16	0.00	39.96	0.00	0.00
MnO	0.00	0.69	0.80	0.00	0.75	0.00	0.00	1.53
Cl	0.06	0.00	0.00	0.00	0.07	0.08	0.00	0.00
SO3	0.17	0.14	0.00	0.00	0.00	0.44	0.00	0.00
Total	96.12	102.05	101.30	102.12	100.78	96.27	96.18	92.05
	Number of cations on the basis of X oxygens							
	X=24	X=6	X=6	X=6	X=6	X=26	X=20	X=32
Si	6.64	1.91	1.88	1.97	1.93	0.17	4.11	0.00
Al	6.10	0.11	0.14	0.03	0.13	0.03	0.24	0.44
Fe	0.34	0.35	0.55	0.14	0.47	0.00	0.30	28.07
Mg	0.10	0.65	0.43	0.91	0.48	0.00	0.00	0.25
Ca	0.00	0.90	0.88	0.91	0.85	10.32	4.06	0.00
Na	0.00	0.12	0.12	0.00	0.16	0.10	0.00	0.00
K	2.02	0.00	0.00	0.01	0.01	0.00	0.01	0.00
Ti	0.03	0.01	0.02	0.01	0.02	0.01	3.53	1.25
P	0.00	0.00	0.01	0.00	0.00	6.01	0.00	0.00
Mn	0.00	0.02	0.03	0.00	0.02	0.00	0.00	0.51
Cl	0.01	0.00	0.00	0.00	0.00	0.02	0.00	0.00
S	0.02	0.00	0.00	0.00	0.00	0.06	0.00	0.00

* Total Fe as FeO

Sample key: I=Sample 34-316=Muscovite; J=Sample 21-85B=Salite (phenocryst); K=Sample 21-85B=Salite (phenocryst); L=Sample 21-85B=Salite (phenocryst-core); M=Sample 21-85B=Salite (phenocryst-rim); N=Sample 27-220=Apatite; O=Sample 21-85B=Sphene; P=Sample 21-85B=Titanian magnetite.

Figure 13. Photomicrograph of analcime phonolite porphyry (sample 21-85B). Secondary analcime (A) rimming the margins of a large sanidine phenocryst (S). Other phenocryst minerals include salite (Sa) and titanian magnetite (Tm). Groundmass consists of sanidine microlites with interstitial albite, anorthoclase, and analcime. Bar scale represents 0.25 mm. Plane-polarized light.

Figure 14. Photomicrograph of analcime phonolite porphyry (sample 21-85B). Phenocrysts of zoned salite (Sa), an altered feldspathoid mineral (F), sphene (Sp), and titanian magnetite (Tm) enclosed within a microcrystalline groundmass composed of sanidine microlites with interstitial albite, anorthoclase, and analcime. Bar scale represents 0.25 mm. Plane-polarized light.

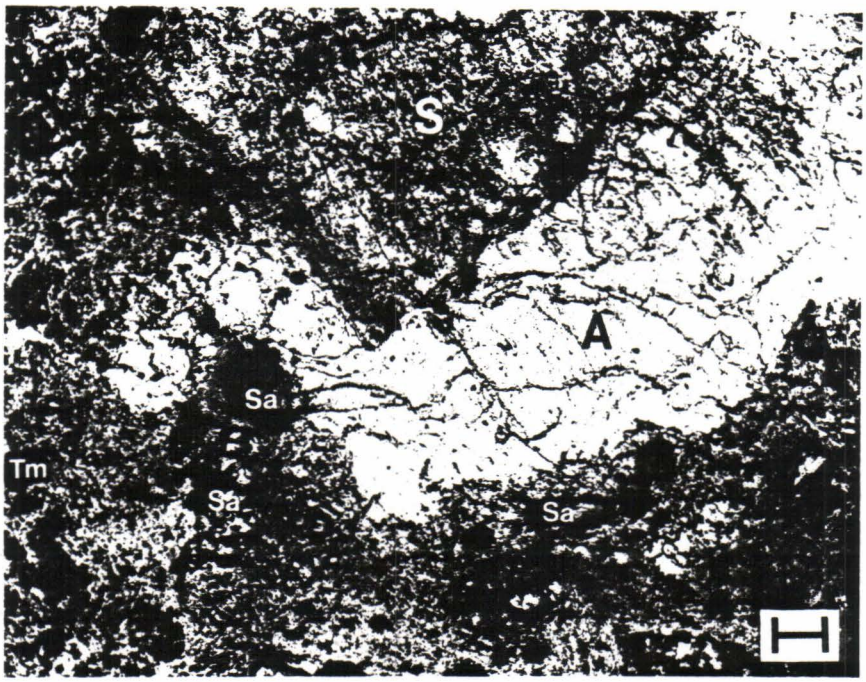
S
A
Sa
Tm
Sa
Sa


Tm
Sp
Tm
Tm
F
Sa
Tm

the groundmass sanidine microlites (Table 5, columns G and H).

Hexagonal phenocrysts of an altered feldspathoid mineral, possibly sodalite or haüyne, occur in most rocks (Figs. 12 and 14). Sizes range between 0.5 and 2.0 mm. In many specimens the alteration material consists of an aphanitic mixture of analcime, sericite, and strontian calcite. In others it is composed of fine-grained flakes of muscovite.

Fresher samples of phonolite and trachyte porphyries invariably contain elongate ferrosalite and salite phenocrysts that range up to 5 mm in length (Fig. 14). Crystals generally display simple or oscillatory normal zoning with pale green, usually salite cores, and darker green ferrosalite rims. Magnesium contents decrease from core to rim while sodium, iron, and titanium show marked enrichments (Table 5, columns L and M). In more altered samples the crystals are either replaced by secondary minerals, usually a mixture of chlorite, calcite, and iron oxides, or are completely destroyed with only small prismatic casts as remnants.

Accessory minerals in the rocks include apatite, sphene, and titanian magnetite. Apatite occurs in both altered and unaltered rocks and displays subhedral, prismatic and hexagonal forms up to 1 mm in size. Sphene only occurs in fresh samples where it forms rhombic crystals that vary between 0.1 and 1.0 mm in size. In altered samples it is usually replaced by leucoxene or forms small casts as a result of complete dissolution. Titanian magnetite crystals display square and triangular cross-sections up to 0.3 mm in size. They are ubiquitous in fresh specimens but are commonly replaced by iron and titanium oxides in more altered rocks.

Chemistry

Major element chemical analyses and CIPW normative mineralogies of six samples of phonolite and trachyte porphyries are presented in Table 6. The specimens range from slightly altered (21-85B) to moderately altered (21-73A) to severely altered (21-24B, 27-220, 34-233, and 34-316). The occurrence in most samples of normative quartz, a feature that would appear to contradict the presence of modal analcime and altered feldspathoid minerals, can be attributed to chemical changes associated with hydrothermal alteration. This conclusion is based upon the marked increase in SiO_2 contents displayed by more altered samples relative to less altered samples. Hydrothermal chemical changes also appear to result in a significant decrease in both MgO and CaO.

Natrolite-Garnet Syenites and Malignites

General

The third and final group of rocks asociated with the initial episode of igneous activity in the Bear Lodge Mountains is termed "natrolite-garnet syenites and malignites". It consists of a series of megascopically similar rock types that include natrolite-bearing garnet syenite, natrolite-garnet syenite, and natrolite-garnet malignite (Table 7). These plutonic rocks occur in the subsurface of the main igneous dome in a region where the effects of later potassic fenitization are most intense. This younger metasomatic event, which has obliterated contacts with surrounding rocks, undoubtedly had a significant effect on the original chemistry, mineralogy, and textures of the natrolite-garnet syenites and malignites.

TABLE 6

MAJOR ELEMENT CHEMICAL ANALYSES AND CIPW NORMATIVE MINERALOGIES OF PHONOLITE AND TRACHYTE PORPHYRIES

SAMPLE	A	B	C	D	E	F
SiO_2	55.45	51.32	61.71	60.62	59.79	59.97
Al_2O_3	17.53	18.66	18.65	19.00	20.17	20.99
Fe_2O_3*	3.47	2.63	3.96	4.44	3.86	3.24
MgO	1.47	1.62	0.28	0.42	0.39	0.29
CaO	5.28	6.03	0.55	0.31	0.34	0.23
Na_2O	3.46	1.89	4.60	3.17	2.88	4.36
K_2O	5.91	8.72	6.34	8.35	8.28	6.43
TiO_2	0.51	0.63	0.69	0.67	0.57	0.55
P_2O_5	0.14	0.12	0.20	0.14	0.11	0.13
MnO	0.14	0.16	0.04	0.03	0.04	0.17
Total	93.36	91.78	97.02	97.15	96.43	96.36
Qz	1.76	0.00	9.77	8.97	10.39	9.79
Co	0.00	0.00	3.81	4.65	6.34	7.00
Or	37.40	56.15	38.62	50.80	50.76	39.44
Ab	31.36	4.68	40.11	27.61	25.27	38.29
An	15.90	18.17	1.47	0.64	1.00	0.30
Ne	0.00	6.90	0.00	0.00	0.00	0.00
Wo	0.00	0.58	0.00	0.00	0.00	0.00
Di	8.81	9.48	0.00	0.00	0.00	0.00
Hy	0.25	0.00	1.11	2.44	1.74	0.75
Mt	3.12	0.34	3.27	3.24	3.11	2.90
Hm	0.00	2.09	0.00	0.00	0.00	0.13
Il	1.04	1.30	1.35	1.31	1.12	1.08
Ap	0.36	0.31	0.49	0.34	0.27	0.32

* Total Fe as Fe_2O_3

Sample key: A=Sample 21-85B; B=Sample 21-73A; C=Sample 21-24B; D=Sample 27-220; E=Sample 27-233; F=Sample 34-316

TABLE 7

MODAL ANALYSES OF NATROLITE-GARNET SYENITES AND MALIGNITES

SAMPLE	A	B	C	D	E
Primary					
Sanidine	34.2	37.8	40.8	44.0	32.6
Aegirine	0.8	0.2	3.8	8.4	5.8
Melanite	5.0	7.6	5.6	2.6	13.2
Apatite	0.4	1.0	0.6	0.2	0.2
Sphene	0.6	0.4	0.8	1.6	1.4
Magnetite	1.8	0.4	1.4	2.4	0.4
Manganian ilmenite	0.0	tr.	0.0	tr.	0.0
Secondary					
Biotite	12.6	14.0	8.8	7.8	17.8
Strontian calcite	17.8	17.0	12.2	9.8	6.2
Strontianite	0.0	0.0	pr.	0.0	0.0
Natrolite	3.6	2.4	2.4	11.8	18.4
Pyrite	1.4	0.4	0.4	1.4	0.8
Pyrrhotite	0.0	tr.	0.0	tr.	tr.
Chalcopyrite	0.6	0.2	tr.	0.0	tr.
Sericite/clays	19.0	18.0	22.8	6.0	3.2
Iron/titanium oxides	2.2	0.6	0.4	1.6	tr.
Uralite	0.0	0.0	0.0	2.4	0.0

tr.=trace, less than 0.2% detected
pr.=present, determined qualitatively by microprobe analysis

Sample key: A=Sample WBD-7/310.6=Natrolite-bearing garnet syenite
B=Sample WBD-13/1339.7=Natrolite-bearing garnet syenite
C=Sample WBD-13/1394.6=Natrolite-bearing garnet syenite
D=Sample WBD-13/1376.0=Natrolite-garnet syenite
E=Sample WBD-13/736.8=Natrolite-garnet malignite

Petrography

Natrolite-garnet syenites and malignites are holocrystalline, calcareous, and fine to medium-grained (Fig. 15). They have a mottled light gray and greenish black appearance when fresh and a mottled reddish brown and yellowish brown appearance when altered. Microprobe analyses of the major minerals of the rock are presented in Table 8.

Light gray patches of potassium feldspar and natrolite, 1 to 10 mm in diameter, are a distinctive feature of natrolite-garnet syenites and malignites, composing between 20 and 40 percent of the rocks (Fig. 16). They exhibit rounded to hexagonal cross-sections and are enclosed within a black matrix of fine to medium-grained biotite, melanite garnet, and aegirine. The macroscopic appearance of the patches is similar to pseudoleucite described in the pseudoleucite-garnet syenites from Magnet Cove, Arkansas (Erickson and Blade, 1963) and in the pseudoleucite borolanites from the Borralan complex, Assynt, Scotland (Wooley, 1973).

Potassium feldspar within the pseudoleucite-like patches occurs as granular aggregates. The feldspar is biaxial negative and termed sanidine on the basis of its low 2V angles which never exceed 25 degrees. Individual crystals are anhedral, untwinned, and generally less than 0.2 mm in diameter. Many of the crystals are partially replaced by strontian calcite along grain boundaries. Microprobe analyses of the sanidine crystals indicate potassium-rich compositions (Table 8, columns A, B, and C).

The natrolite within the pseudoleucite-like patches occurs as irregular-shaped masses intergrown with sanidine and possibly represents an alteration product of original nepheline. Natrolite also forms large anhedral masses along the margins of the patches. Fibrous habits are

Figure 15. Slab photograph of natrolite-bearing garnet syenite (sample WBD-13/1339.7). Light colored, rounded to hexagonal patches composed of sanidine and natrolite enclosed within a darker, fine-grained matrix rich in biotite, melanite garnet, and aegirine.

Figure 16. Photomicrograph of natrolite-bearing garnet syenite (sample WBD-5/166.0). Light colored, rounded to hexagonal patches (S+N) composed of sanidine and turbid natrolite, and dark, rounded to hexagonal crystals of melanite garnet (G) enclosed within within a mafic, fine-grained matrix rich in biotite, melanite garnet, and aegirine (B+G+A). Bar scale represents 0.25 mm. Plane-polarized light.

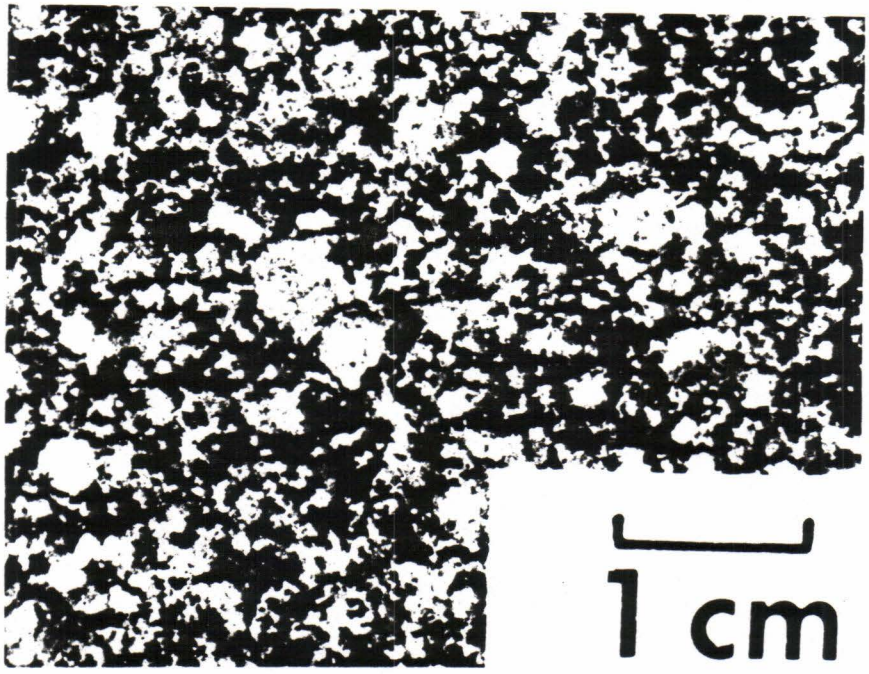
1 cm

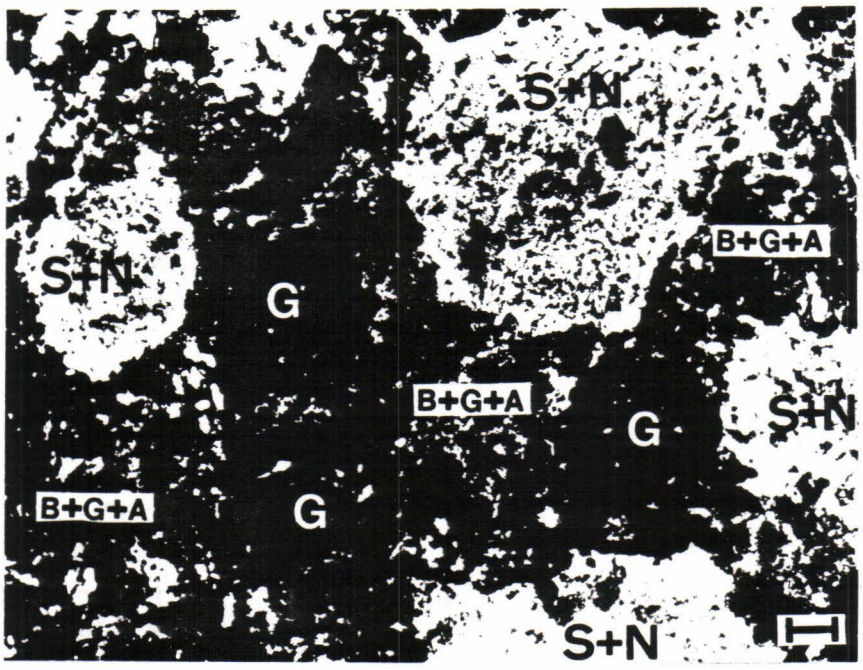
S+N
B+G+A
S+N
G
B+G+A
G
S+N
B+G+A
G
S+N

TABLE 8

MICROPROBE ANALYSES OF MINERALS IN NATROLITE-GARNET SYENITES AND MALIGNITES

SAMPLE	A	B	C	D	E	F	G	H
SiO2	66.48	65.39	64.82	44.80	48.78	47.57	54.12	53.30
Al2O3	18.42	18.88	18.93	30.76	27.81	27.86	1.82	0.76
FeO*	0.43	0.37	0.53	0.23	0.48	0.00	26.56	27.07
MgO	0.00	0.00	0.00	0.00	0.00	0.00	0.32	0.51
CaO	0.00	0.00	0.00	0.93	1.35	0.62	2.10	3.32
Na2O	0.99	1.29	0.90	14.55	13.36	15.61	13.45	12.82
K2O	14.84	14.00	13.95	0.20	0.06	0.12	0.15	0.00
TiO2	0.00	0.21	0.61	0.00	0.00	0.00	0.25	2.42
P2O5	0.17	0.00	0.00	0.00	0.15	0.00	0.00	0.18
MnO	0.00	0.00	0.00	0.00	0.00	0.00	0.21	0.39
Cl	0.06	0.00	0.14	0.00	0.00	0.00	0.05	0.04
SO3	0.00	0.13	0.00	0.00	0.00	0.00	0.00	0.00
Total	101.39	100.27	99.88	91.47	91.99	91.78	99.03	100.81
	Number of cations on the basis of X oxygens							
	X=32	X=32	X=32	X=80	X=80	X=80	X=6	X=6
Si	12.04	11.94	11.90	22.48	24.11	23.75	2.16	2.11
Al	3.93	4.06	4.10	18.19	16.20	16.39	0.08	0.03
Fe	0.06	0.06	0.08	0.09	0.20	0.00	0.89	0.89
Mg	0.00	0.00	0.00	0.00	0.00	0.00	0.02	0.03
Ca	0.00	0.00	0.00	0.50	0.71	0.33	0.09	0.14
Na	0.35	0.46	0.32	14.15	12.80	15.11	1.04	0.98
K	3.43	3.26	3.27	0.13	0.04	0.03	0.01	0.00
Ti	0.00	0.03	0.08	0.00	0.00	0.00	0.01	0.07
P	0.03	0.00	0.00	0.00	0.06	0.00	0.00	0.01
Mn	0.00	0.00	0.00	0.00	0.00	0.00	0.01	0.01
Cl	0.02	0.00	0.04	0.00	0.00	0.00	0.00	0.00
S	0.00	0.02	0.00	0.00	0.00	0.00	0.00	0.00

* Total Fe as FeO

Sample key: A=Sample WBD-7/310.6=Sanidine; B=Sample WBD-13/1339.7= Sanidine; C=Sample WBD-13/736.8=Sanidine; D=Sample WBD-7/310.6= Natrolite; E=Sample WBD-13/1376.0=Natrolite; F=Sample WBD-13/736.8= Natrolite; G=Sample WBD-13/1394.6=Aegirine; H=Sample WBD-13/1376.0= Natrolite.

TABLE 8

(continued)

SAMPLE	I	J	K	L	M	N	O	P
SiO2	35.17	35.75	39.55	37.63	0.70	30.87	0.00	0.34
Al2O3	2.48	1.05	11.64	11.45	0.00	1.39	0.00	0.00
FeO*	22.49	25.57	17.59	24.76	0.00	2.12	93.81	41.13
MgO	0.34	0.37	16.01	10.44	0.00	0.00	0.15	0.34
CaO	33.45	33.33	0.00	0.00	52.48	28.52	0.24	0.42
Na2O	0.29	0.61	0.00	0.20	0.68	0.29	0.43	0.00
K2O	0.00	0.00	9.74	9.02	0.00	0.06	0.00	0.00
TiO2	4.66	3.36	0.88	2.07	0.00	36.81	0.71	49.95
P2O5	0.24	0.17	0.00	0.00	37.85	0.32	0.00	0.15
MnO	0.58	0.61	0.80	0.77	0.00	0.00	0.33	8.25
Cl	0.00	0.08	0.12	0.00	0.32	0.00	0.10	0.00
SO3	0.00	0.00	0.00	0.00	0.41	0.00	0.00	0.00
Total	99.70	100.90	96.33	96.34	92.44	100.38	95.77	100.58
	Number of cations on the basis of X oxygens							
	X=24	X=24	X=24	X=24	X=26	X=20	X=32	X=6
Si	6.11	6.24	6.48	6.38	0.13	4.04	0.00	0.02
Al	0.51	0.21	2.25	2.29	0.00	0.21	0.00	0.00
Fe	3.27	3.73	2.41	3.51	0.00	0.23	31.11	1.75
Mg	0.09	0.09	3.91	2.64	0.00	0.00	0.09	0.03
Ca	6.22	6.23	0.00	0.00	10.49	4.00	0.10	0.02
Na	0.10	0.21	0.00	0.07	0.24	0.07	0.33	0.00
K	0.00	0.00	2.04	1.95	0.00	0.01	0.00	0.00
Ti	0.61	0.44	0.11	0.26	0.00	3.62	0.21	1.89
P	0.03	0.02	0.00	0.00	5.98	0.03	0.00	0.01
Mn	0.09	0.09	0.11	0.11	0.00	0.00	0.11	0.36
Cl	0.00	0.02	0.03	0.00	0.10	0.00	0.07	0.00
S	0.00	0.00	0.00	0.00	0.06	0.00	0.00	0.00

* Total Fe as FeO

Sample key: I=Sample WBD-7/310.6=Melanite (primary); J=Sample WBD-13/736.8=Melanite (secondary); K=Sample WBD-7/310.6=Biotite; L=Sample WBD-13/1339.7=Biotite; M=Sample WBD-7/310.6=Apatite; N=Sample WBD-13/736.8=Sphene; O=Sample WBD-13/1376.0=Magnetite; P=Sample WBD-13/1339.7=Manganian ilmenite.

common with first order interference colors (Fig. 17). Partial alteration to clay minerals and local replacement by strontian calcite imparts a distinct cloudy appearance that facilitates the identification of this zeolite in plane-polarized light.

Melanite garnet is ubiquitous in the rocks. This titaniferous variety of andradite varies in color from brownish red to honey-yellow and appears to be of 2 distinct generations. An older generation is represented by euhedral and subhedral crystals that commonly display octagonal cross-sections up to 2 mm in diameter (Fig. 16). They usually contain inclusions of sphene, magnetite, manganian ilmenite, and apatite and are frequently rimmed by fine-grained biotite and magnetite.

A younger generation of garnets occurs as small anhedral masses embedded within biotite flakes (Fig. 18). These biotite-garnet aggregates frequently display prismatic cross-sections and probably represent pseudomorphs of biotite and garnet after pyroxene. Chemical differences between the two types of garnet appear to be negligible (Table 8, columns I and J).

Aegirine occurs as equant subhedral crystals less than 2 mm in size. It also forms irregular-shaped microcrystalline aggregates that surround and possibly replace melanite garnet. Crystals are unzoned and moderately to strongly pleochroic with X=emerald green, Y=yellowish green, and Z=pale green.

Biotite is the major mafic constituent of the rocks. The majority of crystals are of secondary origin and form, as previously noted, pseudomorphs after original aegirine. Individual crystals range up to 2 mm in length and are strongly pleochroic with X=yellowish tan and Y=Z=brownish green.

Figure 17. Photomicrograph of natrolite-garnet malignite (sample WBD-13/736.8). Fibrous crystal of natrolite (N) surrounded by sanidine (S) and melanite garnet (G). Bar scale represents 0.25 mm. Crossed polars.

Figure 18. Photomicrograph of natrolite-bearing garnet syenite (sample WBD-5/166.0). Fine-grained intergrowths of biotite (B) and melanite garnet (G) surrounded by sanidine (S) and altered natrolite (N). Note prismatic shape of biotite-garnet intergrowth located near center of photograph which suggests pseudomorphing of biotite and garnet after pyroxene. Bar scale represents 0.25 mm. Plane-polarized light.

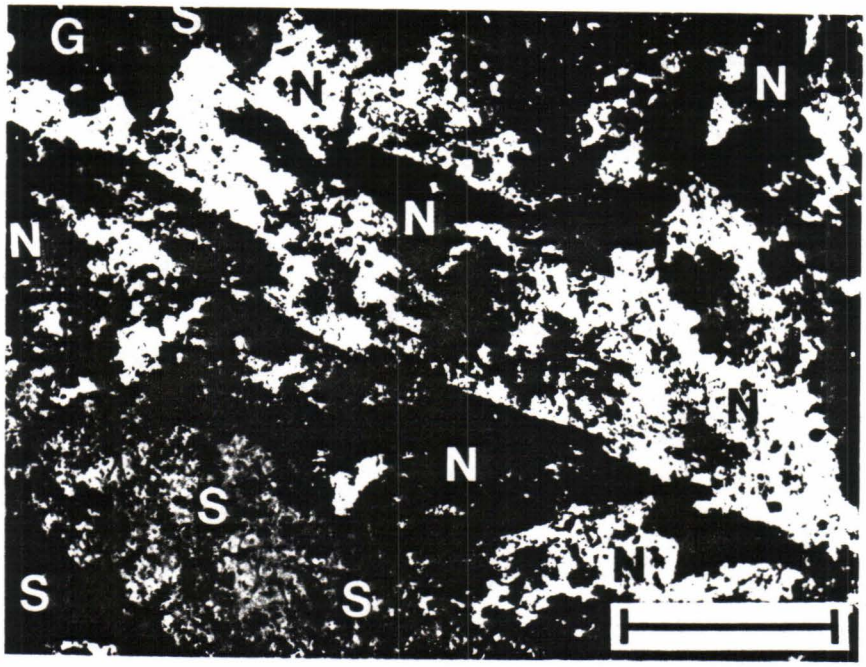
G
S
N
N
N
N
N
N
S
S
S
N

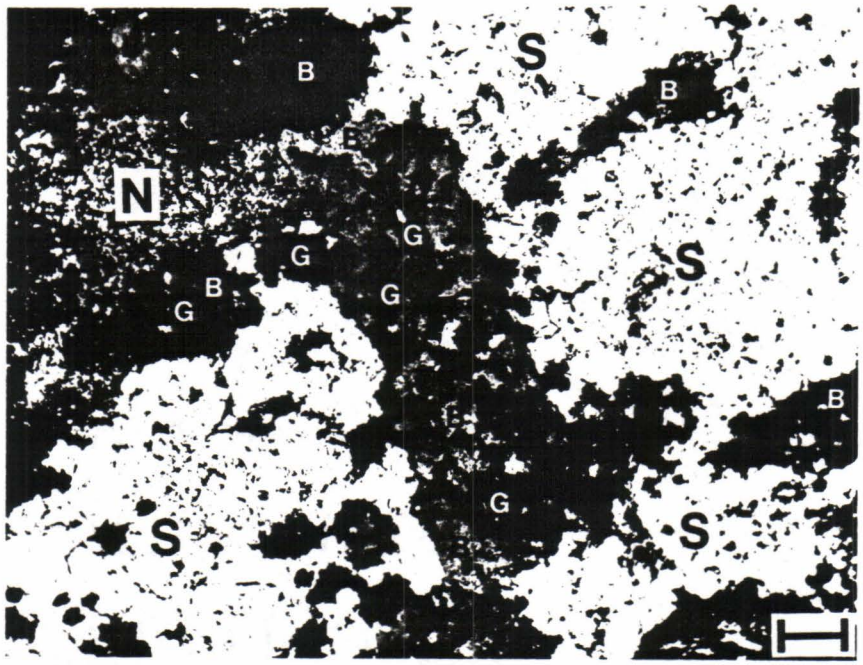
B
S
B
N
G
G
B
G
G
S
B
G
S
S

Strontianite, pyrite, pyrrhotite, and chalcopyrite occur in accessory amounts as small disseminated grains less than 1 mm in size. They frequently display replacement textures and are considered to be of secondary origin in the rocks. They were probably deposited by the CO_2-rich fluids associated with both potassic fenitization and the emplacement of strontium-rich carbonatite dikes and veins.

Chemistry

Major element chemical analyses and CIPW normative mineralogies of five samples of natrolite-garnet syenites and malignites are presented in Table 9. The extreme silica-undersaturation of the rocks is shown by the abundance of both normative nepheline and normative leucite. The undersaturation is partially an artifact and can be attributed to the occurrence of strontian calcite which varies between 6 and 18 percent in modal abundance (Table 7). The presence of this secondary carbonate mineral explains the inverse relationship displayed between values of SiO_2 and Al_2O_3 relative to CaO and also accounts for the poor closures of the five analyses.

The values of total alkalis (Na_2O+K_2O) and the values of the other major oxides in natrolite-garnet syenites and malignites show little variation between samples. The high ratios of K_2O/Na_2O are similar to the ratios displayed by the rock types associated with potassic fenitization and are probably related to the chemical effects of this later metasomatic event.

TABLE 9

MAJOR ELEMENT CHEMICAL ANALYSES AND CIPW NORMATIVE MINERALOGIES OF NATROLITE-GARNET SYENITES AND MALIGNITES

SAMPLE	A	B	C	D	E
SiO_2	43.72	43.67	46.27	45.56	43.72
Al_2O_3	14.91	15.47	17.00	15.82	15.62
Fe_2O_3*	8.91	9.02	7.93	8.00	7.74
MgO	2.78	1.97	1.53	1.46	2.01
CaO	11.04	11.51	8.90	8.89	8.32
Na_2O	2.03	0.63	2.20	3.11	3.73
K_2O	7.68	8.32	7.81	7.17	6.51
TiO_2	1.59	1.69	1.51	1.56	1.39
P_2O_5	0.51	0.32	0.27	0.27	0.35
MnO	0.29	0.30	0.27	0.29	0.23
Total	93.46	92.90	93.69	92.13	89.62
Qz	0.00	0.00	0.00	0.00	0.00
Or	1.27	2.70	27.97	30.78	25.30
An	9.51	15.92	14.35	8.71	7.42
Lc	37.06	39.37	16.69	11.92	13.79
Ne	9.96	3.11	10.76	15.47	19.08
Wo	4.74	6.43	3.91	6.68	4.04
Di	28.15	23.21	17.92	17.71	21.81
Mt	4.79	4.98	4.66	4.82	4.68
Il	3.23	3.46	3.06	3.22	2.95
Ap	1.29	0.82	0.68	0.69	0.93

* Total Fe as Fe_2O_3

Sample key: A=Sample WBD-7/310.6; B=Sample WBD-13/1339.7; C=Sample WBD-13/1394.6; D=Sample WBD-13/1376.0; E=Sample WBD-13/736.8

Potassic Fenitization

The second event in the petrologic history of the Bear Lodge Mountains is termed "potassic fenitization". Fenitization is a type of metasomatic wall-rock alteration that is characteristic of many alkalic igneous complexes. Its effects can be observed in alkalic complexes containing carbonatites, in alkalic complexes without carbonatites, and in areas where carbonatites are exposed but associated alkalic silicate rocks are lacking (Heinrich, 1966).

The term fenitization was first employed by Brögger (1921) to describe a process of alkali enrichment observed in rocks from the Fen complex of southern Norway. Inherent in Brögger's definition is the notion that the process occurs in situ, without appreciable melting or mobilization of the original wall rocks. Subsequent work in other complexes resulted in the recognition of mobilized rocks associated with the fenitization process. These igneous-looking rocks are commonly refered to as "rheomorphic fenites".

The mineralogic changes accompanying fenitization have been summarized by Heinrich (1966). They include:

1. Concentration of K in the feldspars with recrystallization to larger euhedral crystals.
2. Oxidation of Fe^{+2} to Fe^{+3}, and its concentration in sodic pyroxene and as hematite dispersed in potassium feldspar.
3. Concentration of early available Na and Ca in pyroxene.
4. Formation of variable amounts of sodic plagioclase with introduced Na.
5. Elimination of quartz.

The above changes are generally associated with a net increase in the values of K_2O, Na_2O, Fe_2O_3, CaO, TiO_2, P_2O_5, CO_2, H_2O, and F in the

original wall rocks while values of SiO_2 and FeO usually show a net decrease (Heinrich, 1966).

In many alkalic complexes the rock types associated with fenitization show a progression from a higher temperature assemblage dominated by sodium-rich alkali feldspar and sodic pyriboles to a lower temperature assemblage consisting of almost pure potassium feldspar and iron oxides. Temporal and spatial relationships indicate that the higher temperature, sodic fenites usually form earlier and at deeper structural levels than the lower temperature, potassic fenites (Heinrich and Moore, 1970; Le Bas, 1977; Wooley, 1969, 1982). The type of fenite produced, either sodic or potassic, has been shown to be dependent upon the temperature, pressure, CO_2 content, and K/Na ratio of the fenitizing fluid (Rubie and Gunter, 1983).

Fenitization in the Bear Lodge Mountains has generated the lower temperature, potassic variety of fenites. This variation of fenitization has been termed feldspathization by Heinrich (1966) and potassic fenitization by Wooley (1982). Other complexes where an analogous process has occurred are located in East Africa and include Chilwa Island and Tundulu, Malawi (Garson, 1966; Wooley, 1969); Muambe, Mozambique (Dixie and others, 1955); Toror Hills, Uganda (Sutherland, 1965); Wasaki, Kenya, (Le Bas, 1977, p. 113-128); and Myeba, Musensi Hills, and Songwe scarp, Zambia (Fawley and James, 1955; Miller and Brown, 1963; Brown, 1964).

The initial stage of fenitization in the Bear Lodge Mountains is marked by the shattering and elimination of quartz within the Precambrian granitic rocks. The dissolved silica resulting from this phenomenon is often reprecipitated as irregular-shaped pods of quartz in

adjacent granite (Fig. 19) or as microcrystalline patches of chalcedony in surrounding fenites and alkalic igneous rocks (Fig. 20). Granitic breccias, consisting of subrounded to subangular fragments of Precambrian granite in a matrix of granulated quartz and feldspar, are also a product of this desilicification process.

The potassic fenites found in the Bear Lodge Mountains are of two types, metasomatic and rheomorphic. The metasomatic units represent fenitized analogues of the alkalic rocks emplaced during the initial episode of igneous activity. Phenocrysts and other primary igneous features are commonly preserved in the rocks. The rheomorphic units occur as dikes and small plugs which crosscut earlier formed metasomatic units and unfenitized alkalic igneous rocks. Both varieties of fenite are ultrapotassic with values of K_2O significantly greater than values for the surrounding igneous rocks (Fig. 21).

The principle mineral occurring in both metasomatic and rheomorphic fenites is potassium feldspar. It is designated sanidine on the basis of its biaxial negative sign and low 2V angles which never exceed 25 degrees. The sanidine occurs both in shallower level, hypabyssal rock types and in deeper level, plutonic rock types. Minute inclusions of hematite are commonly disseminated in the sanidine of the hypabyssal rock types resulting in the red, orange, and brown colors that are characteristic of many of these rocks.

The episode of potassic fenitization in the Bear Lodge Mountains is of considerable economic interest. The thorium and rare-earth deposits described by Staatz (1983) are especially significant. The numerous veins and veinlets that compose the deposits crosscut earlier formed metasomatic and rheomorphic rock types and mark the waning stages of

Figure 19. Slab photograph of Precambrian granite (sample 27-444B). Discontinuous, irregular-shaped patches of quartz (Q) in granite (Gr). Quartz mobilized from groundmass of granite during potassic fenitization.

Figure 20. Photomicrograph of latite porphyry (sample 27-13). Irregular-shaped pods of secondary quartz (Q) in groundmass of latite porphyry. Quartz mobilized from adjacent xenoliths of Precambrian granite during potassic fenitization and reprecipitated in groundmass of specimen. Bar scale represents 0.25 mm. Crossed polars.

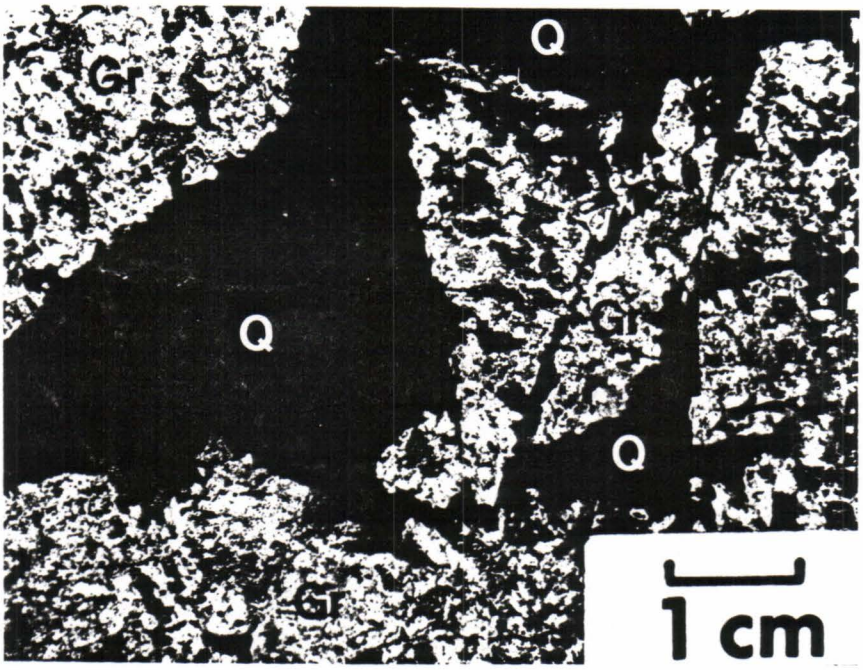
Gr
Q
Q
Gr
Q
Gr
1 cm

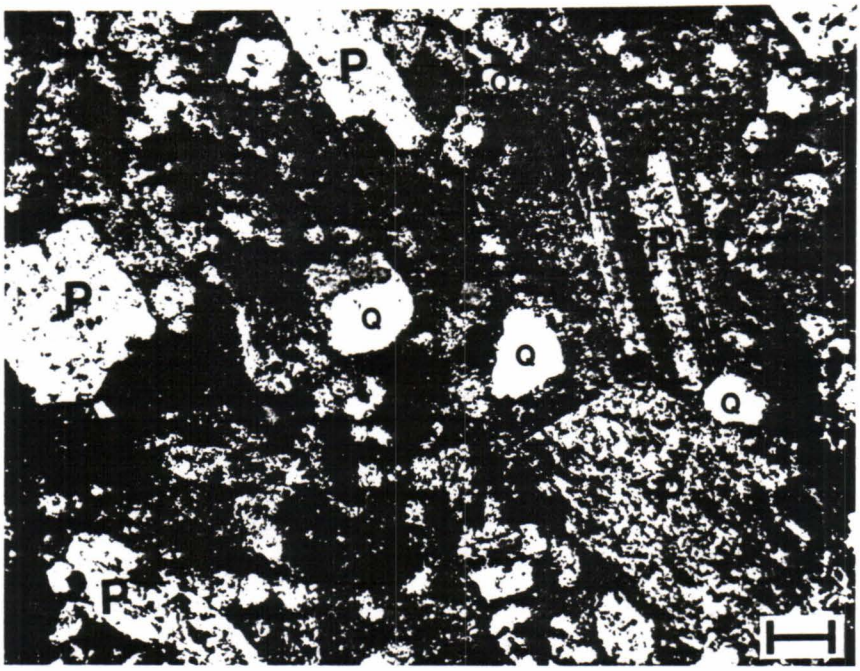
P
P
Q
Q
Q
P
P

Figure 21. Triangular plot of ($MgO+Fe_2O_3+FeO+MnO$) versus K_2O versus Na_2O showing compositional differences between the rock types associated with the episode of early igneous activity (open circles) and the rock types associated with the episode of potassic fenitization (closed circles) in the southeastern and central Bear Lodge Mountains.

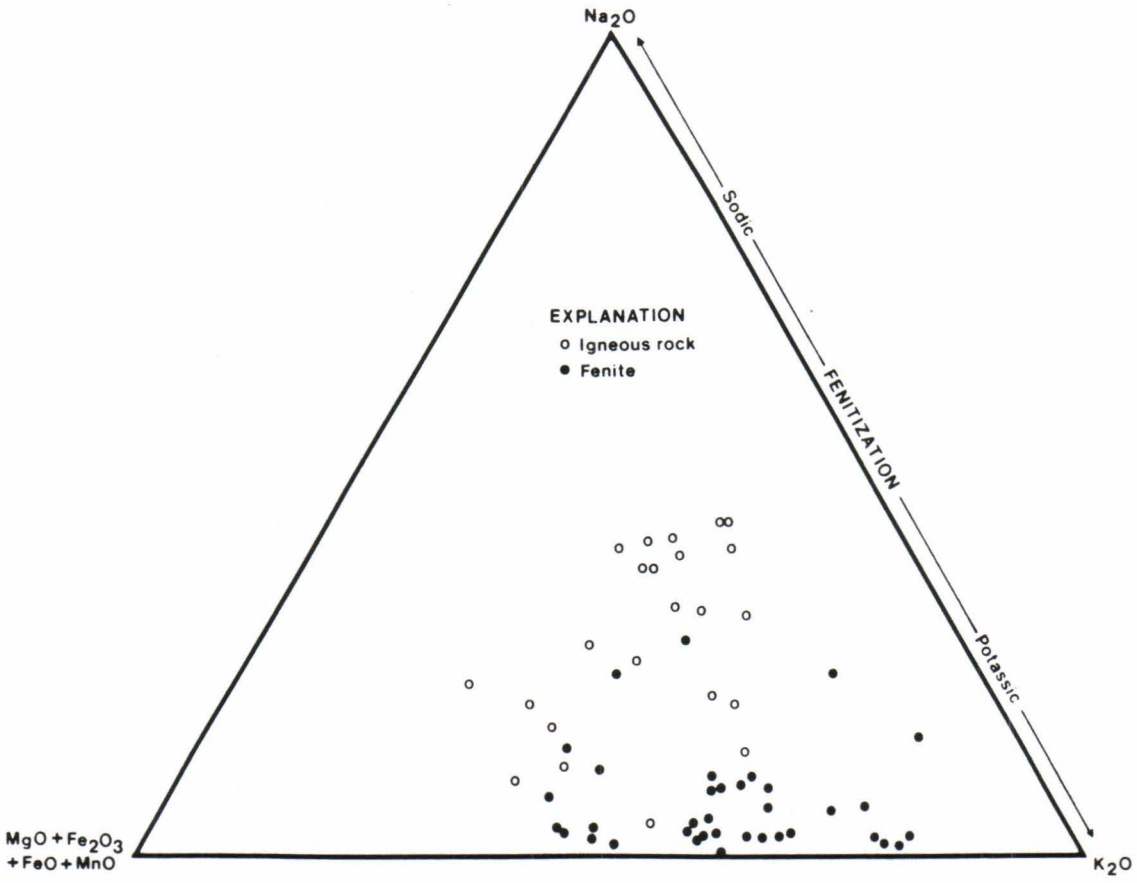
Na_2O
Sodic
FENITIZATION
Potassic
EXPLANATION
o Igneous rock
• Fenite
$MgO + Fe_2O_3$
$+ FeO + MnO$
K_2O

fenitization in the region (Figs. 22 and 23). They are common in oxidized rocks at the surface but diminish in abundance with increasing depth. They contain up to 1.2 percent thorium and 9.8 percent total rare-earths and possess a complex and highly variable mineralogy that includes, in approximate order of decreasing abundance, sanidine, quartz, hematite, limonite, goethite, manganese oxide, monazite, fluorite, montmorillonite, kaolinite, cryptomelane, barite, rutile, magnetite, calcite, chlorite, brockite, bastnaesite, lepidocrocite, anatase, brookite, biotite, sphalerite, and zircon (Staatz, 1983).

Other deposits of potential economic interest that are associated with potassic fenitization in the Bear Lodge Mountains are copper, lead, zinc, and gold. Copper-lead-zinc deposits occur in both metasomatic and rheomorphic rock types and consist of disseminated chalcopyrite, galena, and sphalerite with associated pyrite and pyrrhotite. These sulfides are rare in oxidized surface rocks but occur in significant amounts in deeper, unoxidized fenites. Chalcopyrite is the most abundant economic sulfide and locally approaches ore-grade concentrations in the subsurface.

Low-grade gold mineralization has recently been recognized in the southeastern Bear Lodge Mountains (Lorson, 1984, oral communication). The mineralization reportedly occurs within oxidized samples of intrusive feldspathic breccia. A microprobe survey of six samples failed to reveal any gold within this rock type and the nature of the mineralization and its relationship to the fenitization process remain an enigma.

Six rock types are associated with potassic fenitization in the Bear Lodge Mountains. They are: (1) alkali trachyte, (2) alkali

Figure 22. Slab photograph of Th/REE vein crosscutting pseudoleucite alkali trachyte porphyry (sample BL-6/764.0).

Figure 23. Photomicrograph of Th/REE vein crosscutting alkali trachyte (sample 27-6A). Vein composed mostly of iron oxides (FeOx), chlorite (Ch), and quartz (Q). Holes (Ho) in specimen due to polishing. Note microfracturing with mineralization in alkali trachyte (T) adjacent to the vein. Bar scale represents 0.25 mm. Plane-polarized light.


1 cm

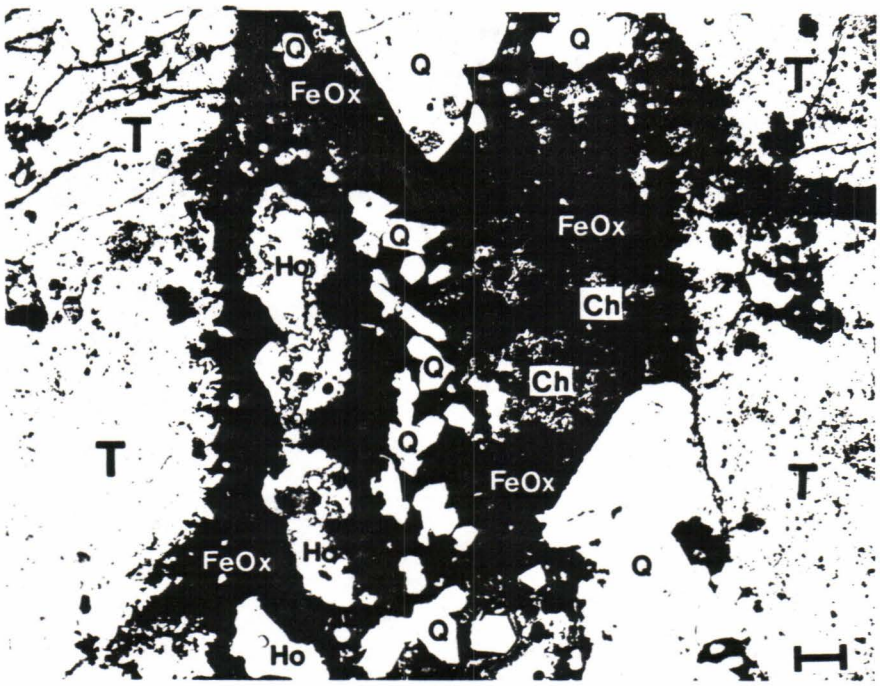
Q
FeOx
T
Q
Q
T
FeOx
Ho
Q
Ch
Ch
Q
Q
T
FeOx
T
FeOx
Ho
Q
Ho
Q
H

trachyte porphyry, (3) alkali melasyenite, (4) alkali leucosyenite, (5) pseudoleucite alkali trachyte porphyry, and (6) intrusive breccias.

Alkali Trachyte

General

The most common variety of fenite exposed at the surface along the southeastern flank of the Bear Lodge Mountains is classified as alkali trachyte (Table 10). It occurs in other areas of the uplift and is analogous to many of the samples of alkali trachyte porphyry reported by Wilkinson (1982) in the central portions of the main igneous dome in the same region where drilling activity indicates it forms one of the major rock types in the shallow subsurface. It also corresponds to the ultrapotassic varieties of altered felsite described by O'Toole (1981) in the southwestern Bear Lodge Mountains and to many of the altered samples of "older" trachyte reported in areas of thorium and rare-earth mineralization by Staatz (1983).

Alkali trachyte consists of both metasomatic and rheomorphic varieties. The metasomatic types are megascopically similar to the latite and trachyte porphyries emplaced during the initial episodes of igneous activity and essentially represent fenitized equivalents of these older alkalic igneous rocks. As such, distinguishing samples of metasomatic alkali trachyte from samples of latite and trachyte porphyries is usually impossible in hand sample and generally necessitates chemical analysis with alkali trachyte recognizable on the basis of its ultrapotassic chemical composition.

The rheomorphic varieties of alkali trachyte occur as dikes and

TABLE 10

MODAL ANALYSES OF ALKALI TRACHYTE

SAMPLE	A	B	C	D	E	F
Primary						
Groundmass						
Sanidine	57.0	57.3	52.1	51.0	51.1	57.4
Albite	0.0	2.1	1.7	8.9	16.6	2.7
Anorthoclase	0.0	0.0	0.0	0.0	0.0	3.4
Calcite	3.6	9.6	0.0	2.6	3.6	4.1
Quartz	0.0	0.0	3.4	1.3	0.7	0.0
Sanidine	1.6	2.0	12.4	8.0	6.2	1.4
Albite	tr.	15.2	8.6	6.8	8.4	0.0
Aegirine	0.0	0.0	0.0	7.2	0.4	0.0
Biotite	4.2	0.0	0.0	3.6	0.4	7.4
Apatite	0.2	0.0	0.0	0.2	0.4	0.8
Zircon	0.0	0.0	tr.	0.0	0.0	0.0
Strontian calcite	4.8	0.0	0.0	0.6	6.0	4.4
Strontianite	0.0	0.0	0.0	0.0	pr.	0.0
Barite	0.0	0.0	pr.	0.0	0.0	0.0
Fluorite	0.0	tr.	0.0	0.0	0.0	tr.
Quartz/chalcedony	0.4	5.6	1.8	0.0	0.0	0.0
Titanian magnetite	5.2	0.2	0.0	0.0	0.8	0.4
Manganian ilmenite	1.2	0.4	0.2	0.0	0.0	tr.
Brookite	pr.	0.0	0.0	0.0	pr.	0.0
Pyrite	0.0	0.6	1.0	3.4	2.4	8.0
Pyrrhotite	0.0	0.0	0.0	0.0	0.0	0.6
Chalcopyrite	0.0	0.0	0.0	tr.	tr.	tr.
Secondary						
Sericite/clays	12.6	4.2	3.0	4.6	2.4	8.8
Iron/titanium oxides	9.2	2.8	15.2	1.8	0.6	0.6
Chlorite	0.0	0.0	0.6	0.0	0.0	0.0

tr.=trace, less than 0.2% detected
pr.=present, determined qualitatively by microprobe analysis

Sample key: A=Sample 10-393=Alkali trachyte
B=Sample 21-368=Alkali trachyte
C=Sample 27-6B=Alkali trachyte
D=Sample WBD-8/348.2=Alkali trachyte
E=Sample WBD-12/906.8=Alkali trachyte
F=Sample BL-4/1146.0=Alkali trachyte

small plugs which crosscut both older fenites and alkalic igneous rocks. They commonly contain xenoliths of these earlier formed rock types and, with an increase in the ratio of xenoliths to groundmass, grade into another variety of fenite termed intrusive feldspathic breccia.

Petrography

Alkali trachyte is holocrystalline and variably porphyritic (Fig. 24). Samples range from light gray to medium gray in color when fresh but more commonly have an ocherous appearance due to hematite staining associated with alteration and oxidation. Microprobe analyses of the major minerals of the rock are presented in Table 11.

Groundmasses are aphanitic to very fine-grained and compose 60 to 95 percent of the rock. The principle groundmass constituent is sanidine. In metasomatic units it tends to form Carlsbad twinned microlites that vary from felty to strongly trachytic in texture (Fig. 25) while in rheomorphic units it typically occurs as untwinned, aphanitic crystals that exhibit an allotriomorphic granular texture (Fig. 26). In both types of units cryptocrystalline albite and/or anorthoclase may occur interstitially within the groundmass.

Sanidine phenocrysts range up to 10 percent in abundance. They vary from 1 to 5 mm in size and possess potassium-rich compositions (Table 11, columns E and F). Crystals typically display subhedral forms with corroded and embayed margins. Carlsbad twinning is common in many samples but rare or absent in others. In rheomorphic units the crystals often appear fractured or broken and possibly represent xenocrysts derived from included fragments of surrounding wall rocks rather than true phenocrysts.

Albite phenocrysts occur in many samples of the rock and are

Figure 24. Slab photograph of alkali trachyte (sample 27-250). Anhedral phenocrysts (xenocrysts?) of sanidine (S) enclosed within an aphanitic, altered and iron oxide-stained groundmass rich in sanidine.

Figure 25. Photomicrograph of alkali trachyte (sample 10-393). Fresh, vitreous laths of felted, Carlsbad twinned sanidine (S) enclosing altered and oxidized mafic minerals (M). Typical example of metasomatic variety of alkali trachyte. Bar scale represents 0.25 mm. Crossed polars.


S
S
1 cm

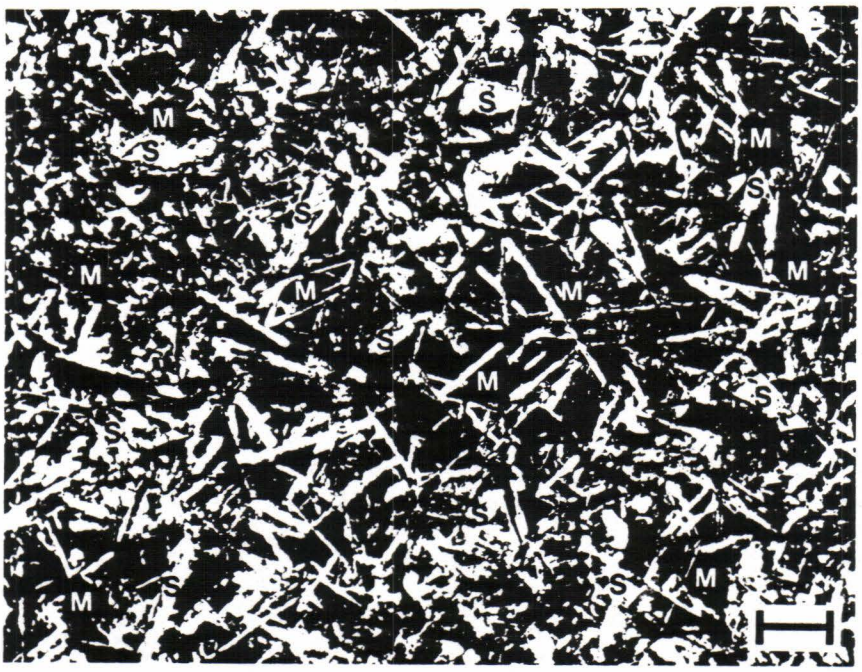
M
S
M
S
M
M
M
M
M
S
S
M
M

TABLE 11

MICROPROBE ANALYSES OF MINERALS IN ALKALI TRACHYTE

SAMPLE	A	B	C	D	E	F	G	H
SiO2	66.19	65.71	69.16	69.14	66.23	66.44	69.43	69.92
Al2O3	18.61	18.65	20.30	21.00	19.26	19.52	20.17	20.14
FeO*	0.50	0.00	0.26	0.51	0.00	0.00	0.00	0.27
MgO	0.00	0.00	0.00	0.00	0.00	0.00	0.00	0.00
CaO	0.00	0.00	0.18	0.00	0.00	0.00	0.07	0.00
Na2O	0.39	0.54	11.31	9.61	0.91	0.29	12.10	11.58
K2O	15.58	15.89	0.58	3.51	14.94	15.16	0.33	0.30
TiO2	0.00	0.00	0.00	0.00	0.22	0.00	0.00	0.00
P2O5	0.27	0.00	0.00	0.17	0.00	0.00	0.00	0.00
MnO	0.00	0.00	0.00	0.00	0.00	0.12	0.17	0.00
Cl	0.05	0.11	0.10	0.00	0.00	0.00	0.00	0.00
SO3	0.00	0.00	0.00	0.00	0.17	0.00	0.00	0.00
Total	101.59	100.90	101.89	103.94	101.73	101.53	102.27	102.21
	Number of cations on the basis of X oxygens							
	X=32	X=32	X=32	X=32	X=32	X=32	X=32	X=32
Si	11.99	12.01	11.90	11.78	11.93	11.98	11.90	11.96
Al	3.97	4.02	4.12	4.22	4.09	4.15	4.07	4.06
Fe	0.07	0.00	0.04	0.07	0.00	0.00	0.00	0.04
Mg	0.00	0.00	0.00	0.00	0.00	0.00	0.00	0.00
Ca	0.00	0.00	0.03	0.00	0.00	0.00	0.01	0.00
Na	0.14	0.19	3.77	3.18	0.32	0.10	4.02	3.84
K	3.60	3.70	0.13	0.76	3.43	3.49	0.07	0.07
Ti	0.00	0.00	0.00	0.00	0.03	0.00	0.00	0.00
P	0.04	0.00	0.00	0.02	0.00	0.00	0.00	0.00
Mn	0.00	0.00	0.00	0.00	0.00	0.02	0.02	0.00
Cl	0.01	0.03	0.03	0.00	0.00	0.00	0.00	0.00
S	0.00	0.00	0.00	0.00	0.02	0.00	0.00	0.00

* Total Fe as FeO

Sample key: A=Sample WBD-8/348.2=Sanidine (groundmass); B=Sample WBD-12/906.8=Sanidine (groundmass); C=Sample WBD-8/348.2=Albite (groundmass); D=Sample BL-4/1146.0=Anorthoclase (groundmass); E=Sample WBD-8/348.2=Sanidine (phenocryst); F=Sample WBD-8/348.2=Sanidine (phenocryst); G=Sample WBD-8/348.2=Albite (phenocryst); H=Sample WBD-8/348.2=Albite (phenocryst).

TABLE 11

(continued)

SAMPLE	I	J	K	L	M	N	O	P
SiO2	54.19	52.84	36.48	42.42	0.67	0.36	0.32	0.22
Al2O3	0.47	0.27	14.32	10.39	0.00	2.32	0.00	0.00
FeO*	25.65	31.00	16.00	13.08	0.31	76.68	31.55	0.70
MgO	1.55	0.00	13.50	18.12	0.22	0.58	0.00	0.00
CaO	0.88	0.34	0.00	0.00	54.28	0.00	0.21	0.00
Na2O	13.97	13.98	0.87	0.56	0.49	0.30	0.00	0.00
K2O	0.20	0.05	8.87	9.98	0.00	0.00	0.00	0.07
TiO2	2.07	0.83	6.73	1.09	0.00	13.24	60.86	99.45
P2O5	0.00	0.00	0.00	0.00	40.50	0.00	0.00	0.00
MnO	0.14	0.00	0.27	0.40	0.00	0.15	8.46	0.00
Cl	0.07	0.00	0.00	0.00	0.22	0.05	0.00	0.00
SO3	0.00	0.00	0.00	0.00	0.40	0.00	0.00	0.00
Total	99.19	99.31	97.04	96.04	97.09	93.68	101.40	100.44
	Number of cations on the basis of X oxygens							
	X=6	X=6	X=24	X=24	X=26	X=32	X=6	X=16
Si	2.16	2.15	5.89	6.78	0.12	0.13	0.01	0.02
Al	0.02	0.01	2.73	1.96	0.00	0.97	0.00	0.00
Fe	0.85	1.06	2.16	1.75	0.05	22.77	1.26	0.06
Mg	0.09	0.00	3.25	4.32	0.06	0.31	0.00	0.00
Ca	0.04	0.01	0.00	0.00	10.27	0.00	0.01	0.00
Na	1.08	1.10	0.27	0.17	0.17	0.20	0.00	0.00
K	0.01	0.00	1.83	2.04	0.00	0.00	0.00	0.01
Ti	0.06	0.03	0.82	0.13	0.00	3.53	2.18	7.94
P	0.00	0.00	0.00	0.00	6.06	0.00	0.00	0.00
Mn	0.01	0.00	0.04	0.05	0.00	0.04	0.34	0.00
Cl	0.01	0.00	0.00	0.00	0.06	0.03	0.00	0.00
S	0.00	0.00	0.00	0.00	0.05	0.00	0.00	0.00

* Total Fe as FeO

Sample key: I=Sample WBD-8/348.2=Aegirine; J=Sample WBD-12/906.8= Aegirine; K=Sample 10-393=Biotite; L=Sample WBD-8/348.2=Biotite; M=Sample 10-393=Apatite; N=Sample 10-393=Titanian magnetite; O= Sample WBD-12/906.8=Manganian ilmenite; P=Sample WBD-12/906.8= Brookite.

Figure 26. Photomicrograph of alkali trachyte (sample WBD-8/300.9). Irregular-shaped phenocrysts (xenocrysts?) of sanidine (S) enclosed within a microcrystalline granular groundmass rich in sanidine. Typical example of rheomorphic variety of alkali trachyte. Bar scale represents 0.25 mm. Crossed polars.

Figure 27. Photomicrograph of alkali trachyte (sample 27-155). Phenocryst of plagioclase (P) mantled by sanidine (S). Bar scale represents 0.25 mm. Crossed polars.

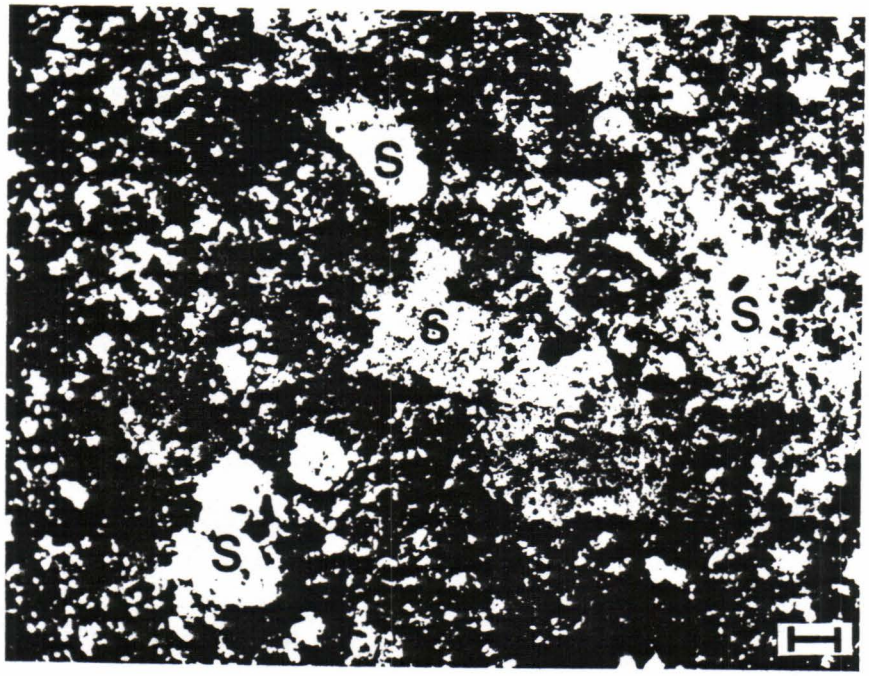
S
S
S
S


S
S
S
S
S
S
P
S
S
S
S
S
P
P

especially common in metasomatic varieties where, with the exception of being unzoned, they are similar in appearance to the oligoclase and andesine phenocrysts found within older latite and trachyte porphyries. They range up to 10 mm in size and generally display both Carlsbad and albite twinning. Crystals are euhedral to subhedral in shape and often possess well-developed mantles of sanidine (Fig. 27).

Amphibole and pyroxene phenocrysts are always altered, even in the freshest samples of alkali trachyte. Aegirine is an exception and may occur in trace amounts associated with strontian calcite in subsurface specimens. Pseudomorphs of brown biotite and titanian magnetite after original amphibole and/or pyroxene are common in some samples while in others the alteration products consist of a microcrystalline mixture of either biotite and calcite or iron oxides and calcite.

Sphene originally occurred as an accessory mineral in the rocks but now appears altered with the rims of the original diamond-shaped crystals composed of leucoxene and the cores replaced by calcite, quartz, or sanidine. Apatite also occurs in accessory amounts but is rarely altered. It displays euhedral to subhedral forms with both hexagonal and prismatic cross-sections.

Other accessory minerals include strontianite, fluorite, barite, zircon, manganian ilmenite, brookite, pyrite, pyrrhotite, and chalcopyrite. These minerals are common in other varieties of fenite occurring in the Bear Lodge Mountains and appear to be intimately associated with the fenitization process. The sulfide minerals (pyrite, pyrrhotite, and chalcopyrite) are usually restricted to less altered subsurface samples where they often poikilitically enclose earlier formed minerals. In altered specimens they generally appear oxidized

with cube-shaped pseudomorphs of iron oxides after pyrite especially common.

Chemistry

Major element chemical analyses of six samples of alkali trachyte are presented in Table 12. Comparison with analyses of the latite and trachyte porphyries emplaced during the episode of early igneous activity (Table 3) illustrates the more potassic character of alkali trachyte relative to these earlier formed igneous rocks. Increases in K_2O are generally accompanied by corresponding decreases in Na_2O, suggesting a net loss of sodium during the fenitization process. The values of K_2O and the other major oxides are similar to the values for rheomorphic potash trachytes from the Toror Hills complex of eastern Uganda (Sutherland, 1965, p. 371).

Alkali Trachyte Porphyry

General

Alkali trachyte porphyry represents the metasomatic analogue of the phonolite and trachyte porphyries emplaced during the initial episode of igneous activity. It is virtually identical to these older alkalic igneous rocks in hand sample and its ultrapotassic composition often serves as the only criterion for distinguishing this fenite from its igneous precursors.

Alkali trachyte porphyry is exposed at the surface along the southeastern flank of the Bear Lodge Mountains and forms one of the major rock types in the shallow subsurface near the center of the main igneous dome. It also corresponds to many of the samples of sanidine

TABLE 12

MAJOR ELEMENT CHEMICAL ANALYSES OF ALKALI TRACHYTE

SAMPLE	A	B	C	D	E	F
SiO_2	53.45	65.22	58.64	54.95	54.18	54.11
Al_2O_3	15.51	14.88	15.53	13.71	14.76	16.30
Fe_2O_3*	6.42	1.41	6.86	3.86	2.54	4.83
MgO	1.03	0.05	0.15	1.92	1.59	2.68
CaO	9.90	0.08	0.11	1.20	4.93	3.36
Na_2O	2.06	1.95	1.59	1.60	3.89	0.79
K_2O	6.09	10.32	11.21	11.00	6.60	11.23
TiO_2	1.41	0.94	0.66	0.94	0.66	1.09
P_2O_5	0.48	0.06	0.20	0.79	0.03	0.40
MnO	0.10	0.03	0.01	0.81	0.18	0.28
Total	96.45	94.94	94.96	90.78	89.36	95.07

* Total Fe as Fe_2O_3

Sample key: A=Sample 10-393
B=Sample 21-368
C=Sample 27-6B
D=Sample WBD-8/348.2
E=Sample WBD-12/906.8
F=Sample BL-4/1146.0

trachyte porphyry described by Wilkinson (1982) in the Warren Peaks area and to several of the samples of "older" trachyte and phonolite porphyries reported within the main igneous dome by Staatz (1983).

Petrography

Alkali trachyte porphyry is holocrystalline and distinctly porphyritic with large tabular phenocrysts of sanidine characteristic (Fig. 28). Fresh samples have only been observed in the subsurface where they range from light gray to medium gray in color Altered samples occur both at the surface and in the shallow subsurface and are hematite stained with colors varying from reddish brown to yellowish brown. Sanidine phenocryts are generally unstained and appear ivory white in color. Modal analyses of six samples of the rock are presented in Table 13 and microprobe analyses of some of the more common minerals are presented in Table 14.

The groundmasses of alkali trachyte porphyries are aphanitic to very fine-grained and compose between 40 and 70 percent of the rocks. Sanidine is the dominant constituent and occurs as Carlsbad twinned microlites that vary from subtrachytic to strongly trachytic in texture. Cryptocrystalline albite and anorthoclase occur interstitial to the microlites in several specimens.

The distinctive sanidine phenocrysts range up to 40 mm in length and frequently exhibit well-developed trachytoid textures. The phenocrysts are generally Carlsbad twinned and compose between 5 and 30 percent of the rock. Microprobe analyses are potassium-rich and similar to the compositions of the groundmass sanidine microlites (Table 14, columns G and H).

Hexagonal phenocryts of an altered feldspathoid mineral are present

Figure 28. Slab photograph of alkali trachyte porphyry (sample 27-172A). Phenocrysts of tabular sanidine and an altered, rounded to hexagonal feldspathoid mineral enclosed within aphanitic, iron oxide-stained groundmass.

Figure 29. Photomicrograph of alkali trachyte porphyry (sample 27-172A). Phenocrysts of sanidine (S) and an altered feldspathoid mineral (F) enclosed within a trachytic, microcrystalline groundmass rich in sanidine. Bar scale represents 0.25 mm. Crossed polars.

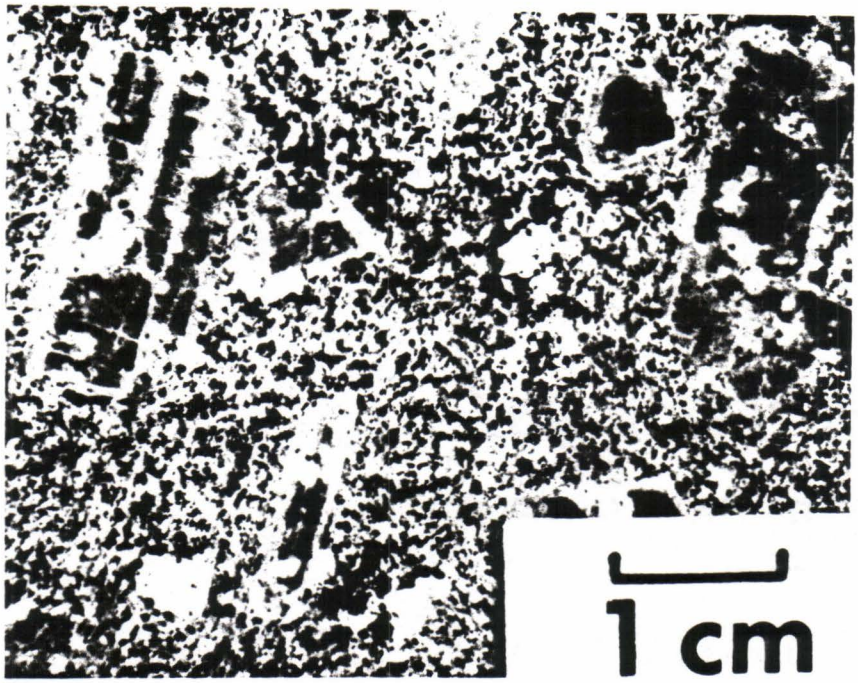
1 cm

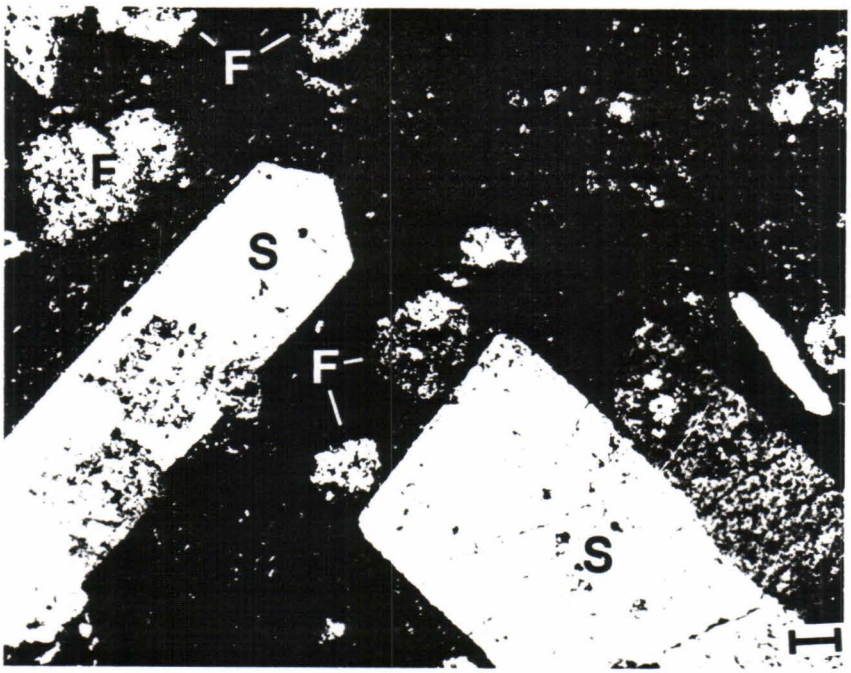
F
F
S
F
S

TABLE 13

MODAL ANALYSES OF ALKALI TRACHYTE PORPHYRY

SAMPLE	A	B	C	D	E	F
Primary						
Groundmass						
Sanidine	55.5	65.6	57.4	55.3	44.0	41.4
Albite	1.2	0.0	0.0	0.0	1.1	1.9
Anorthoclase	0.0	0.0	0.0	0.0	3.2	0.0
Calcite	0.0	0.0	0.0	0.6	2.6	4.3
Quartz	1.7	0.0	1.2	1.7	2.1	0.0
Sanidine	23.2	25.0	10.0	9.0	4.4	12.4
Biotite	0.0	0.0	0.0	0.0	tr.	4.6
Apatite	tr.	tr.	tr.	tr.	0.2	tr.
Strontian calcite	0.0	0.0	0.0	0.0	1.8	13.4
Strontianite	0.0	0.0	0.0	pr.	0.0	0.0
Barite	pr.	0.0	0.0	0.0	0.0	0.0
Fluorite	0.0	0.6	tr.	0.0	0.0	0.0
Quartz/chalcedony	1.0	0.0	tr.	0.0	2.2	0.0
Titanian magnetite	0.0	0.6	0.0	0.0	tr.	0.0
Brookite	0.0	0.0	0.0	0.0	pr.	0.6
Pyrite	1.4	0.0	0.0	0.0	0.0	2.8
Chalcopyrite	0.0	0.0	0.0	0.0	0.0	pr.
Secondary						
Sericite/clays	1.4	0.4	23.6	3.6	3.6	2.8
Iron/titanium oxides	14.6	7.8	7.8	10.4	19.0	2.2
Muscovite	0.0	0.0	0.0	19.4	15.8	13.6

tr.=trace, less than 0.2% detected
pr.=present, determined qualitatively by microprobe analysis

Sample key: A=Sample 16-439C=Alkali trachyte porphyry
B=Sample 21-22B=Alkali trachyte porphyry
C=Sample 27-17=Alkali trachyte porphyry
D=Sample 27-172A=Alkali trachyte porphyry
E=Sample 34-230=Alkali trachyte porphyry
F=Sample WBD-12/804.0=Alkali trachyte porphyry

TABLE 14

MICROPROBE ANALYSES OF MINERALS IN ALKALI TRACHYTE PORPHYRY

SAMPLE	A	B	C	D	E	F	G	H
SiO2	65.66	65.41	66.18	70.59	70.66	65.94	65.59	65.34
Al2O3	18.72	18.98	19.13	20.53	20.96	19.05	18.73	19.02
FeO*	0.28	0.17	0.34	0.00	0.00	0.15	0.00	0.00
MgO	0.00	0.00	0.00	0.00	0.00	0.00	0.00	0.00
CaO	0.00	0.00	0.00	0.16	0.00	0.00	0.00	0.00
Na2O	0.00	0.49	0.00	11.89	12.30	0.30	0.00	0.49
K2O	16.22	15.63	15.95	0.41	0.45	15.35	15.94	15.53
TiO2	0.00	0.00	0.00	0.00	0.00	0.26	0.00	0.20
P2O5	0.00	0.00	0.00	0.28	0.00	0.00	0.00	0.00
MnO	0.00	0.00	0.00	0.00	0.15	0.12	0.00	0.00
Cl	0.06	0.15	0.09	0.00	0.05	0.11	0.05	0.00
SO3	0.00	0.00	0.00	0.11	0.00	0.00	0.16	0.00
Total	100.94	100.83	101.69	103.97	104.57	101.28	100.47	100.58
	Number of cations on the basis of X oxygens							
	X=32	X=32	X=32	X=32	X=32	X=32	X=32	X=32
Si	12.01	11.96	11.99	11.87	11.86	11.97	12.01	11.95
Al	4.03	4.09	4.08	4.07	4.14	4.08	4.04	4.10
Fe	0.04	0.03	0.05	0.00	0.00	0.02	0.00	0.00
Mg	0.00	0.00	0.00	0.00	0.00	0.00	0.00	0.00
Ca	0.00	0.00	0.00	0.03	0.00	0.00	0.00	0.00
Na	0.00	0.17	0.00	3.87	4.00	0.11	0.00	0.17
K	3.78	3.65	3.69	0.09	0.10	3.55	3.72	3.62
Ti	0.00	0.00	0.00	0.00	0.00	0.03	0.00	0.03
P	0.00	0.00	0.00	0.04	0.00	0.00	0.00	0.00
Mn	0.00	0.00	0.00	0.00	0.02	0.02	0.00	0.00
Cl	0.02	0.05	0.03	0.00	0.01	0.03	0.01	0.00
S	0.00	0.00	0.00	0.01	0.00	0.00	0.02	0.00

* Total Fe as FeO

Sample key: A=Sample 21-22B=Sanidine (groundmass); B=Sample 27-172A=Sanidine (groundmass); C=Sample WBD-12/804.0=Sanidine (groundmass); D=Sample 34-230=Albite (groundmass); E=Sample 34-230=Albite (groundmass); F=Sample 16-439C=Sanidine (phenocryst); G=Sample 21-22B=Sanidine (phenocryst); H=Sample 27-172A=Sanidine (phenocryst).

TABLE 14

(continued)

SAMPLE	I	J	K	L	M	N	O	P
SiO2	44.04	45.26	35.96	36.21	0.37	0.85	0.40	0.29
Al2O3	40.89	35.55	22.37	22.88	0.00	0.00	0.00	0.00
FeO*	0.85	2.90	17.08	17.42	0.00	0.00	0.60	0.00
MgO	0.00	0.74	9.36	9.65	0.00	0.00	0.00	0.00
CaO	0.00	0.00	0.00	0.00	53.19	54.55	0.00	0.00
Na2O	0.61	0.00	0.00	0.00	0.28	0.37	0.00	0.00
K2O	9.80	11.09	9.81	9.71	0.16	0.13	0.14	0.00
TiO2	0.00	0.46	2.01	1.97	0.00	0.00	98.76	98.24
P2O5	0.00	0.00	0.00	0.00	38.39	39.20	0.00	0.00
MnO	0.00	0.00	1.60	1.58	0.00	0.00	0.00	0.00
Cl	0.08	0.04	0.00	0.00	0.08	0.00	0.00	0.00
SO3	0.00	0.00	0.00	0.26	0.00	0.52	0.00	0.00
Total	96.27	96.04	98.19	99.68	92.47	95.62	99.90	98.53
	Number of cations on the basis of X oxygens							
	X=24	X=24	X=24	X=24	X=26	X=26	X=16	X=16
Si	6.29	6.60	5.74	5.68	0.07	0.15	0.04	0.03
Al	6.89	6.11	4.21	4.23	0.00	0.00	0.00	0.00
Fe	0.10	0.35	2.28	2.29	0.00	0.00	0.05	0.00
Mg	0.00	0.16	2.23	2.26	0.00	0.00	0.00	0.00
Ca	0.00	0.00	0.00	0.00	10.63	10.50	0.00	0.00
Na	0.17	0.00	0.00	0.00	0.10	0.13	0.00	0.00
K	1.79	2.06	2.00	1.94	0.04	0.03	0.02	0.00
Ti	0.00	0.05	0.24	0.23	0.00	0.00	7.93	7.97
P	0.00	0.00	0.00	0.00	6.06	5.96	0.00	0.00
Mn	0.00	0.00	0.22	0.21	0.00	0.00	0.00	0.00
Cl	0.02	0.01	0.00	0.00	0.03	0.00	0.00	0.00
S	0.00	0.00	0.00	0.03	0.00	0.07	0.00	0.00

* Total Fe as FeO

Sample key: I=Sample 27-172A=Muscovite; J=Sample WBD-12/804.0=Muscovite; K=Sample WBD-12/804.0=Biotite; L=Sample WBD-12/804.0=Biotite; M=Sample 16-439C=Apatite; N=Sample 34-230=Apatite; O=34-230=Brookite; P=Sample 34-230=Brookite.

in the majority of samples (Fig. 29). They range from 0.5 to 3.0 mm in diameter and compose as much as 30 percent of the rock. Alteration material consists either of a microcrystalline mixture of clays and calcite or, more commonly, fine-grained flakes of muscovite.

Mafic phenocrysts are completely altered, even in the freshest samples of alkali trachyte porphyry. Relict prismatic outlines suggest that most were originally pyroxene, probably salite or ferrosalite based upon analogy with the clinopyroxenes observed in phonolite and trachyte porphyries. In fresher samples the replacement material usually consists of a fine-grained intergrowth of biotite and strontian calcite while in more oxidized specimens the rims of the original crystals consist of iron oxides and the cores are completely dissolved to form small vugs. Many of the vugs have been refilled by secondary potassium feldspar, quartz, and/or cristobalite.

Sphene originally occurred in accessory amounts in the rock but now appears completely altered with the rims of the diamond and wedge-shaped crystals composed of leucoxene and the cores consisting of potassium feldspar. In contrast, apatite crystals are always unaltered and exhibit subhedrals forms with prismatic and hexagonal cross-sections up to 1 mm in diameter. Pyrite occurs in less altered samples in the deeper subsurface but is pseudomorphed by iron oxides in more altered surface and subsurface rocks. Other minerals which are commonly found in accessory amounts are strontianite, barite, brookite, fluorite, titanian magnetite, and chalcopyrite.

Chemistry

Major element chemical analyses of six samples of alkali trachyte porphyry are presented in Table 15. The rock is invariably

TABLE 15

MAJOR ELEMENT CHEMICAL ANALYSES OF ALKALI TRACHYTE PORPHYRY

SAMPLE	A	B	C	D	E	F
SiO_2	55.81	56.12	57.16	55.49	58.62	50.90
Al_2O_3	14.54	15.61	22.79	23.47	21.71	18.46
Fe_2O_3*	5.04	3.10	2.91	2.47	4.01	3.00
MgO	0.07	0.05	0.30	0.26	0.61	0.69
CaO	0.36	1.63	0.20	0.11	1.13	6.86
Na_2O	0.46	0.40	0.23	0.37	1.47	0.92
K_2O	12.14	13.65	12.96	13.11	9.13	11.35
TiO_2	0.93	0.47	0.44	0.23	0.70	0.62
P_2O_5	0.24	0.15	0.11	0.03	0.11	0.34
MnO	0.25	0.59	0.20	0.11	0.05	0.22
Total	89.84	91.77	97.30	95.65	97.54	93.36

* Total Fe as Fe_2O_3

Sample key: A=Sample 16-439C
B=Sample 21-22B
C=Sample 27-17
D=Sample 27-172A
E=Sample 34-230
F=Sample WBD-12/804.0

ultrapotassic with values of K_2O commonly in excess of 10 percent. Compared with the analyses of its prefenitization counterparts, phonolite and trachyte porphyries (Table 6), it is less sodic and more potassic. The inverse relationship displayed between values of K_2O and Na_2O suggests a net loss of sodium during the fenitization process.

Alkali Melasyenite

General

A third rock type associated with potassic fenitization in the Bear Lodge Mountains is alkali melasyenite (Table 16). The rock only occurs in the subsurface of the main igneous dome where it represents the metasomatic counterpart of the natrolite-garnet syenites and malignites emplaced during the initial episode of igneous activity. Alkali melasyenite is distinguished from these older igneous rocks by the presence of secondary sanidine crystals and by its more potassic chemical composition.

Petrography

Alkali melasyenite is holocrystalline, calcareous and melanocratic (Fig. 30). Fresh samples appear mottled gray and greenish black in color while altered samples occur in shades of reddish brown, orangish brown, and yellowish brown. Microprobe analyses of the major minerals of the rock are presented in Table 17.

Like its igneous precursors, natrolite-garnet syenites and malignites, alkali melasyenite contains distinct rounded to hexagonal "pseudoleucite-like" patches that range from 1 to 10 mm in diameter. The patches comprise between 5 and 20 percent of the rock and are

TABLE 16

MODAL ANALYSES OF ALKALI MELASYENITE

SAMPLE	A	B	C	D	E
Primary					
Sanidine	48.8	43.0	51.2	40.4	44.4
Aegirine	0.0	0.0	4.2	8.2	0.0
Biotite	16.4	16.8	12.4	7.2	11.2
Melanite	3.4	2.8	1.6	5.8	10.0
Apatite	0.2	0.6	0.2	tr.	0.6
Sphene	0.4	0.8	tr.	tr.	1.0
Strontian calcite	10.4	13.0	9.4	5.2	5.6
Strontianite	pr.	pr.	pr.	0.0	0.0
Ancylite	pr.	0.0	pr.	0.0	0.0
Magnetite	1.4	0.8	2.2	1.4	5.0
Manganian ilmenite	2.2	1.4	2.0	3.8	2.0
Pyrite	1.6	0.6	1.8	0.2	1.0
Pyrrhotite	0.0	0.0	0.8	0.0	tr.
Chalcopyrite	0.0	0.0	tr.	1.2	0.0
Secondary					
Sericite/clays	12.0	17.8	12.2	23.2	18.0
Analcime	0.6	0.0	0.0	0.4	0.0
Iron/titanium oxides	2.6	2.4	2.0	3.0	1.2

tr.=trace, less than 0.2% detected
pr.=present, determined qualitatively by microprobe analysis

Sample key: A=Sample WBD-5/609.5=Alkali melasyenite
B=Sample WBD-5/1545.0=Alkali melasyenite
C=Sample WBD-8/1631.0=Alkali melasyenite
D=Sample WBD-13/848.3=Alkali melasyenite
E=Sample WBD-13/1651.9=Alkali melasyenite

Figure 30. Slab photograph of alkali melasyenite (sample WBD-13/859.9). Sanidine (light colored areas) enclosed within a darker, fine-grained matrix rich in biotite, melanite garnet, and aegirine.

Figure 31. Photomicrograph of alkali melasyenite (sample WBD-5/1664.4). Large poikilitic crystal of sanidine (S) enclosing patches of microcrystalline sanidine (SP), biotite (B), sphene (Sp), and magnetite (M). Bar scale represents 0.25 mm. Crossed polars.


1 cm

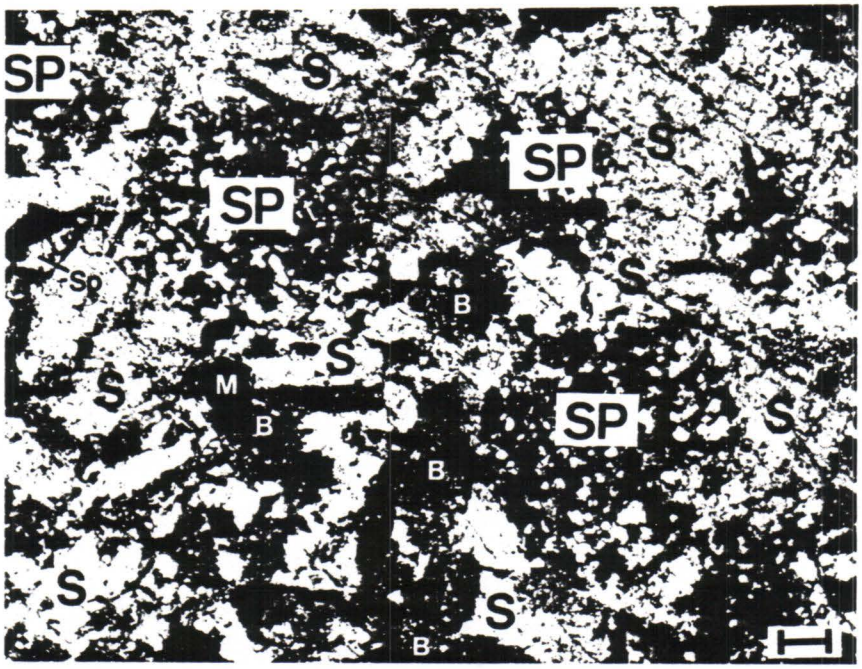
SP
S
SP
S
SP
S
S
B
S
M
B
S
SP
S
B
S
S
B

TABLE 17

MICROPROBE ANALYSES OF MINERALS IN ALKALI MELASYENITE

SAMPLE	A	B	C	D	E	F	G	H
SiO2	64.35	65.62	65.55	65.53	56.17	54.18	53.35	52.71
Al2O3	19.40	20.04	18.72	19.23	23.86	25.50	0.98	0.73
FeO*	0.38	0.00	0.36	0.26	0.00	0.22	19.17	29.23
MgO	0.00	0.00	0.00	0.00	0.00	0.00	5.65	0.00
CaO	0.00	0.00	0.00	0.00	0.00	0.78	12.67	4.14
Na2O	0.68	1.35	0.53	1.20	14.12	12.51	7.30	12.08
K2O	14.53	14.08	15.08	14.04	0.00	0.08	0.17	0.00
TiO2	0.20	0.00	0.17	0.45	0.00	0.00	0.19	0.24
P2O5	0.00	0.00	0.00	0.00	0.26	0.00	0.00	0.00
MnO	0.00	0.00	0.00	0.00	0.00	0.00	0.88	0.63
Cl	0.09	0.08	0.05	0.00	0.00	0.00	0.00	0.04
SO3	0.00	0.00	0.00	0.00	0.00	0.00	0.29	0.00
Total	99.63	100.17	100.46	100.71	94.41	93.27	100.65	99.80
	Number of cations on the basis of X oxygens							
	X=32	X=32	X=32	X=32	X=7	X=7	X=6	X=6
Si	11.87	11.99	11.99	11.91	2.33	2.27	2.06	2.13
Al	4.21	4.10	4.04	4.12	1.17	1.26	0.04	0.03
Fe	0.06	0.00	0.05	0.04	0.00	0.01	0.62	0.99
Mg	0.00	0.00	0.00	0.00	0.00	0.00	0.33	0.00
Ca	0.00	0.00	0.00	0.00	0.00	0.03	0.52	0.18
Na	0.24	0.48	0.19	0.42	1.13	1.02	0.55	0.95
K	3.42	3.28	3.52	3.25	0.00	0.00	0.01	0.00
Ti	0.03	0.00	0.02	0.06	0.00	0.00	0.01	0.01
P	0.00	0.00	0.00	0.00	0.01	0.00	0.00	0.00
Mn	0.00	0.00	0.00	0.00	0.00	0.00	0.03	0.02
Cl	0.03	0.02	0.01	0.00	0.00	0.00	0.00	0.00
S	0.00	0.00	0.00	0.00	0.00	0.00	0.01	0.00

* Total Fe as FeO

Sample key: A=Sample WBD-5/1545.0=Sanidine; B=Sample WBD-8/1631.0= Sanidine; C=Sample WBD-13/848.3=Sanidine; D=Sample WBD-13/1651.9= Sanidine; E=Sample WBD-5/609.5=Analcime; F=Sample WBD-13/848.3= Analcime; G=Sample WBD-8/1631.0=Aegirine-augite; H=Sample WBD-13/ 848.3=Aegirine-augite.

TABLE 17

(continued)

SAMPLE	I	J	K	L	M	N	O	P
SiO2	35.67	35.06	39.32	37.42	0.00	30.49	0.29	0.11
Al2O3	1.19	1.25	11.04	10.60	0.00	1.01	0.14	0.00
FeO*	25.09	26.83	19.88	25.44	0.18	2.07	92.93	43.32
MgO	0.33	0.33	14.45	9.68	0.11	0.00	0.30	0.26
CaO	33.12	32.41	0.00	0.00	54.19	28.58	0.45	0.00
Na2O	0.00	0.31	0.27	1.07	0.26	0.00	0.58	0.00
K2O	0.00	0.00	9.81	9.31	0.07	0.00	0.11	0.25
TiO2	3.86	2.73	1.29	1.86	0.00	36.89	0.76	51.17
P2O5	0.00	0.23	0.00	0.00	40.40	0.00	0.24	0.00
MnO	0.73	0.99	0.54	0.93	0.00	0.00	0.55	5.23
Cl	0.00	0.00	0.00	0.00	0.00	0.00	0.00	0.00
SO3	0.00	0.00	0.00	0.00	0.00	0.00	0.00	0.00
Total	99.99	100.14	96.60	96.31	95.21	99.04	96.35	100.34
	Number of cations on the basis of X oxygens							
	X=24	X=24	X=24	X=24	X=26	X=20	X=32	X=6
Si	6.25	6.20	6.50	6.42	0.00	4.05	0.11	0.01
Al	0.25	0.26	2.15	2.14	0.00	0.16	0.07	0.00
Fe	3.68	3.97	2.75	3.65	0.03	0.23	30.24	1.83
Mg	0.09	0.09	3.56	2.48	0.03	0.00	0.17	0.02
Ca	6.22	6.14	0.00	0.00	10.47	4.07	0.19	0.00
Na	0.00	0.11	0.09	0.35	0.09	0.00	0.44	0.00
K	0.00	0.00	2.07	2.04	0.02	0.00	0.05	0.02
Ti	0.51	0.36	0.16	0.24	0.00	3.68	2.22	1.95
P	0.00	0.03	0.00	0.00	6.17	0.00	0.08	0.00
Mn	0.11	0.15	0.07	0.13	0.00	0.00	0.18	0.22
Cl	0.00	0.00	0.00	0.00	0.00	0.00	0.00	0.00
S	0.00	0.00	0.00	0.00	0.00	0.00	0.00	0.00

* Total Fe as FeO

Sample key: I=Sample WBD-5/1545.0=Melanite; J=Sample WBD-8/1631.0= Melanite; K=Sample WBD-13/848.3=Biotite; L=Sample WBD-13/1651.9= Biotite; M=Sample WBD-5/1545.0=Apatite; N=Sample WBD-5/1545.0= Sphene; O=Sample WBD-13/1651.9=Magnetite; P=Sample WBD-5/609.5= Manganian ilmenite.

enclosed within a black to dark greenish gray matrix composed of fine-grained biotite, melanite garnet, aegirine, and aegirine-augite.

The secondary sanidine crystals of alkali melasyenite are best observed on broken surfaces or in thin section where they occur either as large vitreous plates that range up to 40 mm in size or as smaller needles that vary from 1 to 10 mm in length. They poikilitically enclose other constituents of the rock, including the pseudoleucite-like patches (Fig. 31). The sanidine needles are Carlsbad twinned and vary from randomly oriented to strongly trachytic in texture while the larger plates are untwinned and usually randomly oriented. Both the needles and the plates are partially replaced by small patches of strontian calcite.

Natrolite is lacking in the rock although irregular-shaped patches of microcrystalline clays and strontian calcite may represent alteration products of this zeolite. The patches have a turbid appearance in plane-polarized light that is similar to the partially altered natrolite observed in natrolite-garnet syenites and malignites. Cryptocrystalline analcime is present in several of the patches.

Melanite garnet forms less than 10 percent of the rock and is similar in habit and composition to the garnets occurring in its igneous predecessors. Crystals range from reddish brown to honey-yellow in color and display rounded to hexagonal cross-sections up to 1 mm in diameter. Intergrown biotite and garnet, analogous to the biotite-garnet aggregates observed in natrolite-garnet syenites and malignites, are also present and display similar prismatic outlines that suggest they are pseudomorphs after original pyroxene.

Unzoned aegirine and aegirine-augite occur in several specimens

where they are found either as equant, subhedral crystals up to 2 mm in diameter or as irregular-shaped aggregates composed of anhedral crystals less than 0.2 mm in size. They exhibit varying degrees of alteration to clay minerals and commonly have a turbid or semi-opaque appearance in thin section. Fresher varieties are moderately pleochroic with X=bright green, Y=yellowish green, and Z=pale green.

Biotite is usually the most abundant mafic mineral and may compose as much as 20 percent of the rock. It appears to be of secondary origin, forming pseudomorphs after original pyroxene and possibly garnet. Crystals range up to 1 mm in length and are strongly pleochroic with X=orangish brown and Y=Z=brownish green.

Apatite, sphene, magnetite, and manganian ilmenite occur in accessory amounts either as minute inclusions within garnet or as isolated crystals up to 1 mm in size. Other accessory minerals include strontianite, ancylite, pyrite, pyrrhotite, and chalcopyrite.

Chemistry

Major element chemical analyses of five samples of alkali melasyenite are presented in Table 18. The samples are similar to other metasomatic rock types and show a significant increase in K_2O and marked decrease in Na_2O relative to their igneous counterparts (Table 9). The extreme silica undersaturation of the rock largely reflects an abundance of strontian calcite which ranges up to 13 percent in modal abundance (Table 16). Variations in CaO and MgO and the poor closures of the analyses can also be related to the presence of this carbonate mineral.

TABLE 18

MAJOR ELEMENT CHEMICAL ANALYSES OF ALKALI MELASYENITE

SAMPLE	A	B	C	D	E
SiO_2	42.13	45.97	50.60	45.26	49.16
Al_2O_3	14.14	15.99	14.64	15.10	16.63
Fe_2O_3*	7.55	8.71	4.98	7.03	8.64
MgO	2.06	1.59	1.02	1.33	1.78
CaO	12.04	9.70	6.97	8.97	8.22
Na_2O	0.67	0.46	1.76	1.95	0.56
K_2O	9.12	9.66	10.10	8.13	8.66
TiO_2	1.33	1.83	0.61	1.42	2.10
P_2O_5	0.30	0.29	0.25	0.26	0.25
MnO	0.37	0.26	0.27	0.24	0.32
Total	89.71	94.46	91.20	89.69	96.32

* Total Fe as Fe_2O_3

Sample key: A=Sample WBD-5/609.5
B=Sample WBD-5/1545.0
C=Sample WBD-8/1631.0
D=Sample WBD-13/848.3
E=Sample WBD-13/1651.9

Alkali Leucosyenite

General

Alkali leucosyenite represents a fourth rock type related to the episode of potassic fenitization in the Bear Lodge Mountains. Three textural variations are distinguished: sanidinite, syenite pegmatite, and pulaskite. All three occur in the subsurface of the main igneous dome but have not been reported at the surface in this region by either Wilkinson (1982) or Staatz (1983) nor are they exposed at the surface in the area of study along the southeastern flank of the uplift.

Alkali leucosyenites include both metasomatic and rheomorphic varieties. Sanidinite and syenite pegmatite are generally metasomatic units and essentially represent more fenitized versions of alkali melasyenite. Sanidinite is characterized by an increase in the proportion of the needle-like crystals of secondary sanidine relative to alkali melasyenite while syenite pegmatite exhibits a greater abundance of the large poikilitic sanidine plates. Syenite pegmatite also forms rheomorphic units that occur as veins and dikes that crosscut older varieties of fenite. Pulaskite is exclusively a rheomorphic rock type and also forms dikes and veins that crosscut older fenites.

Petrography

Alkali leucosyenites are holocrystalline rocks rich in sanidine. Colors range from light gray to medium gray to dark greenish gray for fresh samples and from buff to reddish brown to orangish brown for altered samples. They are moderately calcareous and generally effervesce when exposed to dilute HCl. Modal analyses of ten samples of the rocks are presented in Table 19 and microprobe analyses of the

TABLE 19

MODAL ANALYSES OF ALKALI LEUCOSYENITE

SAMPLE	A	B	C	D	E
Primary					
Sanidine	54.4	67.8	86.2	64.4	76.0
Aegirine	0.0	0.0	0.0	0.0	0.2
Biotite	11.0	2.2	3.0	12.2	0.6
Melanite	3.2	0.0	0.0	0.0	0.0
Apatite	0.6	0.4	0.6	0.6	2.0
Sphene	tr.	0.0	0.0	0.0	tr.
Zircon	0.0	0.0	tr.	0.0	0.0
Strontian calcite	9.2	18.2	1.8	8.6	9.4
Siderite	0.0	0.6	2.0	0.4	1.4
Strontianite	2.2	1.8	0.0	0.0	0.6
Ancylite	0.0	0.0	0.0	0.0	0.4
Fluorite	0.0	0.0	0.0	0.0	0.0
Magnetite	3.6	0.6	0.4	0.8	0.6
Manganian ilmenite	0.8	0.8	1.4	0.8	1.0
Pyrite	0.8	3.0	3.6	6.4	5.4
Pyrrhotite	0.0	tr.	0.0	0.0	tr.
Chalcopyrite	0.0	0.6	0.2	tr.	tr.
Sphalerite	0.0	0.0	tr.	0.0	0.0
Galena	0.0	0.0	tr.	0.0	0.0
Secondary					
Sericite/clays	13.8	3.2	0.8	5.2	1.6
Iron/titaniun oxides	0.4	0.8	tr.	0.6	0.8

tr.=trace, less than 0.2% detected

Sample key: A=Sample WBD-5/623.8=Sanidinite
B=Sample WBD-5/1130.5=Sanidinite
C=Sample WBD-5/1527.6=Sanidinite
D=Sample WBD-10/1408.8=Sanidinite
E=Sample WBD-5/1076.0=Syenite pegmatite

TABLE 19

(continued)

SAMPLE	F	G	H	I	J
Primary					
Sanidine	77.4	74.2	78.6	58.6	60.6
Aegirine	0.0	5.8	tr.	12.0	0.8
Biotite	1.2	0.4	1.4	0.0	0.0
Melanite	0.0	0.0	0.0	0.0	0.0
Apatite	0.2	0.6	0.0	0.0	0.0
Sphene	tr.	0.8	0.0	0.0	0.0
Zircon	0.0	tr.	0.0	0.0	0.0
Strontian calcite	9.6	4.0	9.6	25.2	26.8
Siderite	1.2	0.4	1.2	0.2	0.0
Strontianite	1.4	0.4	1.0	0.6	tr.
Ancylite	0.4	tr.	0.4	0.0	0.2
Fluorite	0.0	0.0	0.0	0.0	2.2
Magnetite	0.8	0.4	0.2	0.0	0.0
Manganian ilmenite	3.0	0.0	0.8	0.0	0.0
Pyrite	3.4	0.4	3.8	1.4	4.0
Pyrrhotite	0.0	0.8	0.0	0.0	0.0
Chalcopyrite	0.0	0.8	tr.	tr.	tr.
Sphalerite	0.0	0.0	0.4	tr.	0.0
Galena	0.0	0.0	1.0	0.4	0.0
Secondary					
Sericite/clays	0.8	8.0	1.2	1.0	5.4
Iron/titanian oxides	0.6	3.0	0.4	0.6	0.0

tr.=trace, less than 0.2% detected

Sample key: F=Sample WBD-5/1473.8=Syenite pegmatite
G=Sample WBD-13/830.5=Syenite pegmatite
H=Sample WBD-5/1467.5=Pulaskite
I=Sample WBD-7/1274.7=Pulaskite
J=Sample WBD-9/647.1=Pulaskite

common minerals are presented in Table 20.

The sanidinite variety of alkali leucosyenite is characterized by acicular crystals of Carlsbad twinned sanidine (Fig. 32). The sanidine needles compose as much as 90 percent of the rock and range from 1 to 10 mm in length. They surround and enclose other constituents of the rock with textures that vary from randomly oriented to strongly trachytic (Fig. 33). Many of the laths are partially replaced by irregular-shaped patches of strontian calcite.

Syenite pegmatite, the second variety of alkali leucosyenite, is characterized by coarse-grained to pegmatitic crystals of sanidine (Fig. 34). These large euhedra compose between 60 and 90 percent of the rock and often poikilitically enclose other constituent minerals (Fig. 35). The majority of crystals are untwinned and many are partially replaced by small patches of strontian calcite.

Other minerals common in both sanidinite and syenite pegmatite are melanite garnet, aegirine, aegirine-augite, and biotite. Melanite garnet occurs as rounded crystals up to 2 mm in diameter and as smaller anhedral crystals intergrown with biotite in a manner analogous to the biotite-garnet aggregates observed in alkali melasyenite and natrolite-garnet syenites and malignites. Colors of the garnet range from reddish brown to honey-yellow. Many of the crystals contain inclusions of sphene, apatite, magnetite, and manganian ilmenite and they are often partially to completely replaced by a microcrystalline mixture of iron and titanium oxides.

Aegirine and aegirine-augite are moderately pleochroic with X=bright green, Y=yellowish green, and Z=pale green. They occur either as equant, subhedral crystals up to 2 mm in diameter or as as smaller

TABLE 20

MICROPROBE ANALYSES OF MINERALS IN ALKALI LEUCOSYENITE

SAMPLE	A	B	C	D	E	F	G	H
SiO2	64.31	65.52	65.61	65.53	65.63	65.44	53.45	52.82
Al2O3	19.65	18.79	18.91	18.52	18.03	18.64	0.00	0.00
FeO*	0.31	0.00	0.36	0.31	0.73	0.00	20.79	25.43
MgO	0.00	0.00	0.00	0.00	0.00	0.00	5.36	2.14
CaO	0.00	0.00	0.00	0.00	0.00	0.00	7.79	5.09
Na2O	0.76	0.34	0.48	0.44	0.00	0.43	9.67	11.01
K2O	14.47	15.26	15.37	15.36	15.91	15.28	0.00	0.00
TiO2	0.22	0.00	0.00	0.00	0.00	0.00	1.94	0.97
P2O5	0.00	0.00	0.00	0.00	0.16	0.00	0.00	0.00
MnO	0.00	0.17	0.00	0.00	0.00	0.17	0.39	1.01
Cl	0.05	0.00	0.06	0.09	0.12	0.00	0.00	0.00
SO3	0.00	0.24	0.00	0.00	0.00	0.00	0.00	0.00
Total	99.77	100.32	100.79	100.25	100.58	99.96	99.39	98.47
	Number of cations on the basis of X oxygens							
	X=32	X=32	X=32	X=32	X=32	X=32	X=6	X=6
Si	11.83	11.98	11.98	12.03	12.05	12.02	2.09	2.13
Al	4.26	4.05	4.07	4.01	3.90	4.04	0.00	0.00
Fe	0.05	0.00	0.05	0.05	0.11	0.00	0.68	0.86
Mg	0.00	0.00	0.00	0.00	0.00	0.00	0.31	0.13
Ca	0.00	0.00	0.00	0.00	0.00	0.00	0.33	0.22
Na	0.27	0.12	0.17	0.16	0.00	0.15	0.73	0.86
K	3.40	3.56	3.58	3.60	3.73	3.58	0.00	0.00
Ti	0.03	0.00	0.00	0.00	0.00	0.00	0.06	0.03
P	0.00	0.00	0.00	0.00	0.03	0.00	0.00	0.00
Mn	0.00	0.03	0.00	0.00	0.00	0.03	0.01	0.03
Cl	0.01	0.00	0.01	0.03	0.04	0.00	0.00	0.00
S	0.00	0.03	0.00	0.00	0.00	0.00	0.00	0.00

* Total Fe as FeO

Sample key: A=Sample WBD-5/623.8=Sanidine (Sanidinite); B=Sample WBD-5/1527.6=Sanidine (Sanidinite); C=Sample WBD-5/1076.0=Sanidine (Syenite pegmatite); D=Sample WBD-13/830.5=Sanidine (Syenite pegmatite); E=Sample WBD-5/1467.5=Sanidine (Pulaskite); F=Sample WBD-7/1274.7=Sanidine (Pulaskite); G=Sample WBD-13/830.5=Aegirine; H=Sample WBD-7/1274.7=Aegirine.

TABLE 20

(continued)

SAMPLE	I	J	K	L	M	N	O	P
SiO2	35.50	34.65	40.79	37.33	0.18	30.40	0.31	0.00
Al2O3	2.20	1.15	10.80	11.76	0.29	0.35	0.00	0.00
FeO*	24.86	25.92	13.73	23.31	0.23	0.98	91.44	44.08
MgO	0.30	0.44	17.38	11.57	0.19	0.29	0.00	0.00
CaO	33.22	32.67	0.00	0.00	53.46	27.79	0.60	0.00
Na2O	0.22	0.00	0.00	0.57	0.00	0.89	0.38	0.00
K2O	0.00	0.00	9.82	9.32	0.13	0.07	0.06	0.00
TiO2	3.47	4.10	2.20	1.66	0.00	37.99	0.52	51.98
P2O5	0.00	0.00	0.00	0.00	40.60	0.00	0.13	0.00
MnO	0.63	0.51	1.08	1.00	0.00	0.00	0.30	3.87
Cl	0.00	0.00	0.00	0.00	0.00	0.00	0.00	0.05
SO3	0.00	0.00	0.00	0.17	0.00	0.00	0.00	0.00
Total	100.40	99.44	95.80	96.69	95.08	98.76	93.74	99.98
	Number of cations on the basis of X oxygens							
	X=24	X=24	X=24	X=24	X=26	X=20	X=32	X=6
Si	6.19	6.15	6.59	6.29	0.03	4.04	0.13	0.00
Al	0.45	0.24	2.05	2.33	0.06	0.05	0.00	0.00
Fe	3.62	3.85	1.85	3.28	0.03	0.11	30.79	1.87
Mg	0.08	0.11	4.19	2.91	0.05	0.06	0.00	0.00
Ca	6.20	6.21	0.00	0.00	10.30	3.96	0.26	0.00
Na	0.07	0.00	0.00	0.19	0.00	0.23	0.30	0.00
K	0.00	0.00	2.02	2.00	0.03	0.01	0.03	0.00
Ti	0.45	0.55	0.27	0.21	0.00	3.80	0.16	1.98
P	0.00	0.00	0.00	0.00	6.18	0.00	0.05	0.00
Mn	0.09	0.08	0.15	0.14	0.00	0.00	0.10	0.17
Cl	0.00	0.00	0.00	0.00	0.00	0.00	0.00	0.00
S	0.00	0.00	0.00	0.02	0.00	0.00	0.00	0.00

* Total Fe as FeO

Sample key: I=Sample WBD-5/623.8=Melanite; J=Sample WBD-5/623.8= Melanite; K=Sample WBD-5/1527.6=Biotite; L=Sample WBD-5/623.8= Biotite; M=Sample WBD-13/830.5=Apatite; N=Sample WBD-13/830.5= Sphene; O=Sample WBD-5/623.8=Magnetite; P=Sample WBD-5/1527.6= Manganian ilmenite.

Figure 32. Photograph of sanidinite (sample WBD-5/1045.0). Note acicular crystals of sanidine shown by arrows.

Figure 33. Photomicrograph of sanidinite (sample WBD-5/1527.6). Acicular crystals of Carlsbad twinned sanidine (S) exhibiting well-developed trachytic texture. Note pyrite-filled (Py) microfault located in left half of photograph. Bar scale represents 0.25 mm. Crossed polars.

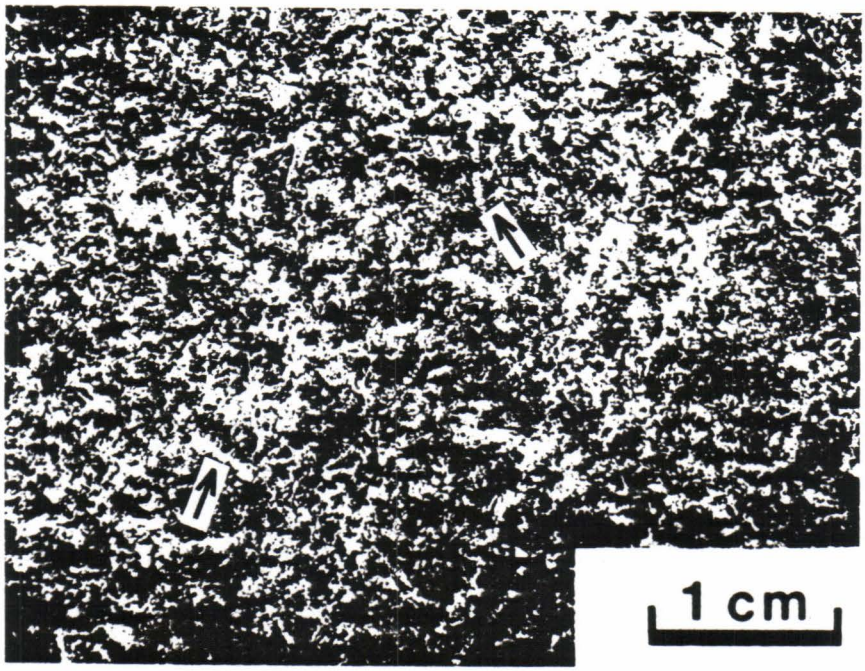
1 cm

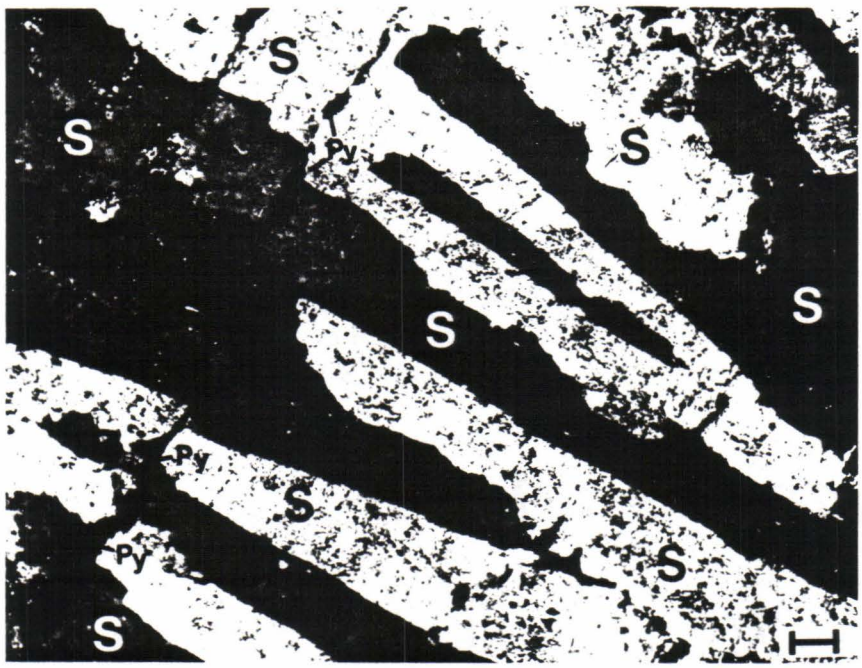
S
S
Py
S
S
S
Py
S
Py
S
S
S
1

Figure 34. Photograph of syenite pegmatite (sample WBD-5/1008.5). Interlocking, coarse-grained to pegmatitic crystals of sanidine.

Figure 35. Photomicrograph of syenite pegmatite (sample WBD-5/830.5). Coarse-grained to pegmatic crystals of sanidine (S) with chalcopyrite (Cp) and partially altered melanite-garnet (aG). Bar scale represents 0.25 mm. Crossed polars.


1 cm

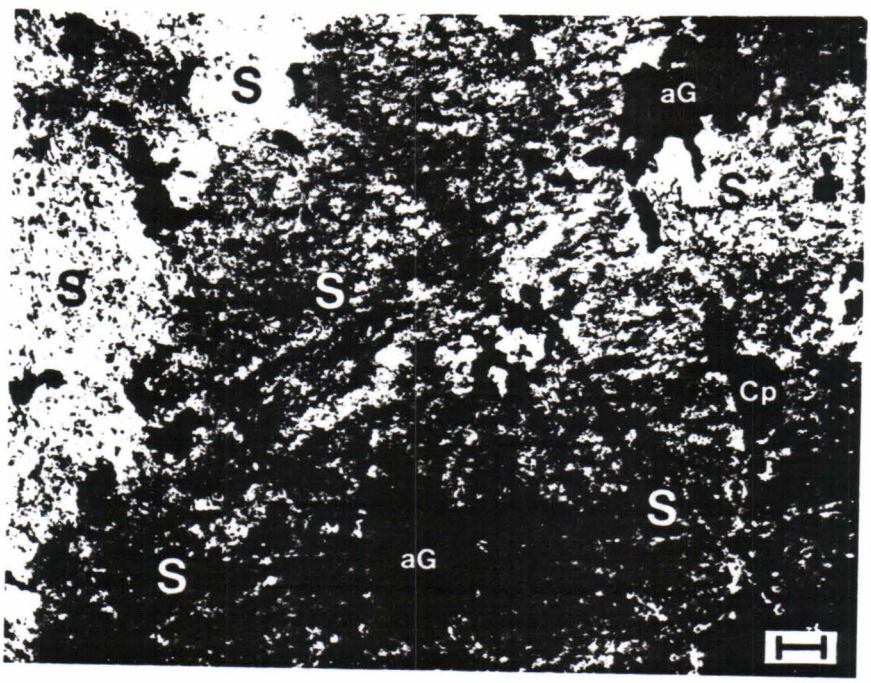
S
aG
S
S
S
Cp
S
aG
S

anhedral crystals that form irregular-shaped microcrystalline aggregates. In most samples the crystals are partially altered to a cryptocrystalline mixture of clays and iron and titanium oxides, resulting in a semi-opaque appearance in plane-polarized light.

Biotite occurs either in pseudomorphs with garnet after pyroxene, or as isolated flakes that range from 0.5 to 2.0 mm in size. Pleochroism is strong with X=orangish brown and Y=Z=greenish brown.

Irregular-shaped patches of cryptocrystalline sericite and strontian calcite occur in both sanidinite and syenite pegmatite. The patches possess a turbid appearance in plane-polarized light that is similar in appearance to the partially altered patches of natrolite occurring in natrolite-garnet syenites and malignites. Presumably the patches represent alteration products of this zeolite.

Pulaskite, the third variety of alkali leucosyenite, is characterized by distinct cube-shaped tablets of untwinned sanidine that vary from 1 to 3 mm in size (Fig. 36). The sanidine tablets have a blocky appearance in thin section and occur in a matrix that is rich in strontian calcite with lesser amounts of aegirine, pyrite, pyrrhotite, chalcopyrite, fluorite, strontianite, and ancylite (Fig. 37). The amount of matrix is highly variable but generally represents between 30 and 50 percent of the rock.

Chemistry

Major element chemical analyses of four samples of sanidinite, three samples of syenite pegmatite, and three samples of pulaskite are presented in Table 21. All of the samples are ultrapotassic with values of K_2O commonly in excess of 10 percent. Values of Na_2O are similar to the values in other varieties of fenite and rarely exceed 1 percent.

Figure 36. Slab photograph of pulaskite (sample WBD-7/1274.7). Cube-shaped crystals of light gray sanidine enclosed within a darker matrix rich in strontian calcite and aegirine.

Figure 37. Photomicrograph of pulaskite (sample WBD-5/1361.0). Cube-shaped crystals of sanidine (S) enlosed within a matrix rich in strontian calcite (Sr-C) and pyrite (Py). Bar scale represents 0.25 mm. Plane-polarized light.

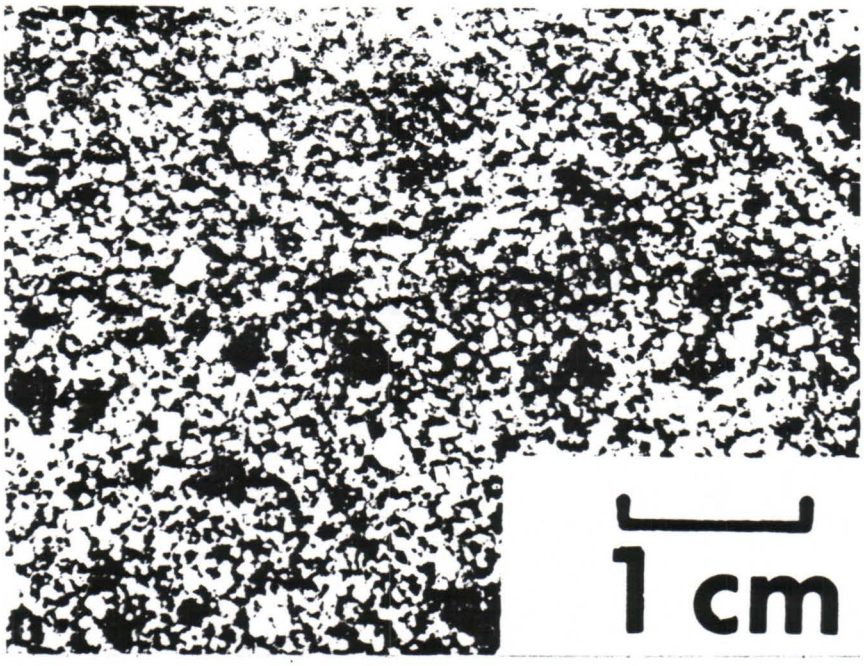
1 cm

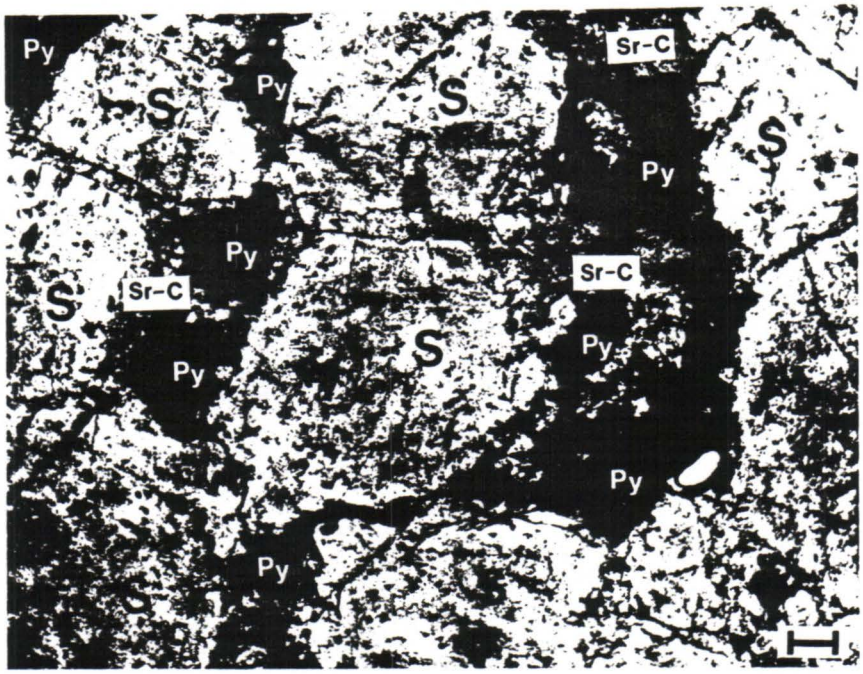
Py
Py
S
S
Sr-C
Py
S
Py
Sr-C
S
Sr-C
Py
S
Py
Py
Py
Py

TABLE 21

MAJOR ELEMENT CHEMICAL ANALYSES OF ALKALI LEUCOSYENITES

SAMPLE	A	B	C	D	E
SiO_2	47.60	48.39	54.82	47.50	42.19
Al_2O_3	20.16	16.21	16.08	15.35	12.10
Fe_2O_3*	5.05	4.86	4.51	6.23	7.52
MgO	0.83	0.81	1.05	1.06	1.39
CaO	7.26	8.31	1.04	8.40	11.48
Na_2O	0.40	0.37	0.45	0.53	0.33
K_2O	9.06	10.76	12.72	10.52	9.78
TiO_2	0.88	1.00	1.36	1.39	1.33
P_2O_5	0.22	0.14	0.23	0.17	0.53
MnO	0.19	0.28	0.43	0.29	0.66
Total	91.65	91.13	92.69	91.44	87.31

* Total Fe as Fe_2O_3

Sample key: A=Sample WBD-5/623.8=Sanidinite
B=Sample WBD-5/1130.5=Sanidinite
C=Sample WBD-5/1527.6=Sanidinite
D=Sample WBD-10/1408.8=Sanidinite
E=Sample WBD-5/1076.0=Syenite pegmatite

TABLE 21

(continued)

SAMPLE	F	G	H	I	J
SiO_2	45.80	49.96	50.53	35.36	43.38
Al_2O_3	13.30	13.22	13.55	8.59	10.12
Fe_2O_3*	4.33	3.87	5.91	2.99	2.36
MgO	0.76	1.17	1.62	0.47	2.91
CaO	9.61	5.53	5.60	23.64	16.90
Na_2O	0.36	1.01	0.41	1.08	0.46
K_2O	10.73	11.06	11.81	7.34	9.87
TiO_2	0.82	2.00	0.54	0.49	0.09
P_2O_5	0.14	0.31	0.11	0.17	0.13
MnO	0.39	0.31	0.27	0.53	0.96
Total	86.24	88.44	90.35	80.66	87.18

* Total Fe as Fe_2O_3

Sample key: F=Sample WBD-5/1473.8=Syenite pegmatite
G=Sample WBD-13/830.5=Syenite pegmatite
H=Sample WBD-5/1467.5=Pulaskite
I=Sample WBD-7/1274.7=Pulaskite
J=Sample WBD-9/647.1=Pulaskite

The wide variations in the values of SiO_2 and the poor closures of the analyses can be attributed to differences in the amount of strontian calcite which ranges up to 26 percent in modal abundance (Table 19).

Pseudoleucite Alkali Trachyte Porphyry

General

Pseudoleucite alkali trachyte porphyry is a volumetrically insignificant rock type in the Bear Lodge Mountains that occurs as small dikes in the shallow subsurface of the main igneous dome. It also forms small dikes at the surface in the central and northern portions of the dome where it corresponds to pseudoleucite trachyte porphyry reported by White (1980) and Wilkinson (1982) and to pseudoleucite porphyry described by Staatz (1983). It is absent in the area of study along the southeastern flank of the uplift.

Crosscutting relationships indicate pseudoleucite alkali trachyte porphyry was generated during the episode of potassic fenitization and represents a rheomorphic variety of fenite. It crosscuts older varieties of fenite and in turn, is crosscut by the rare-earth and thorium veins emplaced during the closing stages of fenitization (Fig. 22, p. 66). The ultrapotassic composition of the rock also suggests that it is genetically related to the fenitization process.

Petrography

Pseudoleucite alkali trachyte porphyry is holocrystalline, moderately calcareous, and variably porphyritic. It is characterized by distinct, light gray, trapezohedral pseudoleucite phenocrysts enclosed within a medium to dark gray aphanitic groundmass (Fig. 38). Modal

Figure 38. Slab photograph of pseudoleucite alkali trachyte porphyry (sample BL-4/1175.0). Trapezohedral phenocrysts of pseudoleucite enclosed within a dark, aphanitic groundmass rich in biotite, strontian calcite, and sanidine.

Figure 39 Photomicrograph of pseudoleucite alkali trachyte porphyry (sample BL-4/1175.0). Rounded to trapezohedral phenocryst of pseudoleucite (Ps) enclosed within a microcrystalline groundmass (Grm) composed mostly of biotite, strontian calcite, and branching crystals of sanidine. Note disseminated crystals of pyrite (Py). Bar scale represents 0.25 mm. Crossed polars.

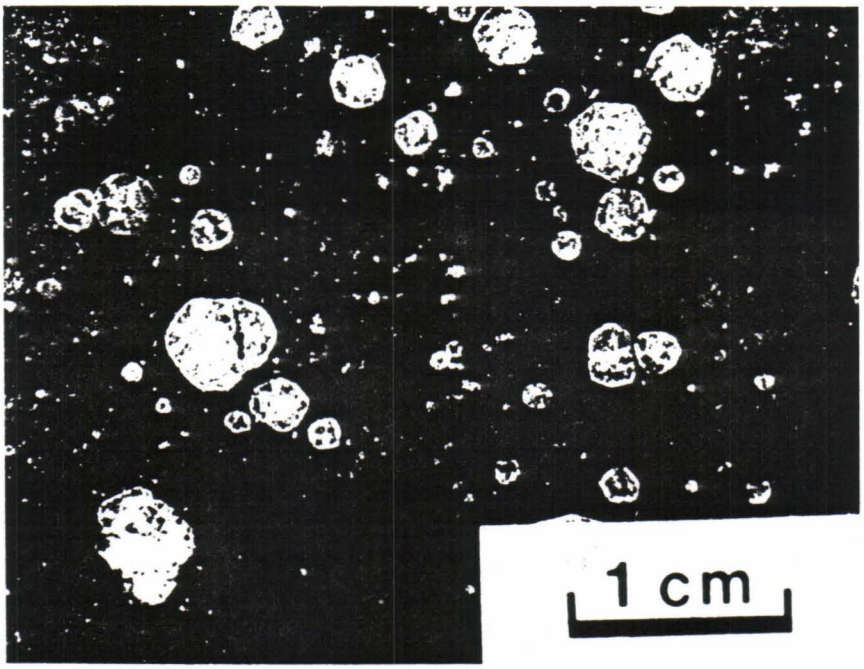
1 cm

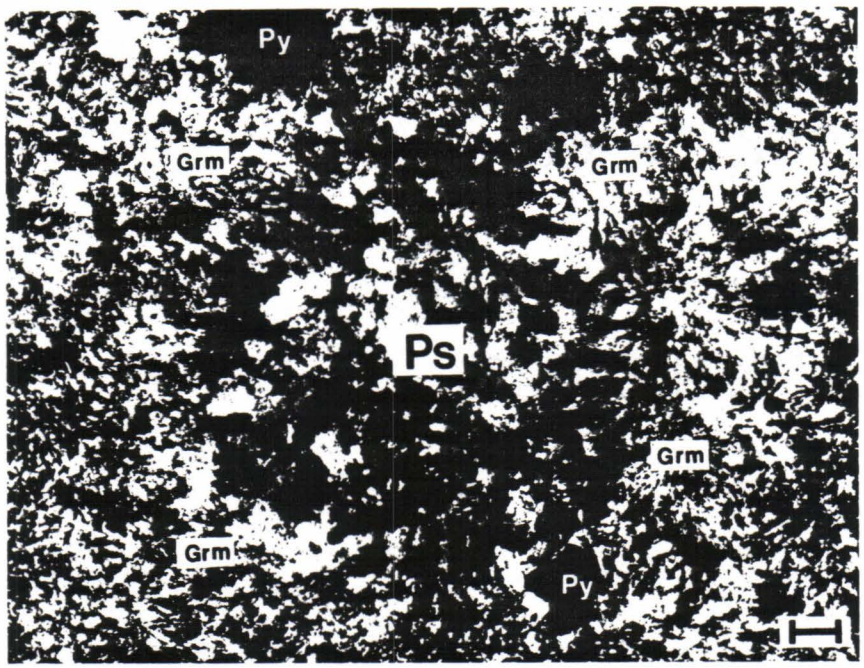
Py
Grm
Grm
Ps
Grm
Grm
Py

analyses of three samples of the rock are presented in Table 22 and microprobe analyses of some of the more common minerals are presented in Table 23.

The pseudoleucite phenocrysts compose between 2 and 30 percent of the rock and range from 0.5 to 5.0 mm in diameter (Fig. 39). They usually occur as isolated crystals but occasionally exhibit glomerophyric arrangements, especially in more phenocryst-rich specimens. Many of the crystals are zoned with cores consisting of mosaic sanidine and rims composed of radially arranged analcime or natrolite. Relict leucite with well-developed multiple lamellar twinning has been reported in several specimens of the rock by White (1980).

Groundmasses are microcrystalline and rich in branching crystals of untwinned sanidine. The crystals range between 0.1 and 0.5 mm in length and are potassium-rich in composition (Table 24 columns A and B). Albite, analcime, biotite, and strontian calcite occur interstitially within the groundmass.

Analcime forms irregular-shaped patches up to 1 mm in size. It has a turbid appearance in plane-polarized light and is partially to completely replaced by clay minerals and strontian calcite.

Microcrystalline biotite and strontian calcite also form irregular-shaped patches. The biotite is strongly pleochroic with X=orangish brown and Y=Z=greenish brown.

Accessory minerals in the rock include apatite, celestite, ancylite, magnetite, and manganian ilmenite. Sulfide minerals, including pyrite, pyrrhotite, chalcopyrite, sphalerite, and galena, occur in trace amounts as disseminated crystals up to 2.0 mm in size.

TABLE 22

MODAL ANALYSES OF PSEUDOLEUCITE ALKALI TRACHYTE PORPHYRY

SAMPLE	A	B	C
Primary			
Groundmass			
Sanidine	47.8	50.2	51.7
Albite	0.0	9.2	0.8
Analcime	3.9	2.5	1.6
Biotite	9.8	15.0	19.7
Calcite	3.9	6.7	8.2
Pseudoleucite			
Sanidine	14.8	2.8	2.0
Analcime	3.4	0.8	0.8
Biotite	1.2	4.2	3.0
Apatite	0.0	0.6	tr.
Strontian calcite	8.4	2.4	5.8
Celestite	pr.	0.0	0.0
Ancylite	pr.	0.0	pr.
Titanian magnetite	0.4	1.2	0.6
Manganian ilmenite	0.8	0.4	1.6
Pyrite	2.6	3.2	2.2
Chalcopyrite	tr.	0.0	0.4
Sphalerite	0.0	0.0	tr.
Galena	0.0	0.0	tr.
Secondary			
Sericite/clays	2.6	0.8	1.6
Iron/titanium oxides	0.4	tr.	tr.

tr.=trace, less than 0.2% detected
pr.=present, determined qualitatively by microprobe analysis

Sample key: A=Sample BL-4/1175.0=Pseudoleucite alkali trachyte porphyry
B=Sample BL-4/1203.6=Pseudoleucite alkali trachyte porphyry
C=Sample WBD-12/819.8=Pseudoleucite alkali trachyte porphyry

TABLE 23

MICROPROBE ANALYSES OF MINERALS IN PSEUDOLEUCITE ALKALI TRACHYTE PORPHYRY

SAMPLE	A	B	C	D	E	F	G	H
SiO2	64.59	65.27	64.71	65.55	69.40	70.53	52.60	55.44
Al2O3	19.07	18.80	18.77	18.95	19.96	20.38	25.06	24.28
FeO*	0.22	0.34	0.00	0.00	0.00	0.00	0.25	0.38
MgO	0.00	0.00	0.00	0.00	0.00	0.00	0.00	0.00
CaO	0.00	0.00	0.00	0.00	0.00	0.15	1.11	0.22
Na2O	0.32	0.42	1.40	1.39	12.29	11.89	11.57	11.64
K2O	15.11	15.17	14.10	14.02	0.17	0.32	0.07	0.08
TiO2	0.19	0.53	0.40	0.00	0.00	0.00	0.00	0.00
P2O5	0.00	0.00	0.00	0.00	0.00	0.29	0.00	0.14
MnO	0.00	0.00	0.00	0.00	0.00	0.10	0.00	0.00
Cl	0.00	0.00	0.06	0.00	0.00	0.00	0.00	0.00
SO3	0.16	0.00	0.00	0.00	0.00	0.00	0.13	0.00
Total	99.66	100.53	99.44	99.91	101.82	103.66	90.79	92.18
	Number of cations on the basis of X oxygens							
	X=32	X=32	X=32	X=32	X=32	X=32	X=7	X=7
Si	11.90	11.94	11.93	11.99	11.93	11.90	2.27	2.34
Al	4.14	4.05	4.08	4.09	4.05	4.05	1.27	1.21
Fe	0.34	0.05	0.00	0.00	0.00	0.00	0.01	0.01
Mg	0.00	0.00	0.00	0.00	0.00	0.00	0.00	0.00
Ca	0.00	0.00	0.00	0.00	0.00	0.03	0.05	0.01
Na	0.11	0.15	0.50	0.49	4.09	3.89	0.97	0.95
K	3.55	3.54	3.31	3.27	0.04	0.06	0.00	0.00
Ti	0.03	0.07	0.05	0.00	0.00	0.00	0.00	0.00
P	0.00	0.00	0.00	0.00	0.00	0.04	0.00	0.01
Mn	0.00	0.00	0.00	0.00	0.00	0.01	0.00	0.00
Cl	0.00	0.00	0.02	0.00	0.00	0.00	0.00	0.00
S	0.02	0.00	0.00	0.00	0.00	0.00	0.00	0.00

* Total Fe as FeO

Sample key: A=Sample BL-4/1175.0=Sanidine; B=Sample BL-4/1203.6= Sanidine; C=Sample BL-4/1203.6=Sanidine; D=Sample WBD-12/819.8= Sanidine; E=Sample BL-4/1203.6=Albite; F=Sample WBD-12/819.8= Albite; G=Sample BL-4/1175.0=Analcime, H=Sample BL-4/1203.6= Analcime.

TABLE 23

(continued)

SAMPLE	I	J	K	L	M	N	O	P
SiO2	36.80	37.84	39.33	0.23	0.00	0.00	0.23	0.17
Al2O3	16.59	13.22	11.49	0.00	0.00	0.64	0.00	0.16
FeO*	21.85	21.00	18.62	0.30	87.39	85.62	39.15	45.86
MgO	9.44	11.85	14.61	0.00	0.25	0.00	0.17	0.00
CaO	0.00	0.00	0.00	54.58	0.00	0.00	1.17	0.00
Na2O	0.22	0.00	0.00	0.00	0.70	0.00	0.00	0.00
K2O	9.31	9.47	9.64	0.17	0.00	0.00	0.07	0.00
TiO2	0.86	2.54	1.81	0.00	7.14	7.50	57.72	50.72
P2O5	0.14	0.17	0.00	40.62	0.00	0.00	0.00	0.00
MnO	0.63	0.77	0.48	0.00	0.73	0.57	1.60	2.27
Cl	0.05	0.00	0.00	0.00	0.05	0.00	0.00	0.00
SO3	0.00	0.00	0.00	0.18	0.00	0.00	0.00	0.00
Total	95.89	96.86	95.98	96.08	96.26	94.33	100.11	99.18
	Number of cations on the basis of X oxygens							
	X=24	X=24	X=24	X=26	X=32	X=32	X=6	X=6
Si	6.15	6.26	6.48	0.04	0.00	0.00	0.01	0.01
Al	3.27	2.57	2.23	0.00	0.00	0.29	0.00	0.01
Fe	3.05	2.90	2.57	0.04	27.35	27.11	1.60	1.96
Mg	2.35	2.92	3.59	0.00	0.14	0.00	0.01	0.00
Ca	0.00	0.00	0.00	10.44	0.00	0.00	0.06	0.00
Na	0.07	0.00	0.00	0.00	0.51	0.00	0.00	0.00
K	1.98	2.00	2.03	0.04	0.00	0.00	0.00	0.00
Ti	0.11	0.31	0.22	0.00	2.01	2.14	2.12	1.95
P	0.02	0.02	0.00	6.14	0.00	0.00	0.00	0.00
Mn	0.09	0.11	0.07	0.00	0.23	0.18	0.07	0.10
Cl	0.01	0.00	0.00	0.00	0.03	0.00	0.00	0.00
S	0.00	0.00	0.00	0.02	0.00	0.00	0.00	0.00

* Total Fe as FeO

Sample key: I=Sample BL-4/1175.0=Biotite; J=Sample BL-4/1203.6= Biotite; K=Sample WBD-12/819.8=Biotite; L=Sample BL-4/1203.6= Apatite; M=Sample BL-4/1203.6=Titanian magnetite; N=Sample BL-4/1203.6=Titanian magnetite; O=Sample BL-4/1175.0=Manganian ilmenite, P=Sample WBD-12/819.8=Manganian ilmenite.

Chemistry

Major element chemical analyses of three samples of pseudoleucite alkali trachyte porphyry are presented in Table 24. The abundance of strontian calcite in the rocks is reflected by the relatively high values of CaO and the anomolously low values of SiO_2 and Al_2O_3. Values of K_2O and Na_2O are comparable to the values observed in other varieties of fenite occurring in the Bear Lodge Mountains with values of K_2O greatly in excess of Na_2O. The values of K_2O are also similar to values for leucite-bearing rocks from other alkalic complexes (Gupta and Yaga, 1980, p. 4).

Intrusive Breccias

General

Intrusive breccias are relatively abundant in the Bear Lodge Mountains and correspond to the intrusive breccias reported by Staatz (1983) at several locations within the main igneous dome. The breccias represent rheomorphic units generated during the episode of potassic fenitization and, like other types of fenite, are ultrapotassic and rich in sanidine. Three varieties are distinguished: granitic breccias, feldspathic breccias, and iron oxide breccias.

Granitic breccias represent a product of the desilicification of the Precambrian granitic rocks. They were emplaced during the early stages of fenitization and occur as small plugs or pipes that crosscut older Tertiary igneous intrusions and undisturbed granitic basement rocks. Several of these intrusive bodies are exposed along the southeastern flank of the uplift but they are absent in the subsurface

TABLE 24

MAJOR ELEMENT CHEMICAL ANALYSES OF PSEUDOLEUCITE ALKALI TRACHYTE PORPHYRY

SAMPLE	A	B	C
SiO_2	49.09	45.15	42.77
Al_2O_3	16.78	13.67	13.52
Fe_2O_3*	4.89	8.40	9.27
MgO	1.63	2.60	2.95
CaO	7.35	10.02	9.47
Na_2O	0.83	1.53	0.74
K_2O	10.51	8.49	9.81
TiO_2	1.10	1.64	1.97
P_2O_5	0.20	0.45	0.65
MnO	0.28	0.32	0.38
Total	92.66	92.27	91.53

* Total Fe as Fe_2O_3

Sample key: A=Sample BL-4/1175.0
B=Sample BL-4/1203.6
C=Sample WBD-12/819.8

in the central portions of the main igneous dome and have not been reported at the surface in this region of the uplift by either Wilkinson (1982) or Staatz (1983).

Feldspathic and iron-oxide breccias are more abundant than granitic breccias and occur as dikes and small plugs that crosscut older alkalic igneous rocks and earlier formed fenites. They are exposed at the surface in the central and southeastern portions of the uplift and also constitute major rock types in the subsurface of the main igneous dome.

Petrography

Granitic breccias are characterized by subrounded to subangular xenoliths of Precambrian granitic rocks enclosed within a microcrystalline matrix of granular quartz and sanidine (Fig. 40). Occassional fragments of sandstone from the Deadwood Formation and xenoliths of older alkalic igneous rocks may also be present. The xenoliths range up to 15 cm in diameter and compose between 50 and 80 percent of the rock. The quartz within the xenoliths appears granulated and optically strained. It grades into the matrix of the breccia along the margins of the xenoliths and frequently contains minute inclusions of acicular rutile. Much of the microcline in the granitic fragments loses its distinct grid twinning and appears to be disordering to untwinned orthoclase or sanidine (Fig. 41).

Feldspathic breccias, the second variety of intrusive breccias, consist of subrounded to subangular fragments of rock, 1 to 10 cm across, set in a microcrystalline matrix rich in granular sanidine (Fig. 42). Deeper subsurface samples appear light gray in color while more altered surface and shallow subsurface samples appear oxidized in shades of light brown or light yellowish brown. The xenoliths consist of older

Figure 40. Slab photograph of granitic breccia (sample 21-52B). Subrounded to subangular xenoliths of Precambrian granite (Gr) and alkali trachyte porphyry (Tp) enclosed within an aphanitic matrix rich in sanidine and quartz.

Figure 41. Photomicrograph of granitic breccia (sample 21-180A). Contact between xenolith of Precambrian granite (Gr) and quartz-rich matrix (Ma). Note twinned microcline crystal (shown by arrow) which appears partially disordered to untwinned sanidine. Bar scale represents 0.25 mm. Crossed polars.

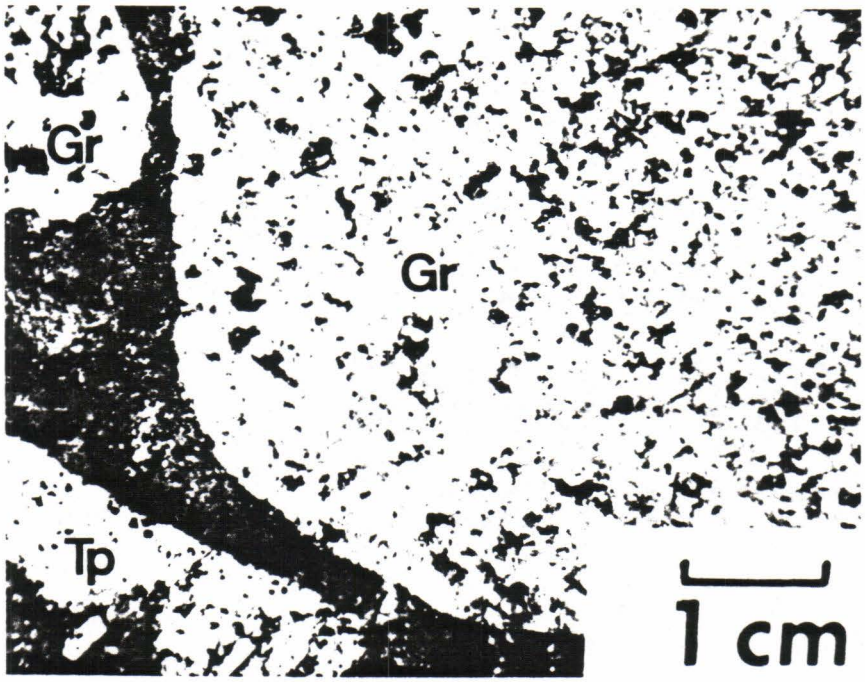
Gr
Gr
Tp
1 cm

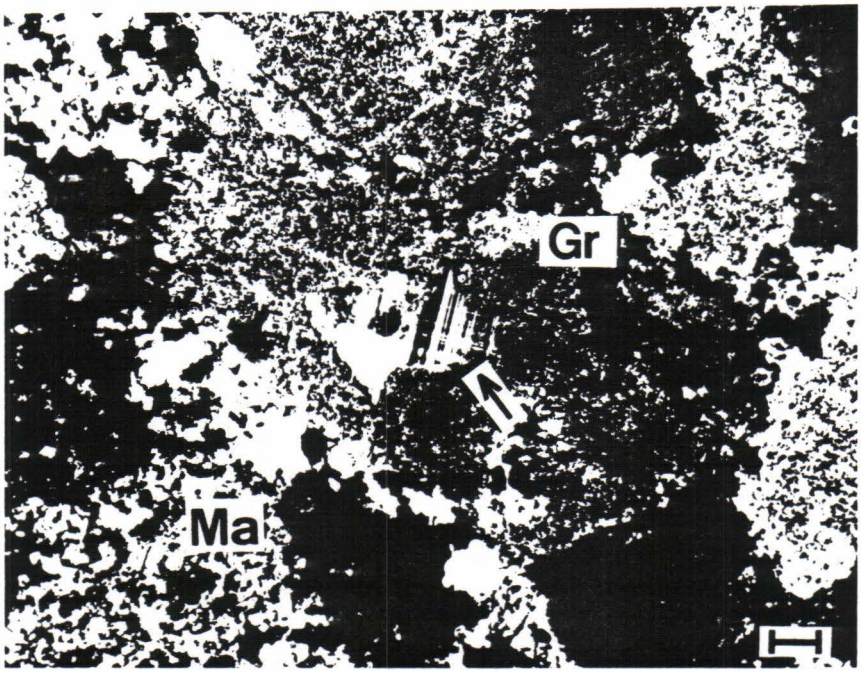
Gr
Ma

Figure 42. Slab photograph of feldspathic breccia (sample 21-33). Subrounded to subangular xenoliths of alkali trachyte enclosed within an aphanitic matrix rich in sanidine.

Figure 43. Photomicrograph of feldspathic breccia (sample 27-239). Subrounded to subangular xenoliths of alkali trachyte (T) enclosed within a microcrystalline to cryptocrystalline matrix rich in sanidine. Bar scale represents 0.25 mm. Plane-polarized light.

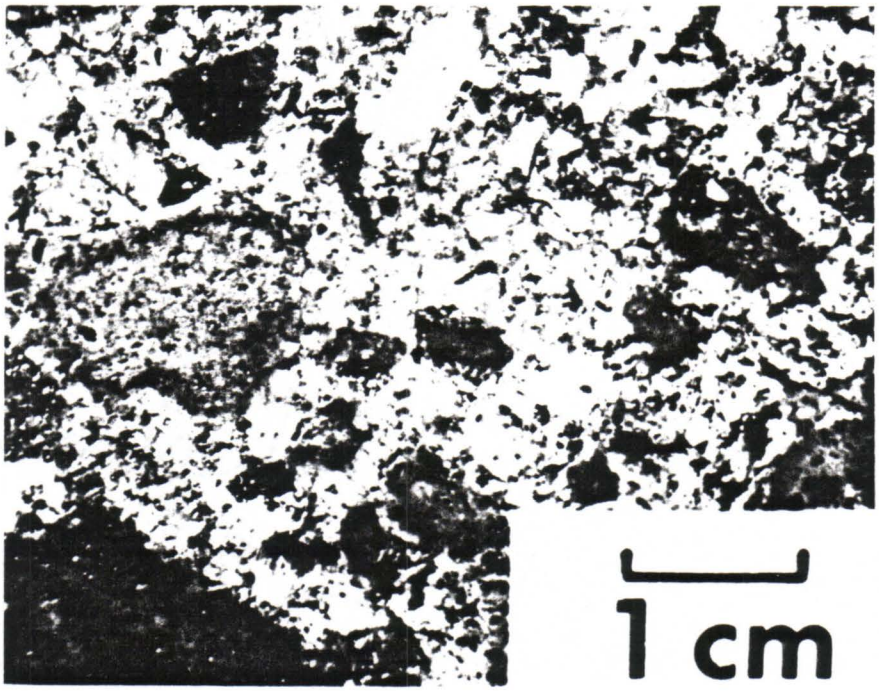
1 cm

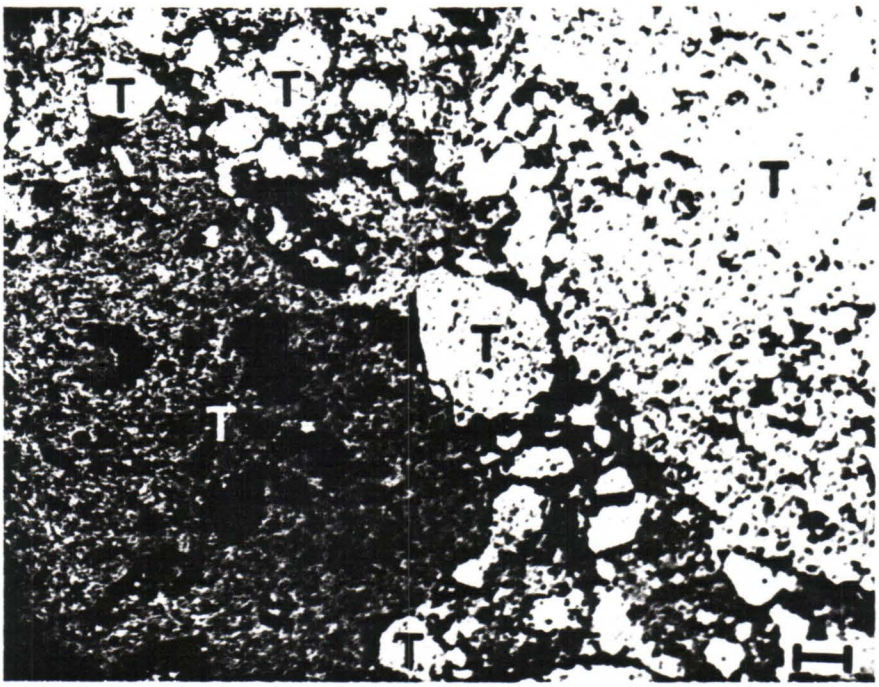
T
T
T
T
T
T
T

alkalic igneous rocks and/or older varieties of fenite but occasional fragments of sandstone from the Deadwood Formation may also be present (Fig. 43). The proportion of xenoliths to matrix is highly variable and the breccia grades into rheomorphic varieties of alkali trachyte with a decreasing ratio of xenoliths to matrix. The majority of samples contain fractured and broken xenocrysts of sanidine, presumably derived from surrounding xenoliths and most specimens also possess irregular-shaped patches of iron oxides and calcite that possibly replaced original mafic minerals. Pyrite is disseminated in fresher samples but is replaced by iron oxides in more altered and oxidized rocks.

The third variety of intrusive breccias, iron-oxide breccias, possess a distinct rust-red to rust-orange ferruginous matrix that is rich in sanidine (Fig. 44). The matrix encloses subangular to subrounded xenoliths of alkalic igneous rocks, older fenites, and in some instances, sandstone of the Deadwood Formation. The xenoliths usually constitute between 30 and 50 percent of the rock and range up to 5 mm in size. The surrounding matrix ranges from microcrystalline to cryptocrystalline and appears opaque to semi-opaque in thin section due to the abundance of iron oxides (Fig. 45).

Chemistry

Major element chemical analyses of two samples of granitic breccia, two samples of feldspathic breccia, and two samples of iron-oxide breccia are presented in Table 25. As expected, granitic breccias are more siliceous than the other two varieties of breccia and iron-oxide breccias are more ferruginous. The values of K_2O and Na_2O are similar to the values occurring in the other types of fenite found in the Bear Lodge Mountains. Feldspathic breccias are especially potassic and

Figure 44. Slab photograph of iron-oxide breccia (sample 21-74C). Subrounded to subangular xenoliths of alkali trachyte enclosed within an aphanitic matrix rich in sanidine and iron oxides.

Figure 45. Photomicrograph of iron-oxide breccia (sample 21-74C). Subrounded to subangular xenoliths of alkali trachyte (T) enclosed within an opaque, microcrystalline to cryptocrystalline matrix rich in sanidine and iron oxides (FeOx). Note sphene crystal (Sp) in trachyte xenolith near center of photomicrograph. Bar scale represents 0.25 mm. Plane-polarized light.

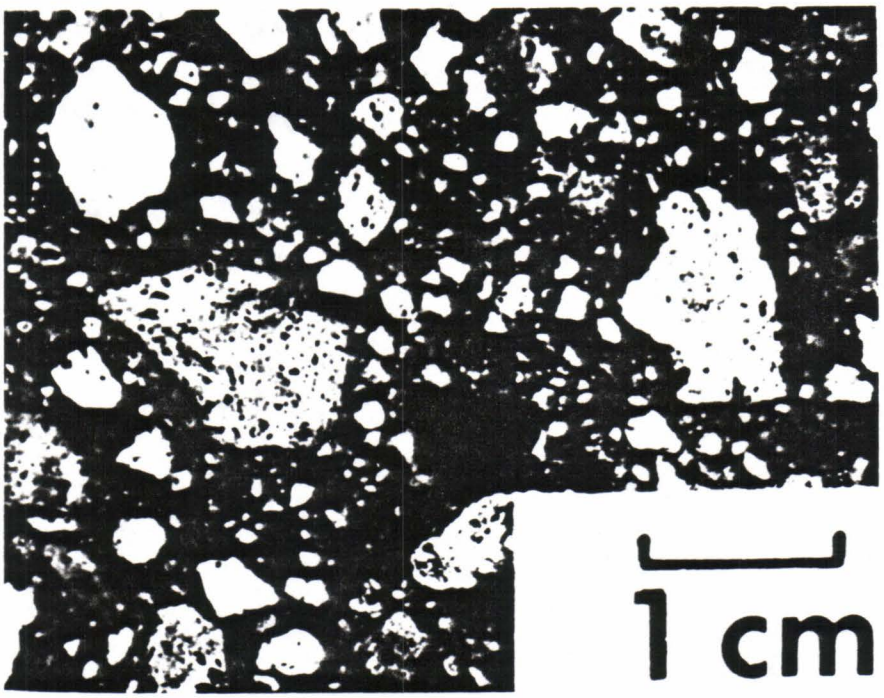
1 cm

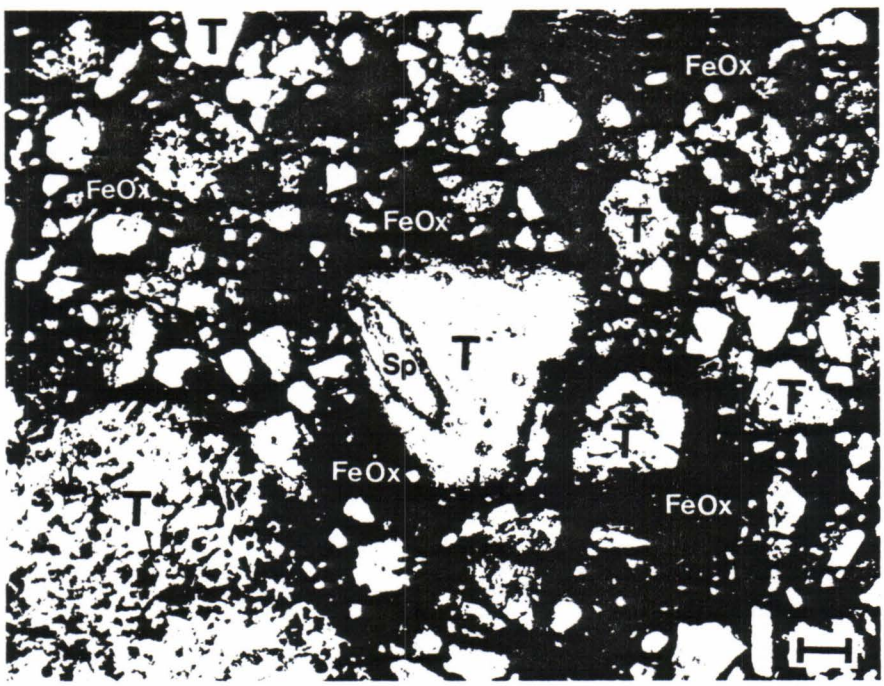
T
FeOx
FeOx
FeOx
T
Sp
T
T
T
FeOx
T
FeOx

TABLE 25

MAJOR ELEMENT CHEMICAL ANALYSES OF INTRUSIVE BRECCIAS

SAMPLE	A	B	C	D	E	F
SiO_2	63.82	68.21	59.26	50.57	53.80	50.34
Al_2O_3	13.22	14.07	16.67	15.89	16.10	16.28
Fe_2O_3*	2.67	1.65	2.95	3.57	5.59	6.77
MgO	0.04	0.09	0.20	0.90	0.37	0.09
CaO	0.12	0.10	0.61	5.61	8.09	6.94
Na_2O	0.18	2.54	0.97	1.43	3.49	0.13
K_2O	11.51	7.08	11.97	10.75	6.12	11.58
TiO_2	0.34	0.09	0.70	1.07	0.98	1.08
P_2O_5	0.05	0.03	0.22	0.65	0.35	0.25
MnO	0.06	0.01	0.12	0.54	0.08	0.22
Total	92.01	93.87	93.67	90.98	94.97	93.68

* Total Fe as Fe_2O_3

Sample key: A=Sample 21-52B=Granitic breccia
B=Sample 16-405=Granitic breccia
C=Sample 21-33=Feldspathic breccia
D=Sample WBD-8/1422.0=Feldspathic breccia
E=Sample 21-74C=Iron oxide breccia
F=Sample BL-5/325.5=Iron oxide breccia

similar in composition to the intrusive feldspathic fenite-breccias from Toror Hills, Uganda (Sutherland, 1965, p. 371).

Carbonatitic Magmatism

A period of carbonatitic magmatism followed the episode of potassic fenitization in the Bear Lodge Mountains. The veins and dikes of carbonatite emplaced during the event crosscut the fenitic rock types both at the surface and in the subsurface of the central igneous core. They are enriched in strontium, thorium, and rare-earth elements and are tentatively termed I-type carbonatites in order to distinguish them from a second variety of carbonatite, termed S-type, which have lower concentrations of these elements and which outcrop in the southeastern portions of the core. Both the I-type carbonatites and S-type carbonatites are rich in calcite and are classified as sovites according to the conventions of Brögger (1921).

I-type Carbonatites

General

Outcrops of I-type carbonatites are rare in the Bear Lodge Mountains. Only two dikes are exposed at the surface, one in the NW ¼, NE ¼, Sec. 20, T.52N., R.63W. and the other in the SE ¼, SE ¼, Sec. 7, T.52N., R.63W. (Wilkinson, 1982). They range from 1 to 9 m in thickness and are highly altered and pervasively stained with iron oxides. The surrounding wall rocks consist of alkali trachyte and intrusive breccia (Wilkinson, 1982; Staatz, 1983). The wallrocks also appear altered and stained and they contain significant amounts of strontian calcite in areas adjacent to the carbonatite dikes.

I-type carbonatites are abundant at depth near the center of the main igneous dome in the general vicinity of the surface exposures.

They range from small veins a few millimeters thick to large dikes several tens of meters thick. Most of the veins and dikes are steeply inclined and they appear to have introduced significant amounts of strontian calcite into the surrounding silicate rocks during emplacement. They are altered and oxidized in the shallow subsurface but gradually become unaltered with increasing depth.

The enrichment of thorium and rare-earth elements in I-type carbonatites is economically significant. Thorium contents range from 54 to 1,510 ppm and total rare-earths from 0.58 to 64 percent (Staatz, 1983). Cerium and lanthanum are the princple rare-earths, accounting for more than 95 percent of the total rare-earth element content of the rocks (Staatz, 1983).

Other deposits of potential economic interest that are associated with I-type carbonatites are copper, lead, and zinc. They occur as sulfides and consist of disseminated crystals of chalcopyrite, galena, and sphalerite with associated pyrite and pyrrhotite. The sulfides are locally abundant at depth but are oxidized at the surface and in the shallow subsurface.

Petrography

I-type carbonatites are holocrystalline and exhibit allotriomorphic granular textures. Altered surface samples are fine to medium-grained and have a mottled appearance in shades of reddish brown, yellowish brown, and grayish brown, often with disseminated blebs of purple fluorite and mustard-yellow patches of powdery rare-earth oxides. Fresh subsurface samples vary from fine-grained to pegmatitic and range from sugary white to light gray to light grayish green in color. They frequently possess flow bands composed of streaks and lenses of dark

sulfide minerals, purple fluorite, cream-white strontianite, and pink rare-earth minerals (Fig. 46).

Strontian calcite is the principle carbonate mineral, comprising between 60 and 95 percent of the rock. Strontianite occurs in variable amounts and in several specimens forms as much as 20 percent of the matrix. It has a turbid appearance in plane-polarized light, commonly with inclusions of barite, and appears to replace strontian calcite along grain boundaries (Fig. 47). Another carbonate mineral, manganese-rich siderite, is found in several specimens but never exceeds more than a few percent in abundance.

Fluorite and the sulfide minerals, pyrite, pyrrhotite, chalcopyrite, galena, and sphalerite, are present in variable amounts in the majority of samples. Fluorite appears to be of late-stage magmatic or hydrothermal origin and occurs with strontianite and rare-earth elements as irregular-shaped microcrystalline patches that replace portions of the coarser-grained strontian calcite matrix. The sulfide minerals also appear to be late-stage, forming disseminated crystals that replace and poikilitically enclose earlier formed strontian calcite.

Other minerals commonly found in the rocks are biotite, aegirine, sanidine, quartz, apatite, and magnetite. They are highly variable in abundance, occurring in trace, accessory, or minor amounts in some samples while in others they are completely lacking. Several dikes also contain significant amounts of sodic actinolite (Fig. 48). The amphibole is dark green in color and forms spectacular clusters of radiating acicular crystals (Fig. 49).

Bastnaesite $\left[(Ce,La)FCO_3\right]$ and synchysite $\left[(Ce,La)Ca(CO_3)_2F\right]$ are the

Figure 46. Slab photograph of I-type carbonatite (sample WBD-5/339.5). Strontian calcite (Sr-C) with irregular-shaped bands of strontianite and ancylite (Sr+A), fluorite (F), and pyrite (Py).

Figure 47. Photomicrograph of I-type carbonatite (sample WBD-5/273.5). Radiating intergrowth of strontianite and ancylite (S+A) enclosed within a fine-grained matrix of strontian calcite (Sr-C). Bar scale represents 0.25 mm. Plane polars.

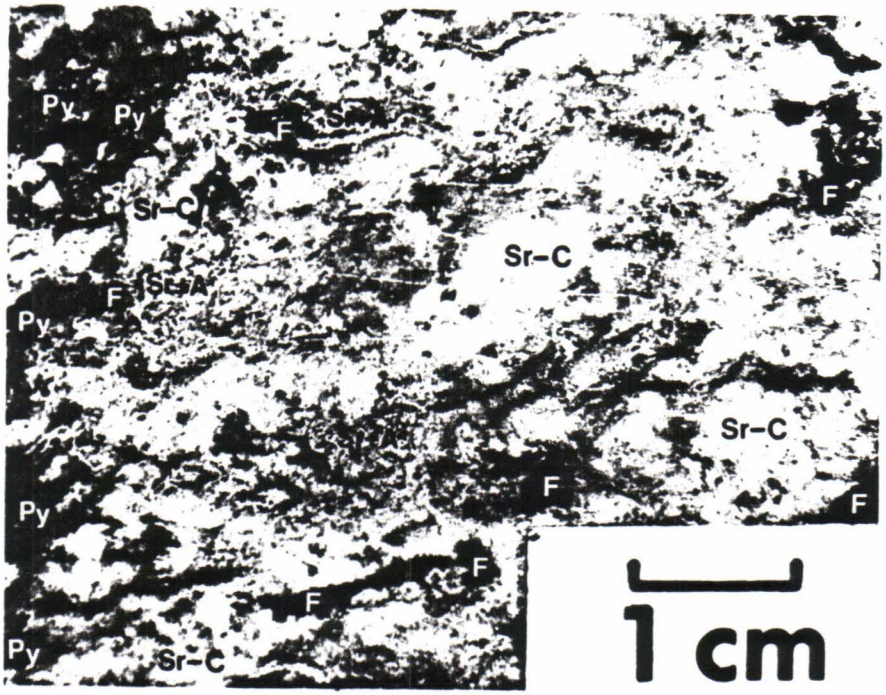
Py
Py
F
Sr-C
F
Sr-C
F
Sr+A
Py
Sr-C
F
Py
F
F
F
Py
Sr-C
1 cm

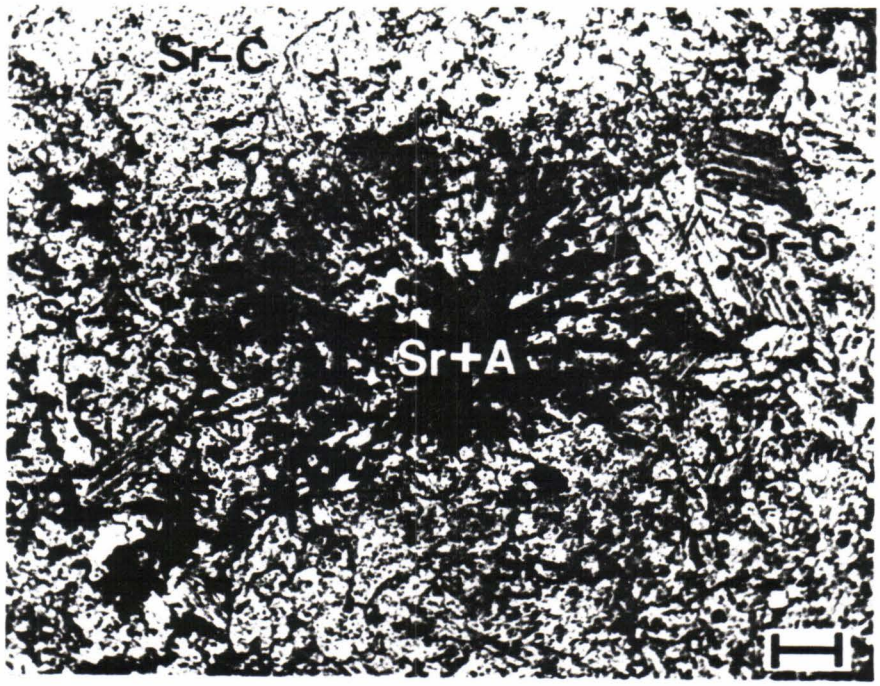
Sr-C
Sr+A
Sr-C

Figure 48. Slab photograph of I-type carbonatite (sample WBD-7/348.4). Strontian calcite (Sr-C) with irregular-shaped bands of sodic amphibole (Amph), strontianite (Sr), and pyrite (Py).

Figure 49. Photomicrograph of I-type carbonatite (sample WBD-7/348.4). Radiating sodic amphibole (Amph) enclosed within a fine to medium-grained matrix of strontian calcite (Sr-C). Bar scale represents 0.25 mm. Crossed polars.

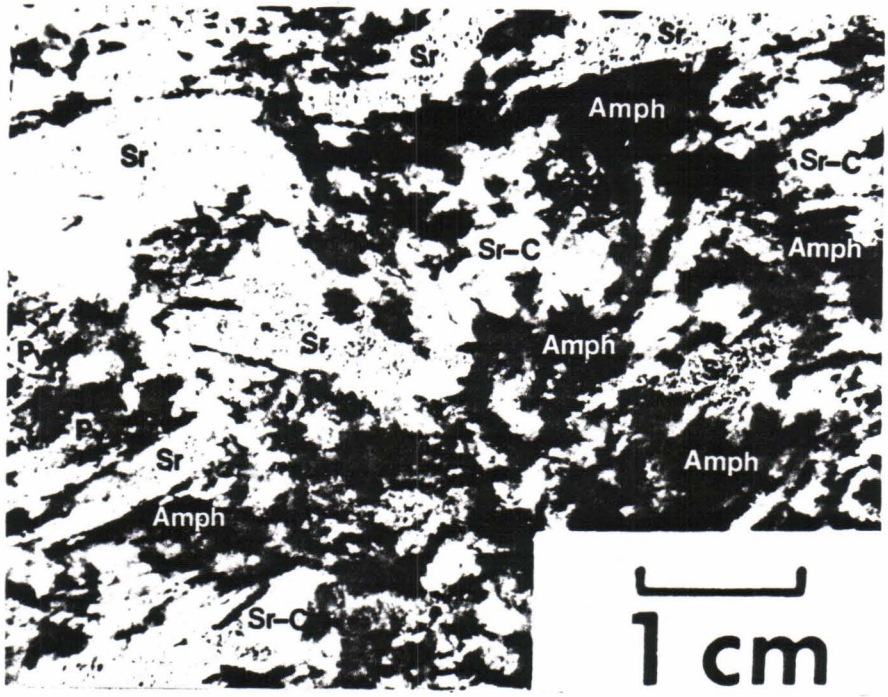
Sr
Sr
Amph
Sr
Sr–C
Sr–C
Amph
Sr
Amph
Sr
Amph
Sr–C
1 cm

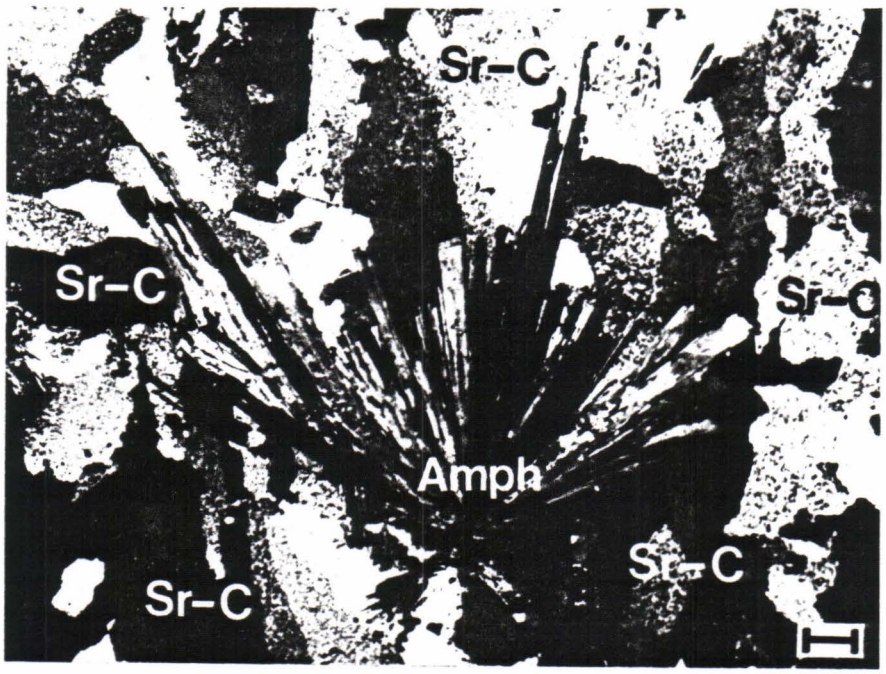
Sr–C
Sr–C
Sr–C
Amph
Sr–C
Sr–C

principle rare-earth minerals in altered surface outcrops of I-type carbonatite (Staatz, 1983). The fresh subsurface dikes and veins contain a more diverse suite of rare-earth minerals that includes ancylite $\left[(Ce,La)_4(Sr,Ca)_3(CO_3)_7(OH)_4\right]\cdot 3H_2O$, burbankite $\left[(Na,Ca,Sr,Ba,Ce)_6(CO_3)_5\right]$, carbocernaite $\left[(Na,Ca,Sr,Ce)CO_3\right]$, and two apparently new rare-earth minerals, one a rare-earth carbonate and the other a rare-earth phosphate.

Ancylite is the most abundant of the rare-earth minerals, forming approximately 10 percent of the matrix in several of the dikes. The mineral possesses a pink color in hand sample and usually occurs with strontianite in irregular-shaped microcrystalline patches that replace the coarser-grained crystals of strontian calcite of the matrix (Fig. 50a). Larger crystals occur in several of the dikes and veins where they commonly exhibit well-developed orthorhombic crystal form (Fig. 50b). A microprobe x-ray energy spectrum of a typical crystal, illustrated in Figure 50c, suggests a composition similar to analyses of ancylite (Palache and others, 1951, p. 292).

Ancylite in many of the dikes and veins alters to a soft micaceous mineral that possesses a burnt orange color in hand sample. The mineral appears as radiating, acicular crystals in thin section (Fig. 51a) and only exhibits its true platy habit when irregular surfaces are observed (Fig. 51b). The composition of the mineral as suggested by its microprobe x-ray energy spectrum is similar to that of ancylite but with an increase in the concentration of calcium relative to strontium (Fig. 51c). Calcioancylite, the calcium-rich, strontium-deficient analogue of ancylite, might be expected to exhibit a comparable spectrum. However, since this micaceous mineral obviously lacks the orthorhombic symmetry

Figure 50. Ancylite.

(a.) Photomicrograph of very fine-grained ancylite (A) replacing strontian calcite (Sr-C) in I-type carbonatite (Sample WBD-10/114.0). Bar scale represents 0.25 mm. Plane-polarized light.

(b.) Secondary electron photomicrograph of euhedral ancylite crystal (A) enclosed within very fine-grained strontianite (Sr) in I-type carbonatite (sample WBD-7/348.4). Bar scale represents 10 microns.

(c.) Electron microprobe x-ray energy spectrum of ancylite in I-type carbonatite (sample WBD-10/114.0).

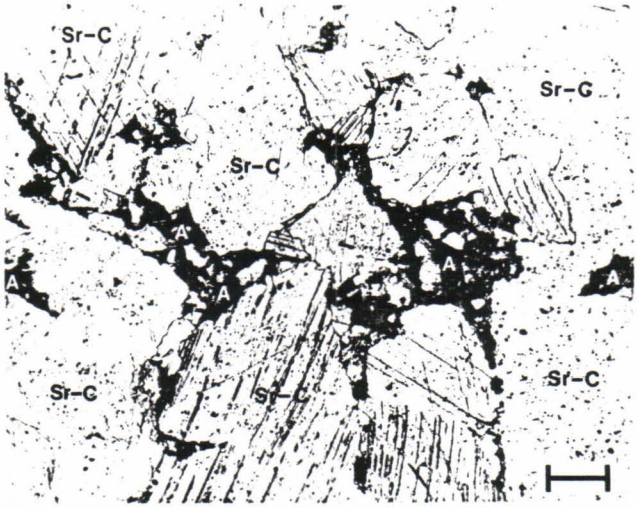
Sr-C
Sr-G
Sr-C
A
A
A
A
A
Sr-C
Sr-C
Sr-C

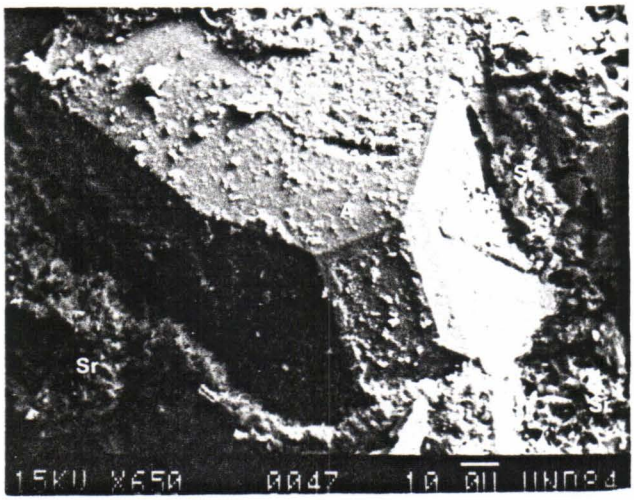
A
Sr
15KV X650 0047 10 UM UNPOL

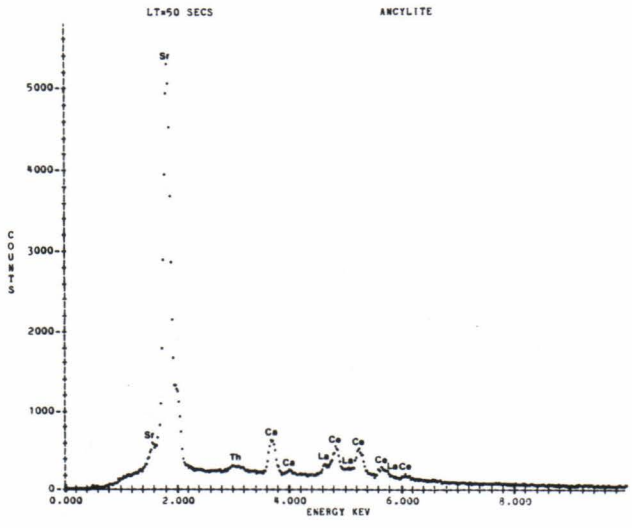
LT=50 SECS
ANCYLITE
Sr
5000
4000
3000
2000
1000
0
COUNTS
Sr
Th
Ce
Ce
La
Ce
Ce
Ce
La
Ce
0.000
2.000
4.000
6.000
8.000
ENERGY KEV

Figure 51. Rare-earth element carbonate mineral.

(a.) Photomicrograph of fine-grained, micaceous, rare-earth carbonate (RC) in I-type carbonatite (sample WBD-8/1573.5). Surrounding matrix consists of strontian calcite (Sr-C). Holes (H) in sample due to polishing. Bar scale represents 0.25 mm. Plane-polarized light.

(b.) Secondary electron photomicrograph of micaceous, rare-earth carbonate (RC) in I-type carbonatite (sample WBD-10/114.0). Note euhedral crystals of siderite (S) and spheres of iron oxide (FeOx). Bar scale represents 10 microns.

(c.) Electron microprobe x-ray energy spectrum of micaceous, rare-earth carbonate in I-type carbonatite (sample WBD-10/114.0).


Sr-C
RC
Ho
Ho
Sr-C
RC
Sr-C

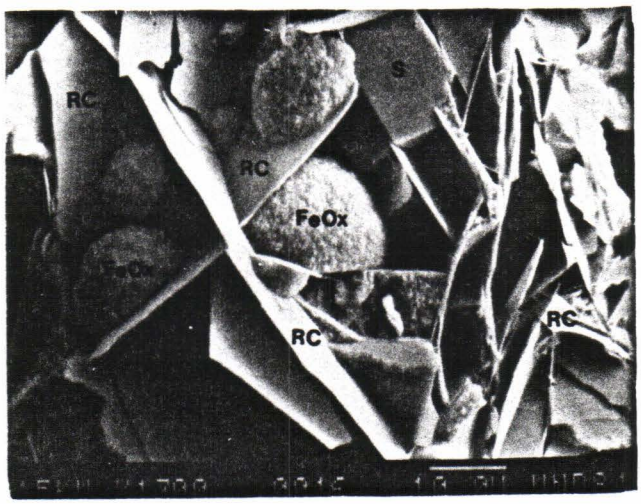
RC
S
RC
FeOx
RC
RC

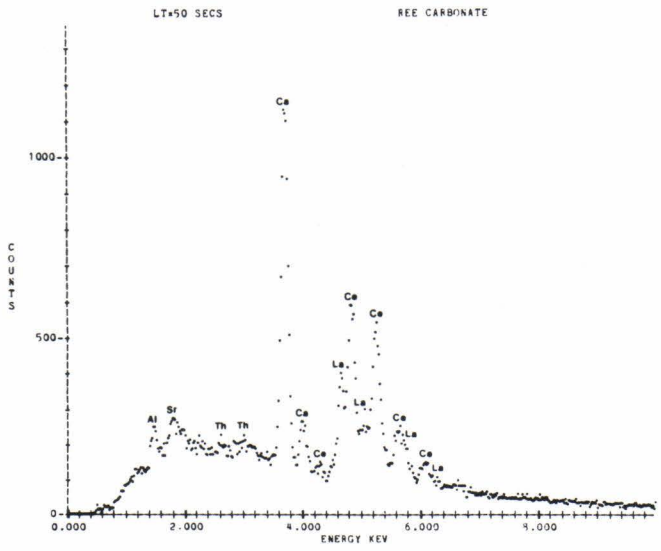
LT=50 SECS
REE CARBONATE
COUNTS
1000
500
0
0.000
2.000
4.000
6.000
8.000
ENERGY KEV
Ce
Al
Sr
Th
Th
Ce
Ce
Ce
Ce
La
La
Ce
La
Ce
La

of calcioancylite it is tentatively identified as a newly recognized rare-earth carbonate.

Burbankite and carbocernaite are relatively rare constituents of I-type carbonatites and are absent in the majority of the dikes and veins. Burbankite forms irregular-shaped microcrystalline aggregates, often with fluorite, that replace the coarser-grained strontian calcite matrix (Fig. 52a). The mineral is colorless in thin section and possesses low birefringence with interference colors restricted to first order grays and whites. The mineral lacks distinct crystal form and exhibits conchoidal fracture with no apparent cleavage (Fig. 52b). A microprobe x-ray energy spectrum of a typical crystal is presented in Figure 52c and suggests a composition comparable to analyses of burbankite from the Bear Paw Mountains of Montana (Pecora and Kerr, 1953, p. 1173).

Carbocernaite forms prismatic crystals up to 2 mm in length that are commonly surrounded by a cryptocrystalline mixture of clays, iron oxides and barite (Fig. 53a). The mineral is biaxial negative with 2V angles between 50 and 60 degrees and interference colors and relief that are slightly lower than the surrounding strontian calcite matrix. The mineral generally exhibits well-developed orthorhombic crystal form with moderate to poor cleavage (Fig. 53b). The approximate composition of the mineral, as suggested by its microprobe x-ray energy spectrum (Fig. 53c), is consistent with analyses of carbocernaite from the Vuorjarvi massif, Kola Peninsula, U.S.S.R. (Bulakh and others, 1961, p. 1202).

A newly recognized rare-earth phosphate occurs in trace amounts in one of the subsurface dikes where it forms radiating clusters composed of minute, cigar-shaped crystals less than 1.0 mm in length (Fig. 54a and b). The mineral is uniaxial negative and ranges in color from

Figure 52. Burbankite.

(a.) Photomicrograph of microcrystalline granular burbankite (B) and fluorite (F) replacing fine to medium-grained strontian calcite (Sr-C) in I-type carbonatite (sample WBD-10/495.5). Bar scale represents 0.25 mm. Crossed polars.

(b.) Secondary electron photomicrograph of anhedral burbankite (B) in I-type carbonatite (sample WBD-10/495.5). Note conchoidal fracture. Bar scale represents 10 microns.

(c.) Electron microprobe x-ray energy spectrum of burbankite in I-type carbonatite (sample WBD-10/495.5).

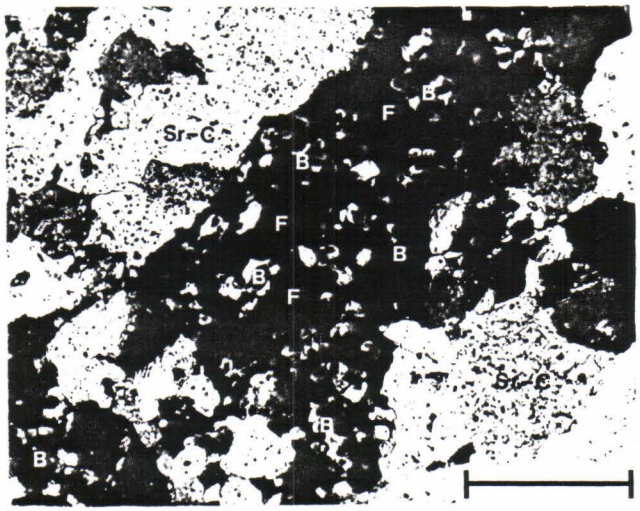
Sr-C
B
F
B
F
B
B
F
B
B
Sr-C
B
B

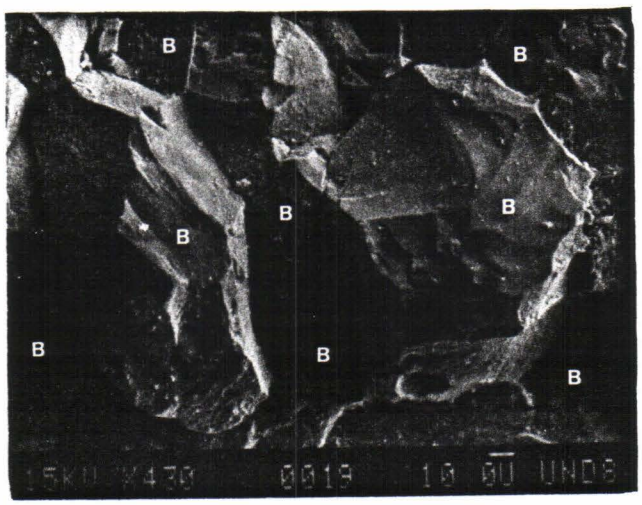
B
B
B
B
B
B
B
B
B
15KV X430 0019 10 00 UNDS

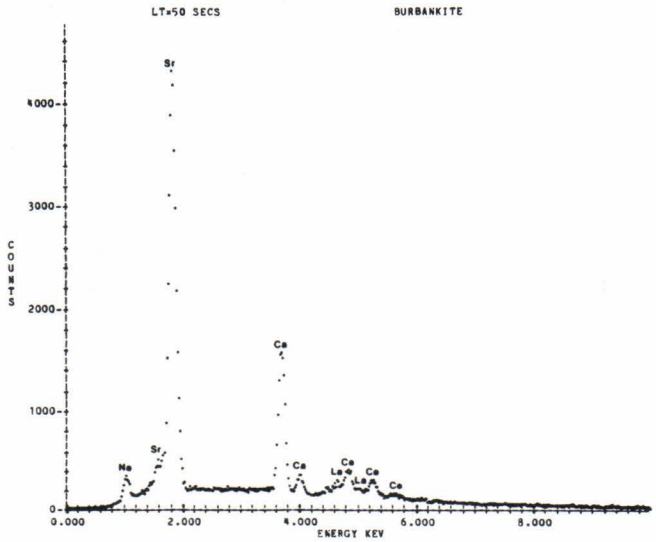
LT=50 SECS
BURBANKITE
Sr
4000
3000
2000
1000
0
COUNTS
Ce
Sr
Na
Ca
Ce
La
Ce
Ca
Ce
0.000
2.000
4.000
6.000
8.000
ENERGY KEV

Figure 53. Carbocernaite

(a.) Photomicrograph of medium-grained, euhedral to subhedral carbocernaite (C) in I-type carbonatite (sample WBD-12/1233.0). Turbid areas composed of clays and iron oxides (F+CL). Surrounding matrix consists of fine to medium-grained strontian calcite (Sr-C). Bar scale represents 0.25 mm. Plane-polarized light

(b.) Secondary electron photomicrograph of euhedral carbocernaite (C) in I-type carbonatite (sample WBD-12/1233.0). Bar scale represents 10 microns.

(c.) Electron microprobe x-ray energy spectrum of carbocernaite in I-type carbonatite (sample WBD-1233.0).

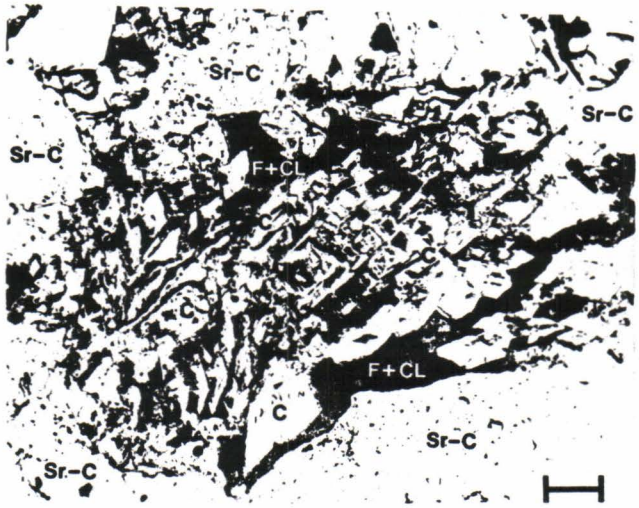
Sr-C
Sr-C
Sr-C
F+CL
C
C
F+CL
C
Sr-C
Sr-C

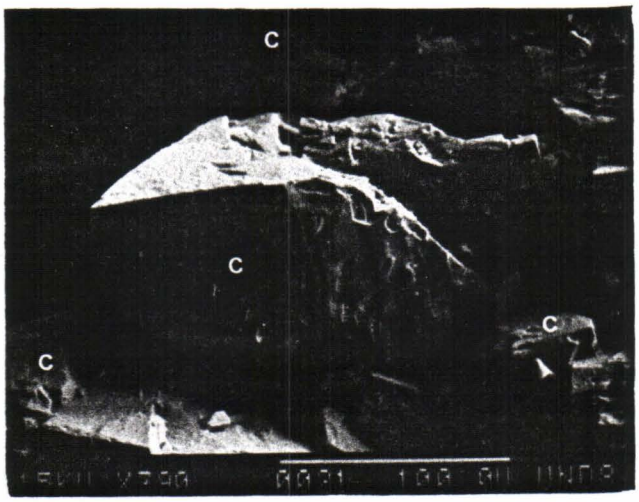
C
C
C
C

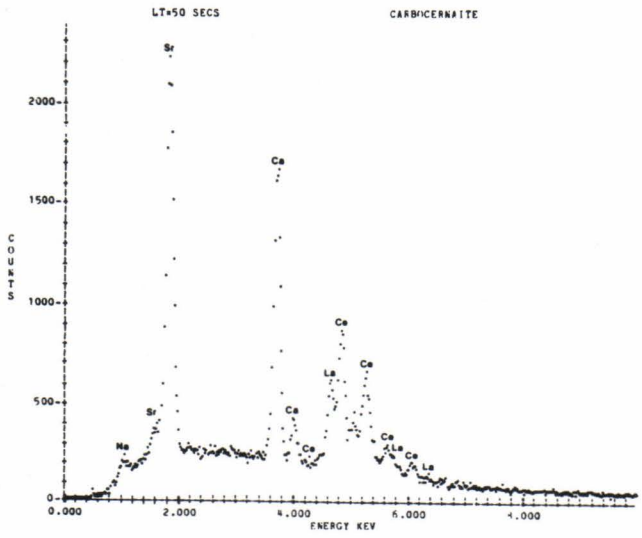
LT=50 SECS
CARBOCERNAITE
Sr
Ca
Ce
Ce
La
Ce
Sr
Ca
Ce
Ce
La
Ce
La
Na
2000
1500
1000
500
0
COUNTS
0.000
2.000
4.000
6.000
8.000
ENERGY KEV

Figure 54. Rare-earth phosphate

(a.) Photomicrograph of radiating rare-earth phosphate (RP) in I-type carbonatite (sample WBD-10/1471.3). Surrounding matrix composed of strontian calcite (Sr-C). Bar scale represents 0.25 mm. Plane-polarized light.

(b.) Secondary electron photomicrograph of radiating, cigar-shaped, crystals of rare-earth phosphate (RP) in I-type carbonatite (sample WBD-10/1471.3). Note strontian calcite (Sr-C) in lower left of photomicrograph. Bar scale represents 10 microns.

(c.) Electron microprobe x-ray energy spectrum of rare-earth phosphate mineral in I-type carbonatite (Sample WBD-10/1471.3).

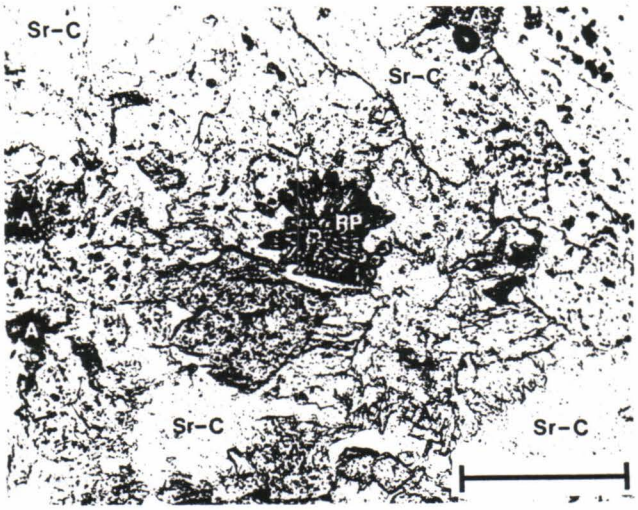
Sr-C
Sr-C
RP
Sr-C
Sr-C


RP
RP
RP
Sr-C

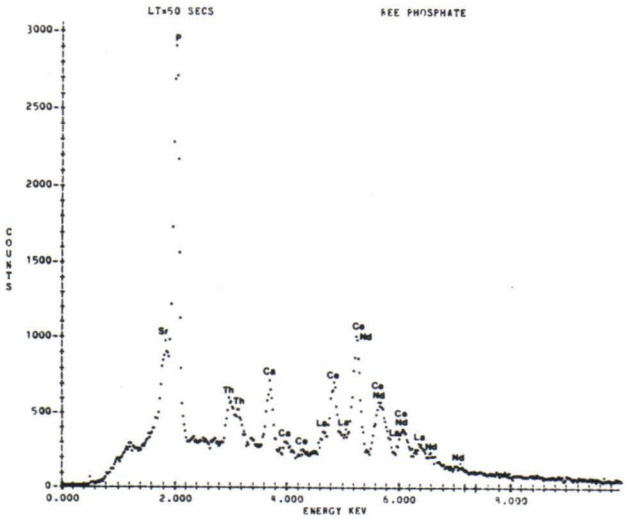
LT=50 SECS
REE PHOSPHATE
3000
2500
2000
1500
1000
500
0
COUNTS
P
Sr
Th
Ce
Nd
La
0.000
2.000
4.000
6.000
8.000
ENERGY KEV

greenish brown to yellowish brown with relief significantly higher than the surrounding strontian calcite matrix. A microprobe x-ray energy spectrum, illustrated in Figure 54c, indicates the presence of phosphorous, strontium, calcium, thorium, cerium, lanthanum, and neodymium, a suite of elements that is similar to the suite for the phosphate mineral brockite from the Wet Mountains of Colorado (Fisher and Meyrowitz, 1962, p. 1351). However, brockite is uniaxial positive and its stoichiometry appears to be significantly different than the stoichiometry suggested by the x-ray energy spectrum of the rare-earth phosphate mineral occurring in the Bear Lodge Mountains.

S-type Carbonatites

General

The second variety of carbonatite occurring in the Bear Lodge Mountains, S-type, outcrop several miles to the southeast of the surface exposures of I-type carbonatite. They are located above the southern wall of Ogden Canyon in the SW ¼, SW ¼, Sec. 27, T.52N., R.63W. and the SE ¼, SE ¼, Sec. 28, T.52N., R.63W. (Plate I). The S-type carbonatites have been mapped as xenoliths of Precambrian marble (Chenowith, 1955) and as xenoliths of Pahasapa Limestone (Staatz, 1983). However, they exhibit several features which indicate they are intrusive bodies and represent dikes of carbonate material that have intruded older alkalic igneous rocks. The evidence includes:

1. The dike-like form of the carbonate bodies and their sharp contacts with the surrounding alkalic igneous rocks (Fig. 55). They are tabular in shape and trend in a NNW direction almost perpendicular to the strike of the nearest Paleozoic sedimentary unit.

Figure 55. Dike of S-type carbonatite outcropping above Ogden Canyon in the SW ¼, SW ¼, Sec. 27, T.52N., R.63W.. Hammer approximately 0.5 m in length.

Figure 56. Brecciated xenoliths of latite and trachyte porphyries (shown by arrows) in dike of S-type carbonatite.

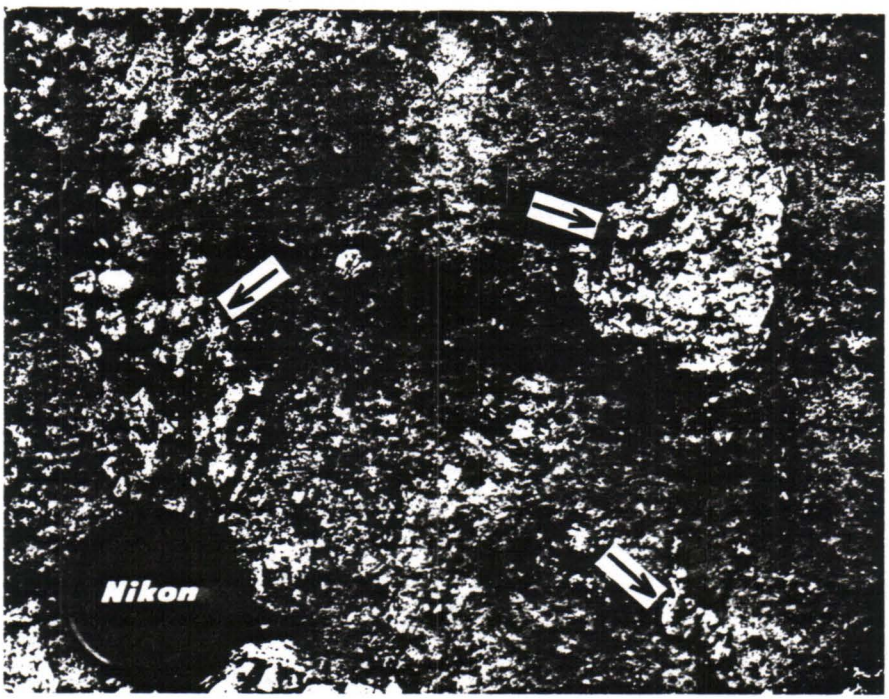
Nikon

2. The lack of bedding, fossils, or other features indicative of a sedimentary origin.

3. The presence of numerous xenoliths of latite and trachyte porphyries (Fig. 56). They are highly fractured and veined which indicates that the carbonate material was injected into older and obviously solidified igneous material.

4. The presence of sandstone xenoliths, presumably derived from the nearby Deadwood Formation. Diagenetic quartz overgrowths are preserved in several of the xenoliths (Fig. 57).

5. The occurrence of small veins of carbonate material in the wall rocks adjacent to the outcrops. Many of the veins "dehydrate" the sericite in altered feldspars of the wall rocks, suggesting that the carbonate material was emplaced at relatively high temperatures (Fig. 58).

The dikes of S-type carbonatite range up to 20 m in thickness with the longest exposed over a distance of approximately 100 m. They are less altered than the surface dikes of I-type carbonatite and appear light gray to medium gray in color with only slight to moderate iron oxide staining.

Petrography

S-type carbonatites are holocrystalline and fine-grained with allotriomorphic granular textures. They have a mottled appearance in shades of light gray, grayish brown, and rust-orange with localized patches of purple fluorite and dendritic coatings of black pyrolusite.

Calcite is the principle carbonate mineral, composing between 90 and 95 percent of the rock. It lacks the strontium enrichment that is characteristic of the calcite of I-type carbonatites. Siderite occurs in several samples but is generally a minor constituent of the rock.

Other minerals that occur in the dikes are sanidine, quartz, chalcedony, barite, and oxides of iron, titanium, and manganese. Most of the sanidine and quartz occurs within the xenoliths of the

Figure 57. Photomicrograph of sandstone xenoliths from the Late Cambrian-Early Ordovician Deadwood Formation (SS) in S-type carbonatite (sample 27-292). Note preservation of diagenetic quartz overgrowths (arrows). Surrounding matrix composed mostly of fine-grained calcite (C). Bar scale represents 0.25 mm. Crossed polars.

Figure 58. Photomicrograph of vein of S-type carbonatite (CV) crosscutting plagioclase phenocryst (P) in latite porphyry (sample 27-191A). Plagioclase phenocryst altered to sericite except in area adjacent to veinlet where it appears clear and devoid of sericite (arrows). Bar scale represents 0.25 mm. Crossed polars.

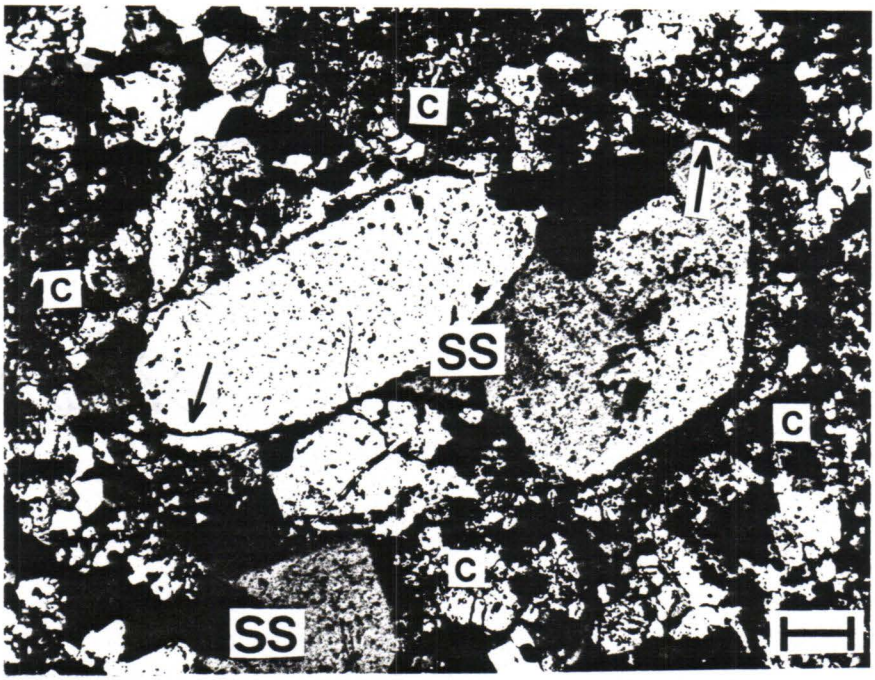
C
C
SS
C
C
SS

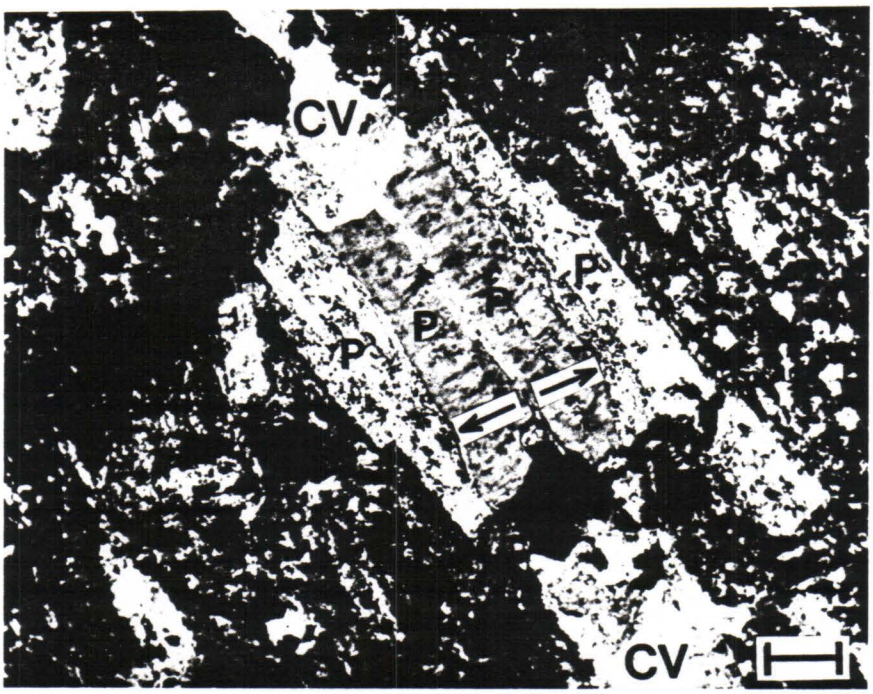
CV
P
P
P
P
CV

surrounding igneous and sedimentary rocks. The chalcedony forms irregular-shaped patches, often with inclusions of barite, that replace the calcite matrix. The oxides of iron, titanium, and manganese occur as alteration materials of original pyrite and manganese-rich ilmenite. Strontianite and rare-earth minerals, important constituents of the I-type carbonatites, are absent in S-type carbonatites.

Stable Isotope Geochemistry

There exist two major schools of thought regarding the origin of carbonatites. One is that carbonatites are derived through the assimilation of either sedimentary limestone or metamorphic marble by an ascending magma, a notion first proposed by Daly (1910, 1933). The second, more widely accepted hypothesis, is that carbonatites are magmatic in origin and form from juvenile CO_2. (Heinrich, 1966, p. 272-329).

Recent studies of the isotopic compositions of carbon and oxygen in carbonatitic calcites provide a strong argument for the magmatic model. Results have shown that values of $\delta^{13}C$ and $\delta^{18}O$ are relatively uniform and significantly lower than values in calcites from marine limestone (Baertschi, 1957; Gonfiantini and Tongorgi, 1964; Kukarenko and Dontsova, 1964; Taylor and others, 1967; Conway and Taylor, 1969; Deines, 1970; Deines and Gold, 1973). Conway and Taylor (1969, p. 618) conclude "it is improbable that limestone could be the source of carbonatitic material except through complete isotopic reconstitution at great depth".

Oxygen isotope geothermometry based upon coexisiting calcite-magnetite pairs from the Oka, Quebec and Magnet Cove, Arkansas carbonatites provide additional evidence in support of the magmatic

model. Equilibration temperatures range between 595° and 855°C, values that are comparable to estimates for the crystallization temperatures of other plutonic igneous rocks such as gabbros and granites (Conway and Taylor, 1969).

Based upon their study of the carbonatites of the Laacher See district of West Germany and the Alnö Island district of Sweden, Taylor and others (1967) have proposed, as a "working hypothesis", that the isotopic range for calcites from primary igneous carbonatites is between -8.0 and -5.0 per mil relative to PDB for carbon and between +6.0 and +8.5 per mil relative to SMOW for oxygen. Because the values of $\delta^{13}C$ for carbonatitic calcites are nearly identical to values determined for mantle-derived diamonds and kimberlitic calcites (Deines and Gold, 1973; Deines, 1980) and the values of $\delta^{18}O$ are virtually the same as values determined for mantle-derived ultramafic and mafic rocks (Taylor, 1968), it has been suggested that carbonatites form from mantle-derived CO_2 of relatively uniform composition.

The isotopic compositions of carbon and oxygen have been determined for calcites from the I-type and S-type carbonatites of the Bear Lodge Mountains. They are compared with compositions determined for sedimentary calcites from the Mississippian Pahasapa Limestone, the major carbonate unit that outcrops along the flanks of the uplift (Table 26).

The isotopic compositions of carbon and oxygen in calcites from the unaltered drill cores of I-type carbonatite exhibit a rather limited range for both carbon (-7.0 to -10.6 per mil) and oxygen (+7.5 to +9.9 per mil). Three of the ten analyses fall within the field proposed by Taylor and others (1967) for primary igneous carbonatites while the

TABLE 26

CARBON AND OXYGEN ISOTOPIC COMPOSITIONS OF CALCITES FROM I-TYPE CARBONATITES, S-TYPE CARBONATITES, AND THE PAHASAPA LIMESTONE

SAMPLE	SAMPLE TYPE	^{13}C	^{18}O
WBD-5/273.5	ITD	-7.0	+7.7
WBD-5/280.3	ITD	-7.7	+7.5
WBD-5/410.8	ITD	-7.2	+9.0
WBD-5/421.8	ITD	-7.4	+8.3
WBD-5/535.3	ITD	-7.9	+8.7
WBD-7/348.4	ITD	-9.9	+9.5
WBD-7/349.7	ITD	-9.7	+9.2
WBD-10/114.0	ITD	-7.9	+9.9
WBD-12/1402.2	ITD	-10.6	+8.8
WBD-13/1449.3	ITD	-7.7	+9.3
7-795B	ITS	-8.4	+11.6
7-795C	ITS	-7.8	+12.7
8-795D	ITS	-6.9	+11.3
8-795E	ITS	-6.6	+14.4
8-795F	ITS	-6.5	+11.1
27-248	STS	-4.0	+14.7
27-249	STS	-4.1	+12.9
27-292	STS	-2.5	+20.3
27-293	STS	-4.5	+13.9
27-294	STS	-5.5	+12.7
34-229	PLS	-3.2	+22.3
34-343	PLS	+4.1	+21.8
34-345	PLS	-5.0	+24.5
34-356	PLS	-0.1	+10.1
34-443D	PLS	-2.1	+14.9

ITD=I-type carbonatite (drill core); ITS=I-type carbonatite (surface); STS=S-type carbonatite (surface); PLS=Pahasapa Limestone (surface).

remaining seven fall relatively close to the proposed field (Fig. 59). The results are consistent with a primary igneous origin for I-type carbonatites with CO_2 derived from a mantle source region.

In contrast to fresh drill core samples, calcites from the altered and oxidized surface exposures of I-type carbonatite exhibit a significant enrichment in ^{18}O. Differences in the isotopic composition of carbon between the two types of carbonatite are negligible. The enrichment of ^{18}O is probably related to isotopic exchange between the calcites of I-type carbonatites and the hydrothermal solutions responsible for the alteration and oxidation of the samples. One of the notable characteristics of the hydrothermal alteration in the Bear Lodge Mountains is that it appears most severe at or near the surface and gradually diminishes with depth, a feature that strongly suggests a hydrothermal system dominated by heated meteoric groundwaters. However, meteoric groundwaters are typically +5 to +10 per mil lighter in ^{18}O relative to SMOW (Taylor, 1971; Hoefs, 1980) and therefore, much lighter in ^{18}O than the calcites of altered I-type carbonatites. If heated meteoric groundwaters are responsible for the ^{18}O enrichment in the calcites from the altered surface exposures of I-type carbonatites, then isotopic exchange must have occurred at relatively lower, nonmagmatic temperatures where fractionation of ^{18}O into calcite would tend to be greater than the fractionation of ^{16}O.

Calcites fron altered and oxidized surface exposures of S-type carbonatite also exhibit a significant enrichment in ^{18}O relative to the fresh drill core samples of I-type carbonatite as well as a less pronounced enrichment in ^{13}C. The enrichment in ^{18}O is probably, in part, attributable to exchange with hydrothermal solutions in a manner

Figure 59. Plot of $\delta^{13}C$ versus $\delta^{18}O$ comparing compositions of calcites from subsurface I-type carbonatites (closed circles), surface exposures of I-type carbonatites (open circles), surface exposures of S-type carbonatites (open triangles), and surface exposures of the Early Mississippian Pahasapa Limestone (closed squares). Also shown is the probable field of primary igneous carbonatite proposed by Taylor and others (1967).

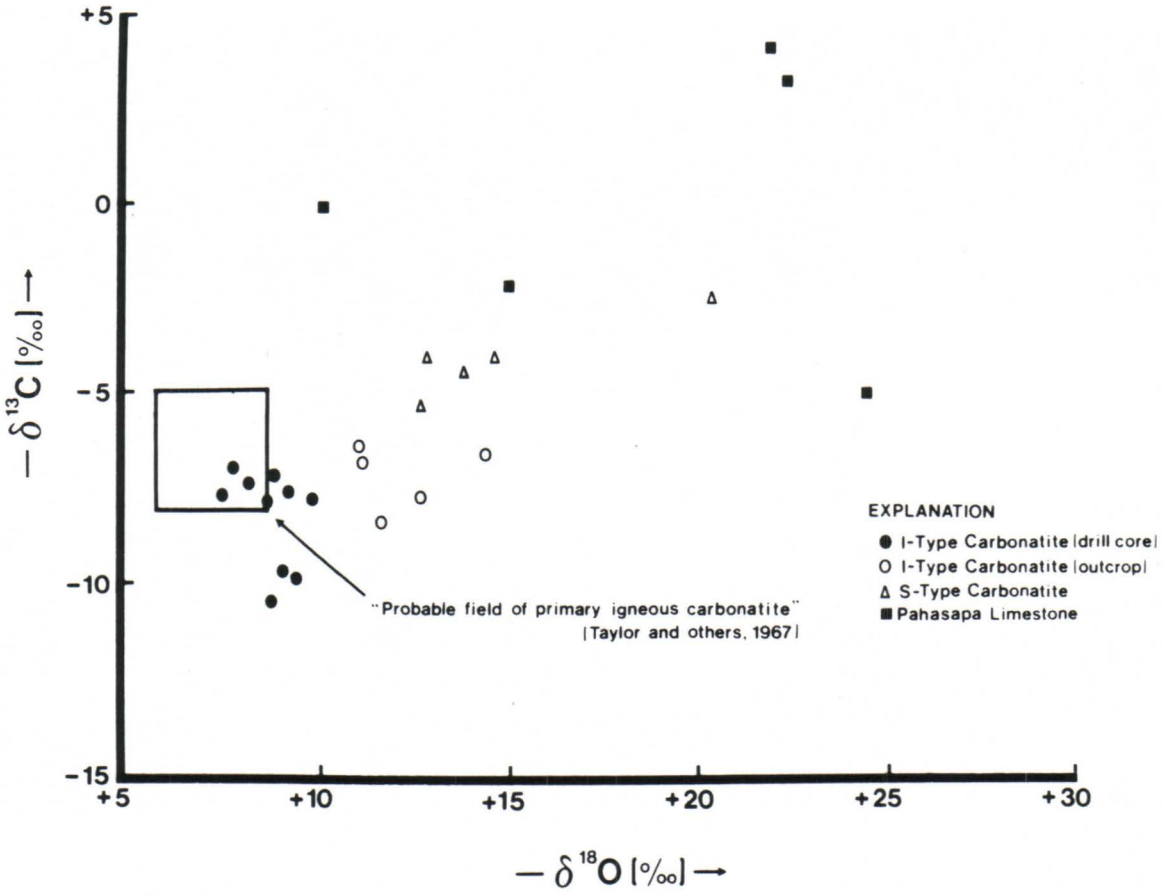
+5
0
-5
-10
-15
+5
+10
+15
+20
+25
+30
$-\delta^{13}C$ [‰] →
$-\delta^{18}O$ [‰] →
"Probable field of primary igneous carbonatite"
(Taylor and others, 1967)
EXPLANATION
● I-Type Carbonatite (drill core)
O I-Type Carbonatite (outcrop)
Δ S-Type Carbonatite
■ Pahasapa Limestone

similar to that proposed for the ^{18}O enrichment in calcites from the altered and oxidized surface exposures of I-type carbonatite. However, the enrichment in ^{13}C is anomolous and, together with the lack of strontianite and rare-earth minerals in S-type carbonatites, suggests a possible genetic difference between S-type and I-type carbonatites.

It is hypothesized that S-type carbonatites resulted from the assimilation of sedimentary limestone by an alkalic silicate magma. The isotopic composition of carbon and oxygen in the calcites from S-type carbonatites approach the compositions determined for sedimentary calcites from the Pahasapa Limestone with one of the analyses of S-type carbonatite (sample 27-292) virtually indistinguishable from Pahasapa Limestone (Fig. 59). The depletion of ^{13}C in S-type calcites relative to Pahasapa Limestone calcites is possibly attributable to loss of CO_2 by degassing during assimilation or by limited isotopic exchange with the intruding magma.

Liquid immiscibility between coexisting silicate and carbonate melts has been demonstrated experimentally in several systems (Koster van Groos and Wyllie, 1966, 1968, 1973; Wendlandt and Harrison, 1979; Freestone and Hamilton, 1980). Thus if sedimentary limestone was assimilated by a silicate magma in the Bear Lodge Mountains it is probable that the resulting carbonate melt existed immiscibly within the silicate magma. A similar interpretation has been proposed for carbonate ocelli occurring in diabase dikes of the Tarr albitite complex of the southeastern Sinai (Bogoch and Magaritz, 1983). The carbonate ocelli, which lack the light rare-element signature of igneous carbonatites (Gold, 1963), are believed to represent immiscible segregations formed by stoping and melting of marble wallrocks by the

intruding diabase magma. It is interesting to note that the calcites of the ocelli are depleted in ^{13}C relative to the calcites of the surrounding marble wallrocks by approximately 1 to 8 per mil, a depletion that is similar in magnitude to that observed between calcites of S-type carbonatites and Pahasapa Limestone in the Bear Lodge Mountains.

To conclude, the isotopic compositions of carbon and oxygen in calcites from I-type carbonatites, S-type carbonatites, and the Pahasapa Limestone suggest: (1) I-type carbonatites are of primary igneous origin and formed from mantle-derived CO_2; (2) hydrothermal alteration, if it involved heated meteoric groundwaters, occurred at lower, nonmagmatic temperatures; and (3) S-type carbonatites formed through the stoping and assimilation of sedimentary limestone by an alkalic silicate magma.

Hydrothermal Activity

Hydrothermal activity in the Bear Lodge Mountains appears to have been intimately associated with the episodes of early igneous activity, potassic fenitization, and carbonatite magmatism. Along the southeastern flank of the uplift dikes of younger and less altered latite and trachyte porphyries frequently crosscut older and more altered dikes of latite and trachyte porphyries (Fig. 60). The sharp contacts between the two types of intrusion indicate that the older dikes were hydrothermally altered prior to the emplacement of the younger dikes, thus proving that the hydrothermal activity was contemporaneous with the episode of early igneous activity and began prior to the episodes of potassic fenitization and carbonatite magmatism. The presence of altered mafic crystals enclosed within fresh, vitreous crystals of fenitic sanidine also indicates that hydrothermal processes were active prior to the periods of potassic fenitization and carbonatite magmatism (Fig. 61). The alteration and oxidation of potassic fenites and I-type carbonatites indicate that hydrothermal processes remained active through the episodes of potassic fenitization and carbonatite magmatism or, alternatively, occurred sometime after these events.

The mineralogic changes associated with hydrothermal alteration are best observed in latite and trachyte porphyries that are exposed along the southeastern flank of the uplift. The rocks exhibit a complete progression from relatively unaltered to severely altered and oxidized (Fig. 62a, b, and c).

Unaltered specimens of latite and trachyte porphyries contain relatively pristine phenocrysts of plagioclase, sanidine, hastingsite,

Figure 60. Dike of lighter colored, younger and less altered latite/trachyte porphyry ($L\text{-}T_Y$) crosscutting older and more altered dike of latite/trachyte porphyry ($L\text{-}T_O$) and altered Precambrian granite (Gr) in the SW ¼, NW ¼, Sec. 27, T.52N., R.63W.. Hammer approximately 0.5 m in length.

Figure 61. Photomicrograph of alkali trachyte (sample 10-393). Fresh, vitreous sanidine (S) mantling altered mafic (M). Bar scale represents 0.25 mm. Crossed polars.

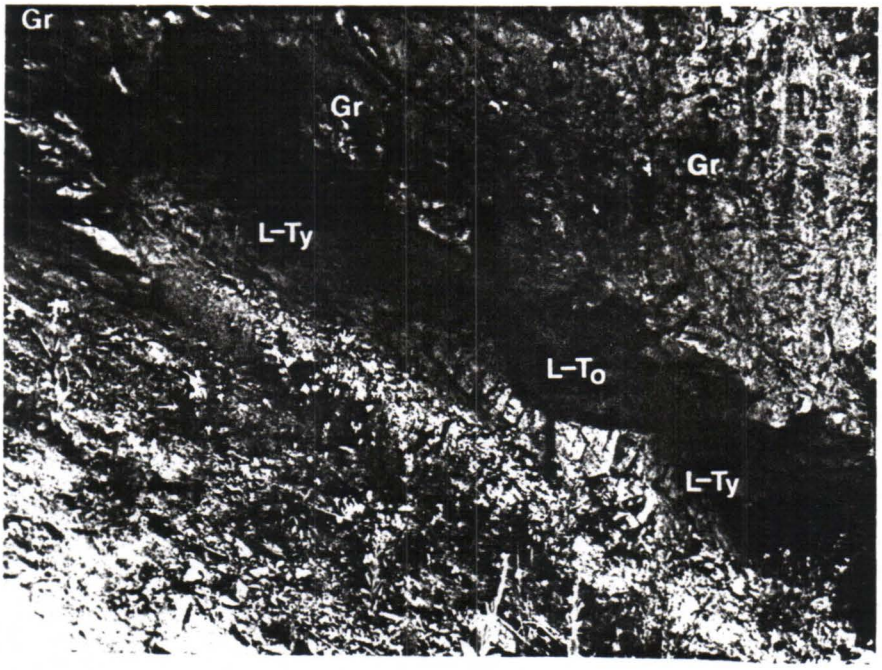
Gr
Gr
Gr
L–Ty
L–To
L–Ty

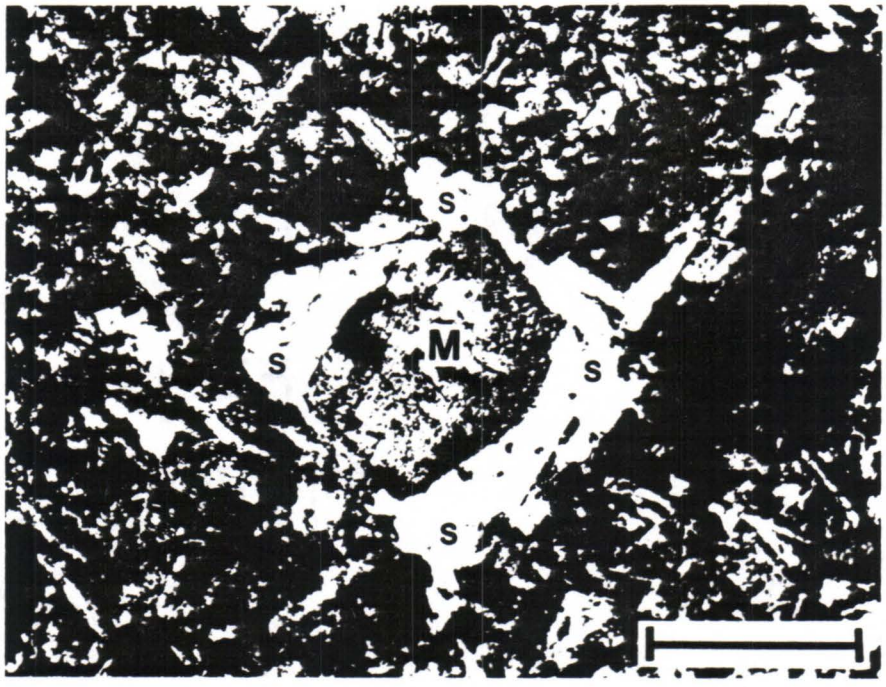
S
S
M
S
S

Figure 62. Photomicrographs showing mineralogic changes associated with hydrothermal changes in latite and trachyte porphyries.

(a.) Photomicrograph of relatively unaltered trachyte porphyry (sample 21-56B). Phenocrysts of plagioclase (P), hastingsite (H), salite (Sa), apatite (Ap), sphene (Sp), and titanian magnetite (Tm) enclosed within a microcrystalline groundmass rich in sanidine. Bar scale represents 0.25 mm. Plane-polarized light.

(b.) Photomicrograph of moderately altered latite porphyry (sample 34-339). Plagioclase phenocrysts (P) altered to a mixture of calcite and clays, especially more calcic cores and growth bands. Original hastingsite (aH) and salite (aSa) are completely replaced by a microcrystalline mixture of biotite and calcite. Titanian magnetite (Tm) exhibits incipient alteration to iron oxides. Bar scale represents 0.25 mm. Plane-polarized light.

(c.) Photomicrograph of highly altered trachyte porphyry (sample 21-54). Plagioclase phenocrysts (P) show more advanced alteration to calcite and clays. Mafic minerals (hastingsite and salite) and opaque (titanian magnetite) are completely dissolved, resulting in prismatic holes (Ho). Bar scale represents 0.25 mm. Plane-polarized light.

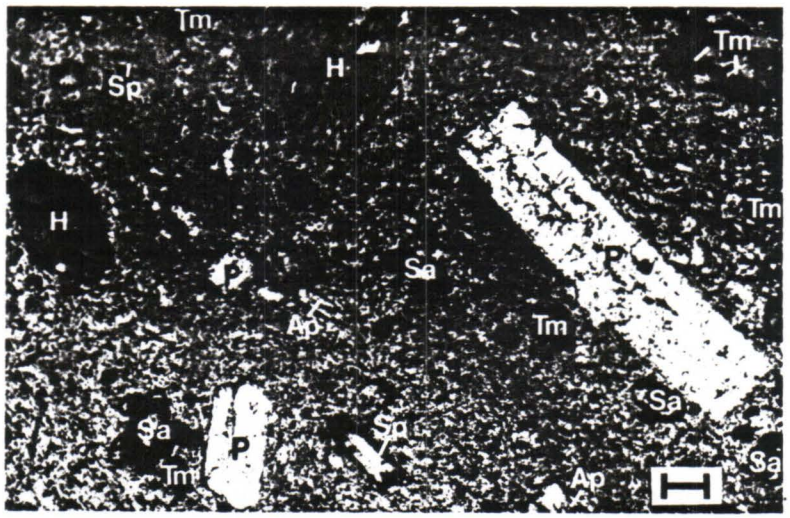
Tm
Sp
H
Tm
H
Tm
P
Sa
Ap
Tm
Sa
Sa
P
Sp
Tm
Ap
Sa
H


aH
aH
P
aH
P
P
aH
P
P
Tm
aSa
aH
P
Tm
aSa
aH
H

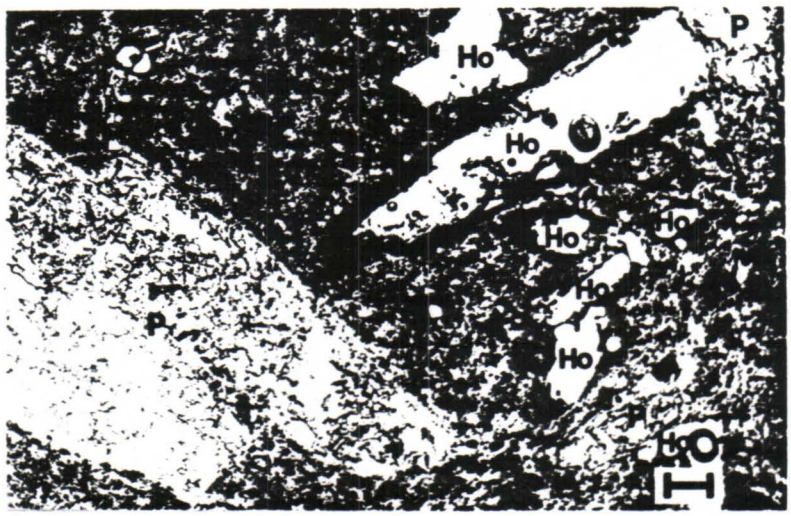
A
Ho
P
Ho
Ho
Ho
Ho
P
Ho
H

salite, apatite, sphene, and titanian magnetite. The phenocrysts are enclosed within a microcrystalline groundmass rich in sanidine (Fig. 62a).

In moderately altered samples of latite and trachyte porphyries the more calcic regions of the zoned plagioclase phenocrysts are replaced by a cryptocrystalline mixture of calcite and clays while the sanidine phenocrysts and groundmass sanidine exhibit incipient sericitization (Fig. 62b). Hastingsite and salite phenocrysts are partially to completely replaced by a fine-grained mixture of biotite and calcite while sphene and titanian magnetite are altered to oxides of iron and titanium. Apatite crystals appear unaffected by the alteration.

In severely altered samples of latite and trachyte porphyries the apatite crystals still remain relatively fresh while the zoned plagioclase phenocrysts exhibit further replacement by calcite and clays (Fig. 60c). The sanidine phenocrysts and groundmass sanidine display more advanced stages of sericitization and the crystals of hastingsite, salite, sphene, and titanian magnetite are replaced by oxides of iron and titanium or, more commonly, are completely dissolved with only prismatic casts as remnants.

The effects of the hydrothermal activity in the Bear Lodge Mountains are most pervasive in the central portions of the uplift where the zone of oxidation and alteration extends to depths of several tens of meters in the subsurface. As noted earlier (p. 158), the observation that the alteration and oxidation gradually diminishes with depth suggests that the hydrothermal system was dominated by the circulation of heated meteoric groundwaters, probably in a fashion similar to modern geothermal areas such as the Yellowstone region in Wyoming, Montana, and

Idaho or the Salton Sea region in California. A high geothermal gradient, which undoubtedly existed in the Bear Lodge Mountains region during Eocene time, could have provided the necessary heat to initiate and maintain circulation of the meteoric groundwaters.

The hydrothermal activity in the Bear Lodge Mountains appears to have been of little economic significance other than to oxidize potentially economic minerals associated with episodes of potassic fenitization and carbonatite magamatism. A possible exception is noted in the NW ¼, NW ¼, Sec. 17, T.52N., R.63W. where a small prospect pit exposes copper oxide mineralization. The copper oxides are probably associated with the hydrothermal activity, although the copper was probably oxidized and leached from chalcopyrite of the surrounding fenites by the hydrothermal solutions.

Late Igneous Activity

The final petrologic event to occur in the Bear Lodge Mountains, termed "late igneous activity", is represented by a suite of unaltered, undersaturated, hypabyssal alkalic igneous rocks which crosscut the older, hydrothermally rock types that are associated with earlier petrologic events. The rocks emplaced during the period of late igneous activity are analcime phonolite porphyries (Table 27) and they represent the final pulse of igneous activity to occur in the Bear Lodge Mountains.

The late emplacement of analcime phonolite porphyries in the Bear Lodge Mountains appears to related to a regional pattern of phonolitic magmatism that occurred in the northern Black Hills during Eocene time. Phonolite porphyries, compositionally and texturally similar to those of the Bear Lodge Mountains, occur at other igneous centers in the northern Black Hills including Devils Tower, Missouri Buttes, and Barlow Canyon in Wyoming (Halvorson, 1980) and Rubicon Gulch, Little Crow Peak, Ragged Top Mountain, Spearfish Canyon, Spearfish Peak, and other centers in South Dakota (Kirchner, 1971). At a number of the South Dakota locations the phonolite porphyries reportedly crosscut older, hydrothermally altered igneous rocks that include quartz latites, latites, and trachytes (Kirchner, 1971), a situation that is remarkably similar to relationships observed in the Bear Lodge Mountains.

Analcime Phonolite Porphyries

General

Two varieties of analcime phonolite porphyries are exposed at the

TABLE 27

MODAL ANALYSES OF ANALCIME PHONOLITE PORPHYRIES

SAMPLE	A	B	C	D	E	F
Primary						
Groundmass						
Sanidine	56.0	50.6	31.1	33.7	38.9	36.4
Anorthoclase	0.0	0.0	1.9	11.4	0.0	2.7
Analcime	16.8	17.5	22.5	4.2	8.0	18.6
Aegirine	8.0	10.5	6.9	8.3	10.9	5.4
Calcite	2.2	1.4	0.0	0.0	0.0	1.3
Sanidine	2.0	1.8	8.2	16.8	3.4	9.8
Analcime	1.8	tr.	4.0	1.2	1.0	3.4
Sodalite	4.4	8.6	0.0	0.0	0.0	0.0
Haüyne	0.0	0.0	2.2	3.6	2.0	5.0
Aegirine-augite	tr.	0.6	2.2	1.6	tr.	6.0
Melanite	0.2	0.8	tr.	0.0	0.0	0.0
Biotite	0.4	0.6	0.0	0.0	0.0	0.0
Apatite	tr.	0.2	0.0	0.2	0.0	0.6
Sphene	tr.	tr.	tr.	0.6	0.0	tr.
Titanian magnetite	0.0	tr.	0.0	0.2	0.0	tr.
Secondary						
Natrolite	5.6	2.0	19.4	15.0	34.2	4.0
Calcite	tr.	1.6	1.0	0.6	0.8	4.0
Sericite/clays	2.0	2.6	0.6	1.0	0.4	2.2
Iron oxides	0.6	1.2	tr.	1.6	0.4	0.6

tr.=trace, less than 0.2% detected

Sample key: A=Sample 21-26A=Sodalite-bearing analcime phonolite porphyry
B=Sample 21-61=Sodalite-bearing analcime phonolite porphyry
C=Sample 21-43=Hauyne-bearing analcime phonolite porphyry
D=Sample 27-126=Hauyne-bearing analcime phonolite porphyry
E=Sample 27-189=Hauyne-bearing analcime phonolite porphyry
F=Sample 22-377=Hauyne-bearing analcime phonolite porphyry

surface in the area of study along the southeastern flank of the Bear Lodge Mountains, haüyne-bearing analcime phonolite porphyry and sodalite-bearing analcime phonolite porphyry. They are found as dikes and small plugs whose characteristically fresh appearances stand in sharp contrast to the altered and oxidized alkalic igneous rocks which they crosscut. They are absent in the subsurface in the central portions of the main igneous dome but are exposed at the surface in other regions of the uplift where they correspond to phonolite, phonolite porphyry, and sodalite-bearing phonolite porphyry reported by O'Toole (1981) in the Houston Creek area, phonolite porphyry reported by Wilkinson (1982) in the Warrens Peaks area, and "younger" trachyte and phonolite dikes described by Staatz (1983) at several locations within the central igneous core.

Petrography

Analcime phonolite porphyries are holocrystalline and distinctly porphyritic. Haüyne-bearing varieties are dark green in color with large phenocrysts of tabular sanidine and small phenocrysts of rounded to hexagonal haüyne (Fig. 63). Sodalite-bearing varieties are dark green to olive green in color and contain small phenocrysts of hexagonal sodalite (Fig. 64). Micrprobe analyses of the major minerals of the rocks are presented in Table 28.

The groundmasses of analcime phonolite porphyries are aphanitic to very fine-grained and compose 60 to 90 percent of the rocks. Sanidine and anorthoclase occur as microlites, 0.1 to 0.2 mm in length, that display trachytic to subtrachytic textures. The microlites are enclosed within an isotropic matrix rich in analcime. Natrolite commonly occurs as an alteration product of the groundmass analcime and often forms

Figure 63. Slab photograph of haüyne-bearing analcime phonolite porphyry (sample 22-377). Large tabular phenocrysts of sanidine (S) and small, rounded to hexagonal phenocrysts of haüyne (Ha) enclosed within a dark, aphanitic groundmass rich in aegirine-augite, sanidine, and analcime.

Figure 64. Slab photograph of sodalite-bearing analcime phonolite porphyry (sample 27-444A). Small, rounded to hexagonal phenocrysts of sodalite enclosed within a dark, aphanitic matrix rich in aegirine-augite, sanidine, and analcime.

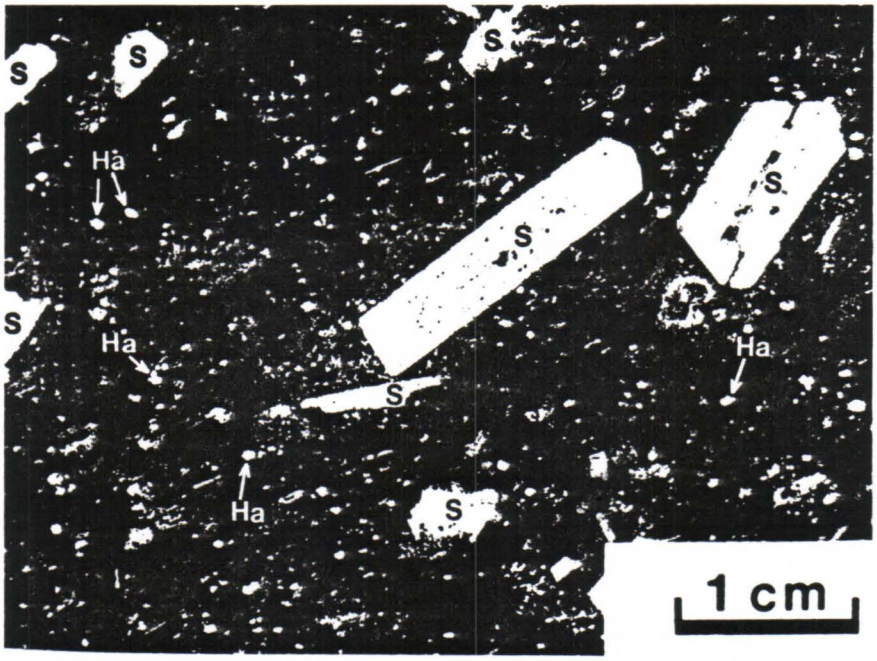
S
S
S
S
S
S
S
S
Ha
Ha
Ha
Ha
1 cm

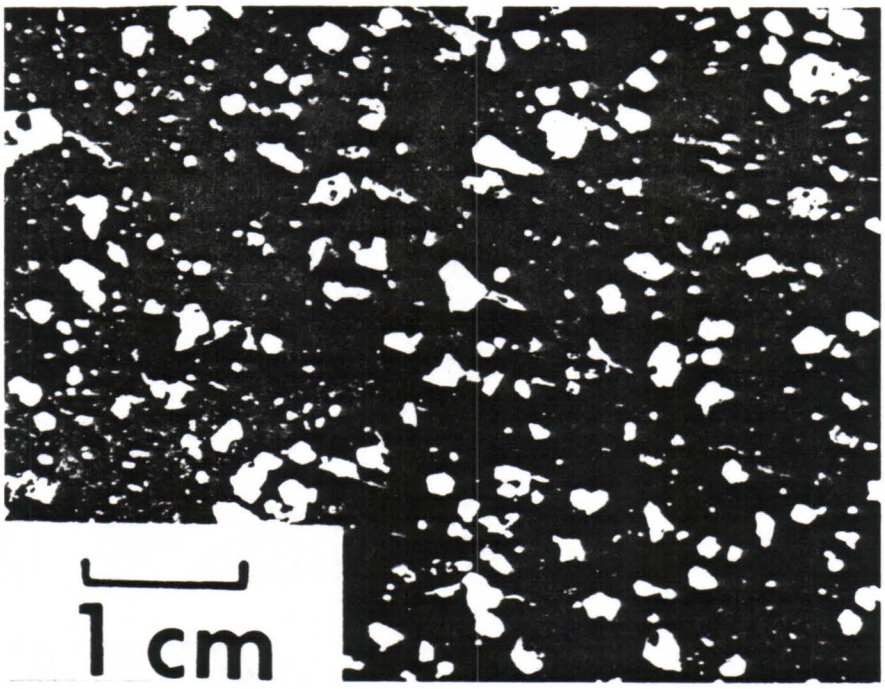
1 cm

TABLE 28

MICROPROBE ANALYSES OF MINERALS IN ANALCIME PHONOLITE PORPHYRIES

SAMPLE	A	B	C	D	E	F	G	H
SiO2	66.82	69.13	68.63	54.50	48.40	66.47	35.40	39.39
Al2O3	19.49	19.22	20.33	24.88	27.63	17.90	28.20	29.74
FeO*	0.00	0.33	0.51	0.40	0.00	0.00	0.47	1.70
MgO	0.00	0.00	0.00	0.00	0.00	0.00	0.00	0.00
CaO	0.00	0.08	0.00	1.16	0.08	0.15	1.56	0.24
Na2O	2.41	11.62	7.41	13.21	15.95	0.46	13.88	23.38
K2O	12.34	0.35	6.62	0.15	0.00	16.00	7.42	0.38
TiO2	0.00	0.00	0.00	0.00	0.00	0.00	0.00	0.00
P2O5	0.00	0.00	0.00	0.00	0.00	0.00	0.00	0.00
MnO	0.20	0.27	0.00	0.10	0.00	0.00	0.00	0.00
Cl	0.00	0.09	0.07	0.00	0.00	0.05	0.00	2.75
SO3	0.00	0.00	0.12	0.00	0.20	0.00	7.36	0.00
Total	101.26	101.09	103.69	94.40	92.26	101.03	94.29	97.58
	Number of cations on the basis of X oxygens							
	X=32	X=32	X=32	X=7	X=80	X=32	X=21	X=21
Si	11.98	12.00	11.85	2.28	23.95	12.13	4.72	5.30
Al	4.12	3.93	4.14	1.23	16.11	3.85	4.43	4.72
Fe	0.00	0.05	0.07	0.01	0.00	0.00	0.05	0.46
Mg	0.00	0.00	0.00	0.00	0.00	0.00	0.00	0.00
Ca	0.00	0.01	0.00	0.05	0.03	0.03	0.22	0.03
Na	0.84	3.91	2.48	1.07	15.30	0.16	3.59	6.10
K	2.82	0.08	1.46	0.01	0.00	3.72	1.26	0.07
Ti	0.00	0.00	0.00	0.00	0.00	0.00	0.00	0.00
P	0.00	0.00	0.00	0.00	0.00	0.00	0.00	0.00
Mn	0.03	0.04	0.00	0.00	0.00	0.00	0.00	0.00
Cl	0.00	0.03	0.02	0.00	0.00	0.01	0.00	0.63
S	0.00	0.00	0.01	0.00	0.07	0.00	0.74	0.00

*Total Fe as FeO

Sample key: A=Sample 217-126=Sanidine (groundmass); B=Sample 22-377=Albite (groundmass); C=Sample 27-126=Anorthoclase; D=Sample 22-377=Analcime (groundmass); E=Sample 27-189=Natrolite (groundmass); F=Sample 21-43=Sanidine (phenocryst); G=Sample 22-377=Haüyne (phenocryst); H=Sample 21-26A=Sodalite (phenocryst).

TABLE 28

(continued)

SAMPLE	I	J	K	L	M	N	O	P
SiO2	51.10	50.15	50.49	34.33	37.56	1.28	30.37	0.00
Al2O3	3.32	2.68	2.03	1.12	12.25	0.18	1.64	0.14
FeO*	11.55	20.98	21.75	24.40	24.55	0.20	2.30	90.97
MgO	10.58	4.38	3.64	0.28	9.54	0.00	0.00	0.00
CaO	21.54	18.48	14.48	32.52	0.00	52.36	27.39	0.00
Na2O	1.41	3.82	5.50	0.00	0.41	0.00	0.00	0.00
K2O	0.00	0.00	0.31	0.00	9.38	0.00	0.00	0.00
TiO2	0.70	0.41	1.33	6.68	2.76	0.00	34.51	2.85
P2O5	0.25	0.00	0.00	0.00	0.00	38.28	0.27	0.00
MnO	0.40	0.82	1.19	0.73	0.89	0.00	0.00	1.06
Cl	0.00	0.00	0.12	0.00	0.06	0.17	0.00	0.00
SO3	0.00	0.00	0.00	0.00	0.00	0.00	0.00	0.00
Total	100.85	101.64	100.84	100.06	97.40	92.47	96.48	95.02
	Number of cations on the basis of X oxygens							
	X=6	X=6	X=6	X=24	X=24	X=26	X=20	X=32
Si	1.92	1.96	1.99	6.01	6.31	0.24	4.12	0.00
Al	0.15	0.12	0.09	0.23	2.43	0.04	0.26	0.06
Fe	0.36	0.68	0.72	3.57	3.45	0.03	0.26	29.87
Mg	0.59	0.25	0.21	0.07	2.39	0.00	0.00	0.00
Ca	0.87	0.77	0.61	6.11	0.00	10.41	3.98	0.00
Na	0.10	0.29	0.42	0.00	0.13	0.00	0.00	0.00
K	0.00	0.00	0.01	0.00	2.01	0.00	0.00	0.00
Ti	0.02	0.01	0.04	0.88	0.35	0.00	3.52	0.84
P	0.01	0.00	0.00	0.00	0.00	6.01	0.03	0.00
Mn	0.01	0.03	0.04	0.11	0.13	0.00	0.00	0.35
Cl	0.00	0.00	0.01	0.00	0.02	0.05	0.00	0.00
S	0.00	0.00	0.00	0.00	0.00	0.00	0.00	0.00

* Total Fe as FeO

Sample key: I=Sample 27-126=Aegirine-augite (phenocryst-core); J=Sample 27-126=Aegirine-augite (phenocryst-rim); K=Sample 21-61=Aegirine-augite (groundmass); L=Sample 21-61=Melanite; M=Sample 21-61=Biotite; N=Sample 22-377=Apatite; O=Sample 27-126=Sphene; P=Sample 27-126=Titanian magnetite.

spectacular clusters of radially arranged crystals (Fig. 65).

The tabular sanidine phenocrysts that are characterstic of haüyne-bearing varieties of analcime phonolite porphyries range from 2 to 30 mm in length and compose between 5 and 20 percent of the rocks. The crystals are typically Carlsbad twinned, euhedral to subhedral in shape, and exhibit well-developed trachytoid textures. Many of the crystals possess corroded and embayed margins, suggestive of magmatic resorbption, and also exhibit partial replacement by analcime and natrolite along microfractures. Smaller untwinned sanidine phenocrysts occur in sodalite-bearing varieties of analcime phonolite porphyries but they are generally minor constituents, composing less than 5 percent of the rocks.

The haüyne phenocrysts of haüyne-bearing analcime phonolite porphyries are chalky white in color and comprise between 1 and 5 percent of the rocks. They occur as equant, subhedral to euhedral crystals with rounded and hexagonal cross-sections between 0.5 and 2.0 mm in diameter. Many of the crystals appear fresh while others are partially to completely replaced by a cryptocrystalline mixture of analcime, clays, and calcite.

The sodalite phenocryts of sodalite-bearing analcime phonolite porphyries are pink to cream white and compose between 2 and 10 percent of the rock. They are often glomerophyrically arranged with individual crystals exhibiting square to hexagonal cross-sections up to 2.0 mm in diameter (Fig. 66). Like the haüyne phenocrysts, they are often partially to completely pseudomorphed by a cryptocrystalline mixture of analcime, clays, and calcite.

Both the haüyne-bearing and sodalite-bearing varieties of analcime

Figure 65. Photomicrograph of haüyne-bearing analcime phonolite porphyry (sample 21-43). Radiating natrolite (N) replacing analcime-rich groundmass (Grm) and sanidine phenocryst (S). Bar scale represents 0.25 mm. Crossed polars.

Figure 66. Photomicrograph of sodalite-bearing analcime phonolite porphyry (sample 21-26A). Rounded to hexagonal phenocrysts of sodalite (So) occurring isolated and cummulophyrically arrranged with zoned melanite garnet (G) and biotite (B). Bar scale represents 0.25 mm. Plane-polarized light.

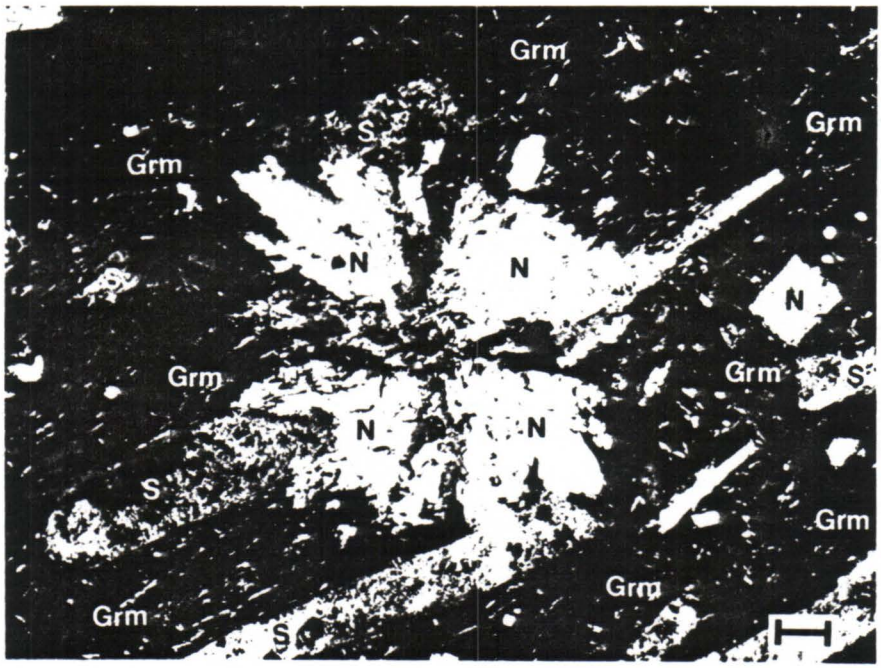
Grm
Grm
S
Grm
N
N
N
Grm
Grm
S
N
N
S
Grm
Grm
Grm
S

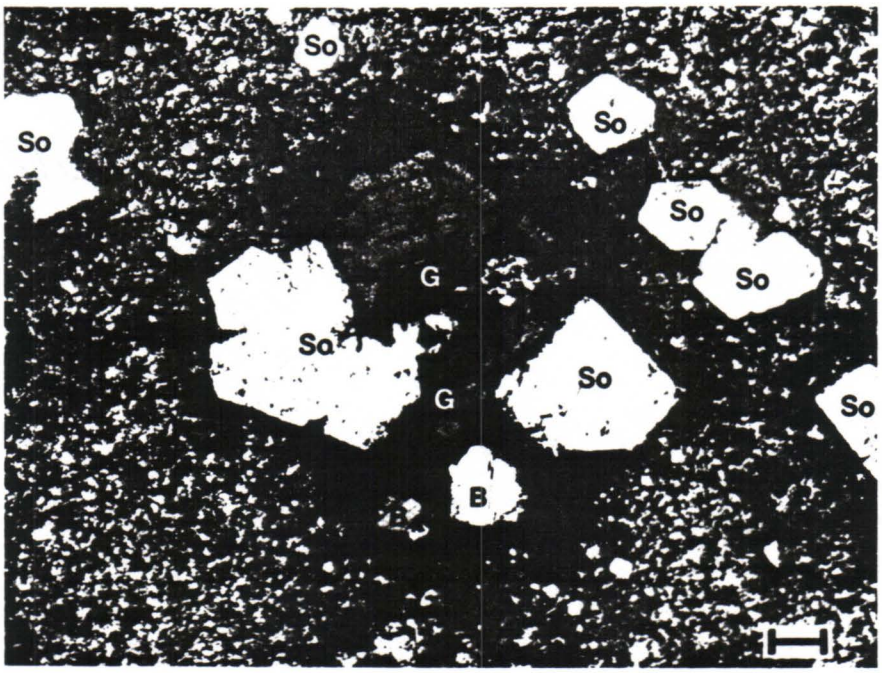
So
So
So
So
So
G
So
So
G
So
B

phonolite porphyries contain clinopyroxene, usually of two generations. An older generation is represented by larger phenocrysts, up to 2.0 mm in length, that typically appear zoned with pale green, aegirine-augite cores, and bright green, aegirine rims. The zoning is normal and oscillatory with sodium and iron concentrations increasing from core to rim and magnesium decreasing (Table 28, columns I and J). Electron microprobe traverses across a typical zoned phenocryst indicate a sawtooth profile with sharp changes in the relative proportions of iron and magnesium from core to rim (Fig. 67a and b). The dark green, iron-rich rims of the crystals are strongly pleochroic with X=emerald green, Y=pale green, and Z=yellowish green.

The younger generation of clinopyroxene occurring in analcime phonolite porphyries consists of acicular aegirine microphenocrysts, up to 0.2 mm in length, that occur within the groundmasses of the rocks. The microphenocrysts are unzoned and possess compositions that are similar to analyses of the aegirine rims of the older clinopyroxene phenocrysts (Table 28, column K). Like the aegirine rims, the microphenocrysts are strongly pleochroic with X=emerald green, Y=pale green, and Z=yellowish green.

Reddish-brown melanite garnet occurs an accessory mineral in the sodalite-bearing varieties of analcime phonolite porphyries but is rare or absent in the haüyne-bearing varieties. The garnet is often found cumulophyrically arranged with sodalite and biotite and occasionally exhibits oscillatory zoning (Fig. 66). Crystals are euhedral to subhedral in shape with hexagonal to rounded cross-sections between 0.5 and 1.0 mm in diameter.

Other accessory minerals occurring in both haüyne-bearing and

Figure 67. Electron microprobe traverse across a zoned aegirine/aegirine-augite phenocryst in haüyne-bearing analcime phonolite porphyry (sample 22-377).

(a.) Photomicrograph of zoned aegirine/aegirine-augite phenocryst showing location of electron microprobe traverse (X-X'). Bar scale represents 0.25 mm. Plane polarized light.

(b.) Electron microprobe traverse (X-X') showing variations in the concentrations of Ca, Na, and K across the zoned aegirine/ aegirine-augite phenocryst shown above.

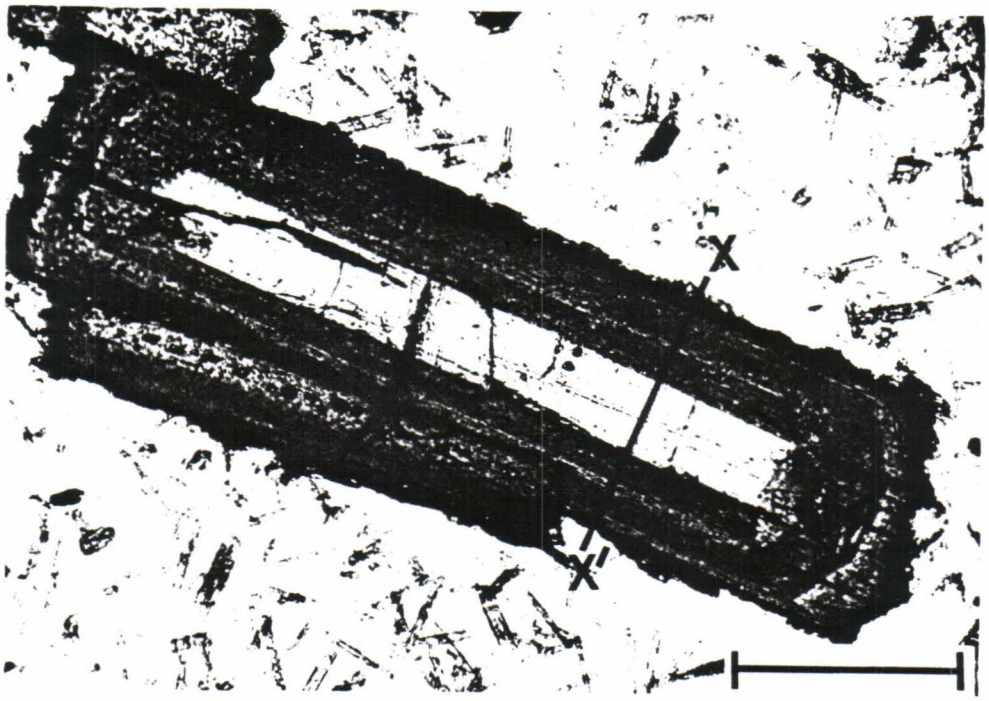
X
X'

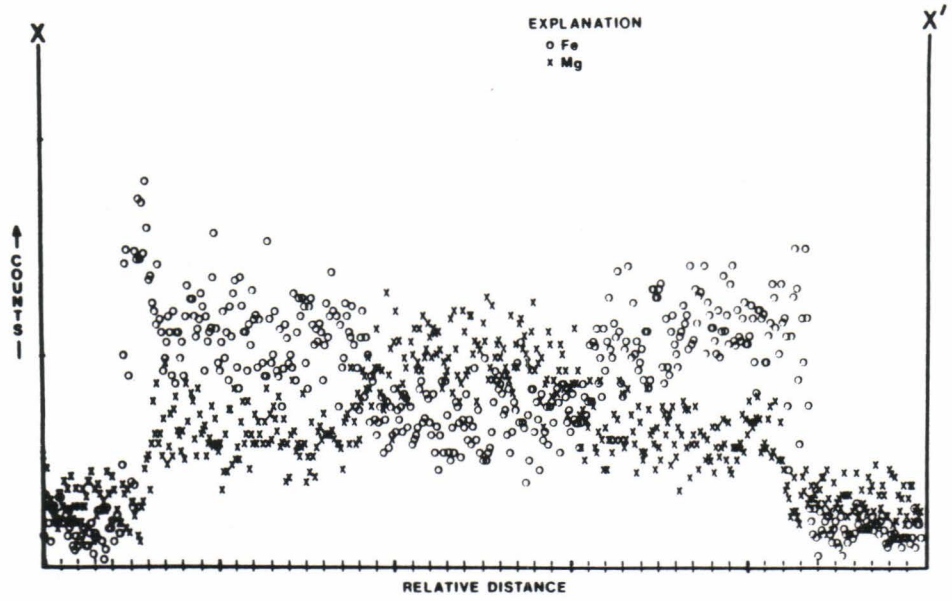
X
X'
EXPLANATION
o Fe
x Mg
COUNTS
RELATIVE DISTANCE

sodalite-bearing varieties of analcime phonolite porphyries are apatite, sphene, and titanian magnetite. Apatite forms euhedral to subhedral crystals with prismatic and hexagonal cross-sections up to 1.0 mm in size. Sphene exhibits diamond or wedge-shaped crystal forms between 0.5 and 2.0 mm in length. Titanian magnetite, which imparts a weakly magnetic character to the rocks, displays square to rectangular cross-sections less than 0.5 mm in size.

Chemistry

Major element chemical analyses and CIPW normative mineralogies of six samples of analcime phonolite porphyries are presented in Table 29. The values of the major oxides are comparable to the values for the average phonolite (Nockolds, 1954, p. 1024). The silica undersaturation of the rocks is reflected by the presence of both normative leucite and nepheline. Sodalite-bearing varieties (columns A and B) are more strongly undersaturated with respect to SiO_2 than the haüyne-bearing varieties (columns C, D, E, and F) although the values of the other oxides are roughly similar. The poor closures of the analyses are, in large part, attributable to the abundance of hydrous phases such as analcime and natrolite.

Differentiation indexes of the samples range from 81 to 90. Their alkalic character is reflected by the relatively high values of total alkalis (Na_2O+K_2O) which vary from 11.6 to 16.6 percent. All of the samples plot in the alkaline field proposed by Irving and Baragar (1971) for volcanic igneous rocks (Fig. 68).

TABLE 29

MAJOR ELEMENT CHEMICAL ANALYSES AND CIPW NORMATIVE MINERALOGIES OF ANALCIME PHONOLITE PORPHYRIES

SAMPLE	A	B	C	D	E	F
SiO_2	44.37	50.37	55.69	57.09	55.14	58.02
Al_2O_3	19.83	20.58	19.23	17.56	18.92	18.64
Fe_2O_3	3.24	3.16	3.40	2.51	3.67	3.28
MgO	0.17	0.19	0.44	0.15	0.97	0.54
CaO	1.70	1.64	1.78	1.63	0.73	2.67
Na_2O	4.93	8.18	6.42	5.58	6.85	5.65
K_2O	8.35	8.38	6.07	6.47	6.18	5.96
TiO_2	0.23	0.29	0.27	0.31	0.27	0.37
P_2O_5	0.02	0.03	0.03	0.08	0.03	0.10
MnO	0.17	0.14	0.16	0.10	0.17	0.12
Total	83.01	92.96	93.49	91.48	92.93	95.35
Or	53.59	45.88	38.37	41.80	39.31	36.94
Ab	0.00	0.00	37.22	44.93	36.76	42.94
An	8.81	0.00	6.12	4.10	2.82	8.28
Lc	4.59	5.80	0.00	0.00	0.00	0.00
Ne	27.23	34.49	11.31	3.62	13.88	3.90
Ac	0.00	5.57	0.00	0.00	0.00	0.00
Nams	0.00	1.04	0.00	0.00	0.00	0.00
Wo	0.00	0.80	0.00	1.27	0.00	0.00
Di	1.02	5.75	2.60	0.88	0.71	3.99
Ol	1.15	0.00	1.00	0.00	3.14	0.12
Mt	3.02	0.00	2.75	1.84	2.76	2.84
Hm	0.00	0.00	0.00	0.71	0.00	0.00
Il	0.53	0.59	0.55	0.64	0.55	0.74
Ap	0.06	0.08	0.08	0.21	0.08	0.25

* Total Fe as Fe_2O_3

Sample key: A=Sample 21-26a; B=Sample 21-61; C=Sample 21-43;
D=Sample 27-126; E=Sample 27-189; F=Sample 22-377

Figure 68. Plot of (Na_2O+K_2O) versus SiO_2 showing Irving and Baragar's (1971) dividing line for making a general distinction between alkaline and subalkaline volcanic igneous rocks. Samples of analcime phonolite porphyry from the southeastern Bear Lodge Mountains (open circles) plot in the alkaline field.

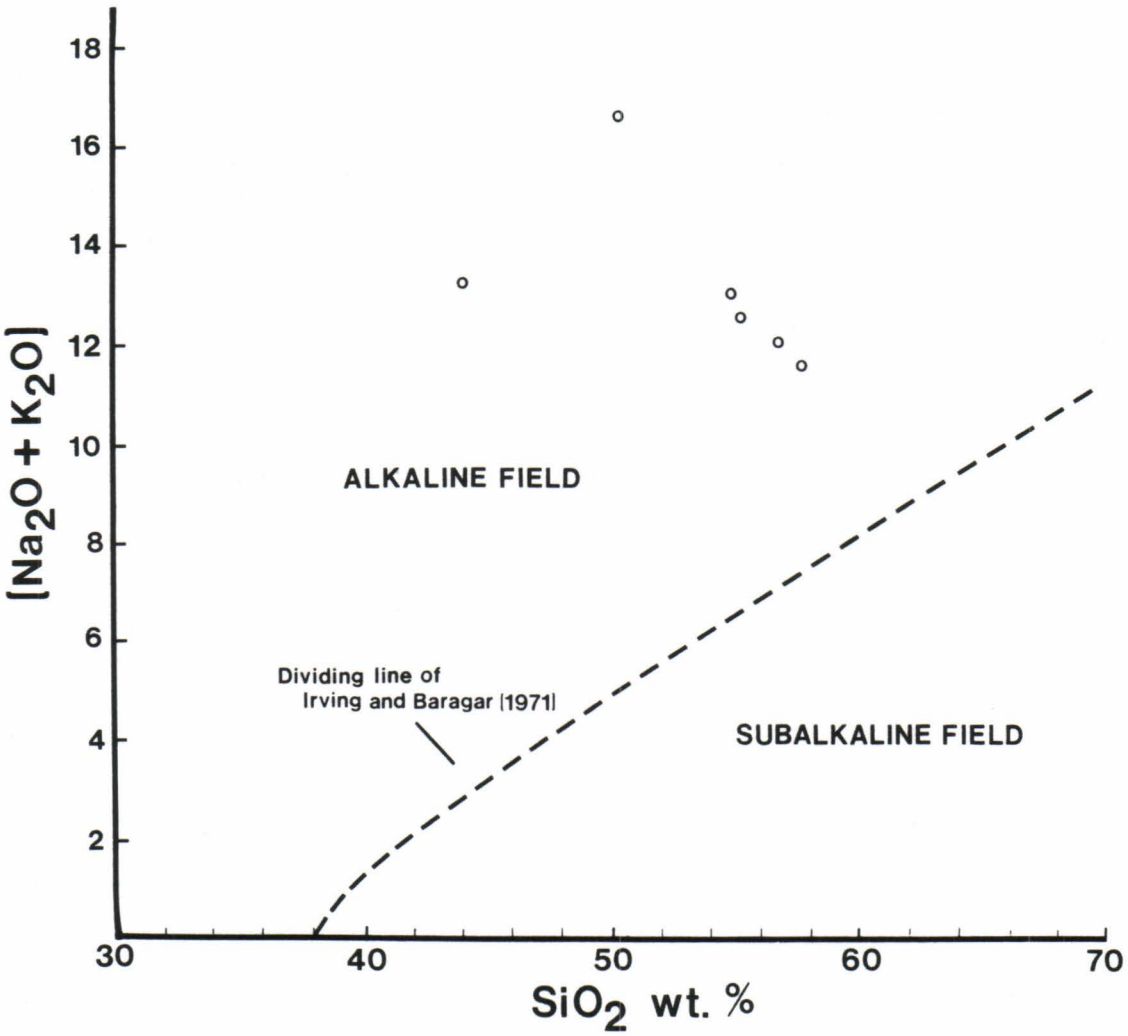
18
16
14
12
10
8
6
4
2
[Na2O + K2O]
ALKALINE FIELD
Dividing line of
Irving and Baragar (1971)
SUBALKALINE FIELD
30
40
50
60
70
SiO2 wt. %

PETROGENETIC MODEL

The petrogenetic scheme envisioned for the alkalic igneous rocks, potassic fenites, and carbonatites of the Bear Lodge Mountains is illustrated diagrammatically in Figure 69. It begins with an alkali-rich mafic magma generated through partial melting of upper mantle material that has been metasomatically enriched in alkalis, strontium, cerium, lanthanum, fluorine, carbon dioxide, water, and other incompatible elements and volatiles. Such metasomatically enriched zones of the upper mantle have been proposed on the basis of petrographic and oxygen, lead, strontium, and neodymium isotopic studies to be the source regions of alkali basalts, nephelinites, kimberlites, and similar types of alkali-rich ultrabasic magmas (Sun and Hanson, 1975; Cox and others, 1976; Boettcher and O'Neil, 1980; Menzies and Murthy, 1980). The metasomatic enrichment of these zones, which in some instances may have occurred billions of years ago, not only account for the characteristically high concentrations of incompatible elements in alkali-rich ultrabasic rocks, but also provides an effective means of concentrating the fluxes and radiogenic heat sources neccessary to initiate mantle fusion.

Although comprehensive isotopic and trace element studies are necessary to prove that the parent magma of the alkalic igneous rocks, potassic fenites, and carbonatites of the Bear Lodge Mountains originated from an enriched portion of the upper mantle, the extremely high concentrations of cerium, lanthanum, thorium, and other incompatible elements in the I-type carbonatites and potassic fenites provide preliminary evidence. The I-type carbonatites are believed to be genetically related to the surrounding silicate rocks and, as

Figure 69. Simplified petrogenetic scheme proposed for the alkalic igneous rocks, potassic fenites, and I-type carbonatites, of the central and southeastern Bear Lodge Mountains.

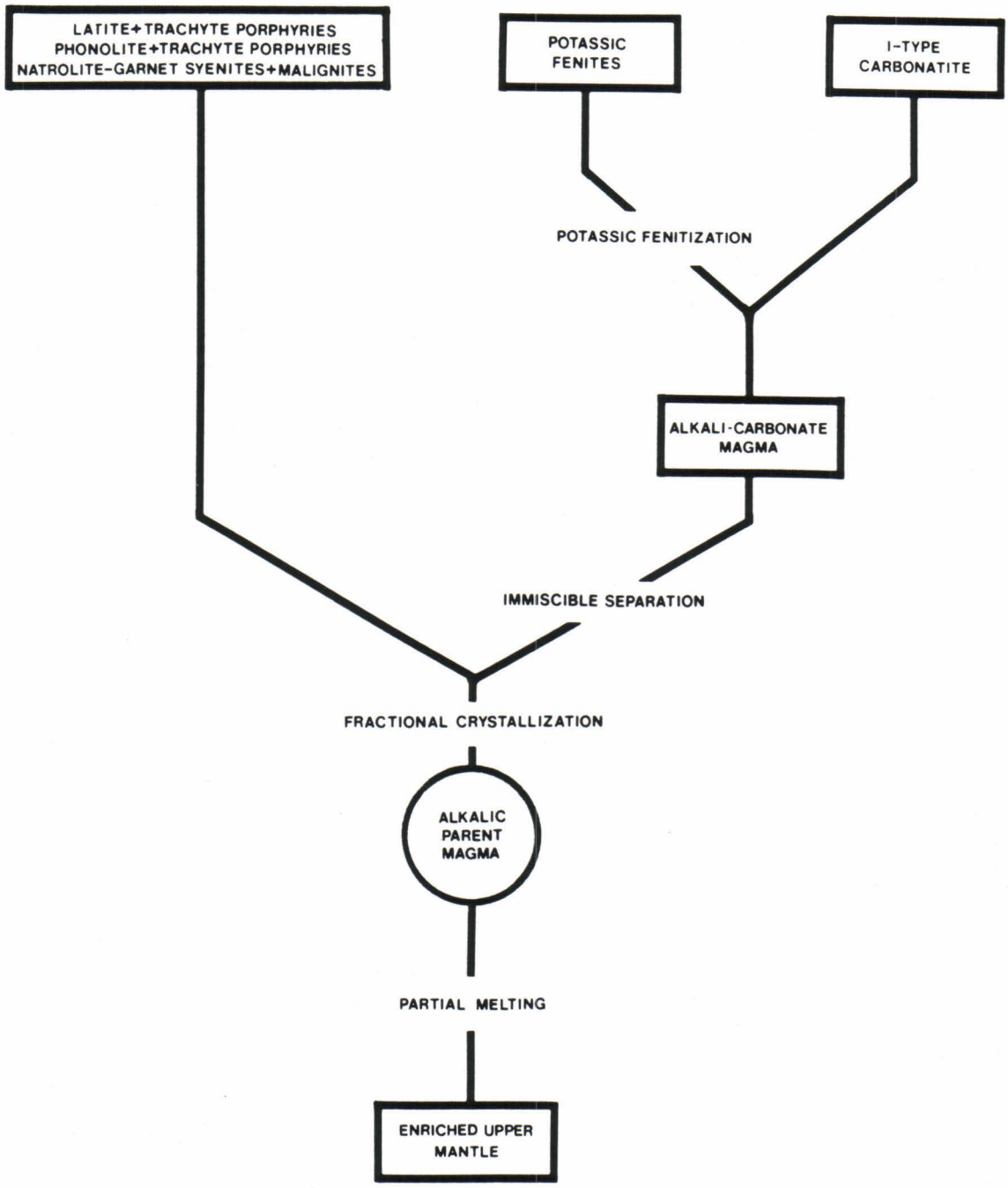
LATITE+TRACHYTE PORPHYRIES
PHONOLITE+TRACHYTE PORPHYRIES
NATROLITE-GARNET SYENITES+MALIGNITES
POTASSIC FENITES
I-TYPE CARBONATITE
POTASSIC FENITIZATION
ALKALI-CARBONATE MAGMA
IMMISCIBLE SEPARATION
FRACTIONAL CRYSTALLIZATION
ALKALIC PARENT MAGMA
PARTIAL MELTING
ENRICHED UPPER MANTLE

discussed earlier (p. 158), carbon and oxygen isotopic data indicate a mantle source for the CO_2 of I-type carbonatites.

The composition of the alkali-rich mafic magma that was parental to the alkalic igneous rocks, potassic fenites, and I-type carbonatites of the Bear Lodge Mountains is speculative. A plot of SiO_2 versus differentiation index which compares analyses of unaltered igneous rocks of the Bear Lodge Mountains with generalized alkali basalt and tholeiitic basalt differentiation lineages suggests that the original parent magma was compositionally similar to an alkali basalt (Fig. 70). An alkali basalt composition is also suggested by the trend defined when the same rocks are plotted on a standard AFM diagram (Fig. 71). Note that the projected origin of the trend delineated on the AFM diagram approaches the composition of the average alkali basalt reported by Nockolds (1954).

The chronology of events during the episode of early igneous activity suggests that differentiation of the original parent magma initially generated, in sequential order, latitic, trachytic, and phonolitic fractions. Petrographic evidence such as zoned pyroxene and plagioclase phenocrysts and the occasional occurrence of pyroxenitic xenoliths indicate that differentiation was dominated by processes of fractional crystallization. Additional evidence for fractional crystallization is provided by a Larson (1938) variation diagram which implies a progressive enrichment of SiO_2, Al_2O_3, Na_2O, and K_2O and a corresponding depletion of CaO, MgO, and total iron during differentiation (Fig. 72). Such trends would be consistent with the fractionation of magnesian olivine, magnesian pyroxene, and calcic plagioclase during crystallization.

Figure 70. Plot of SiO_2 versus differentiation index showing trends of tholeiitic basalt series rocks (open triangles) and alkali basalt series rocks (closed triangles) as determined from analyses presented by Nockolds (1954). Samples of unaltered igneous rocks from the southeastern Bear Lodge Mountains plotted as open circles.

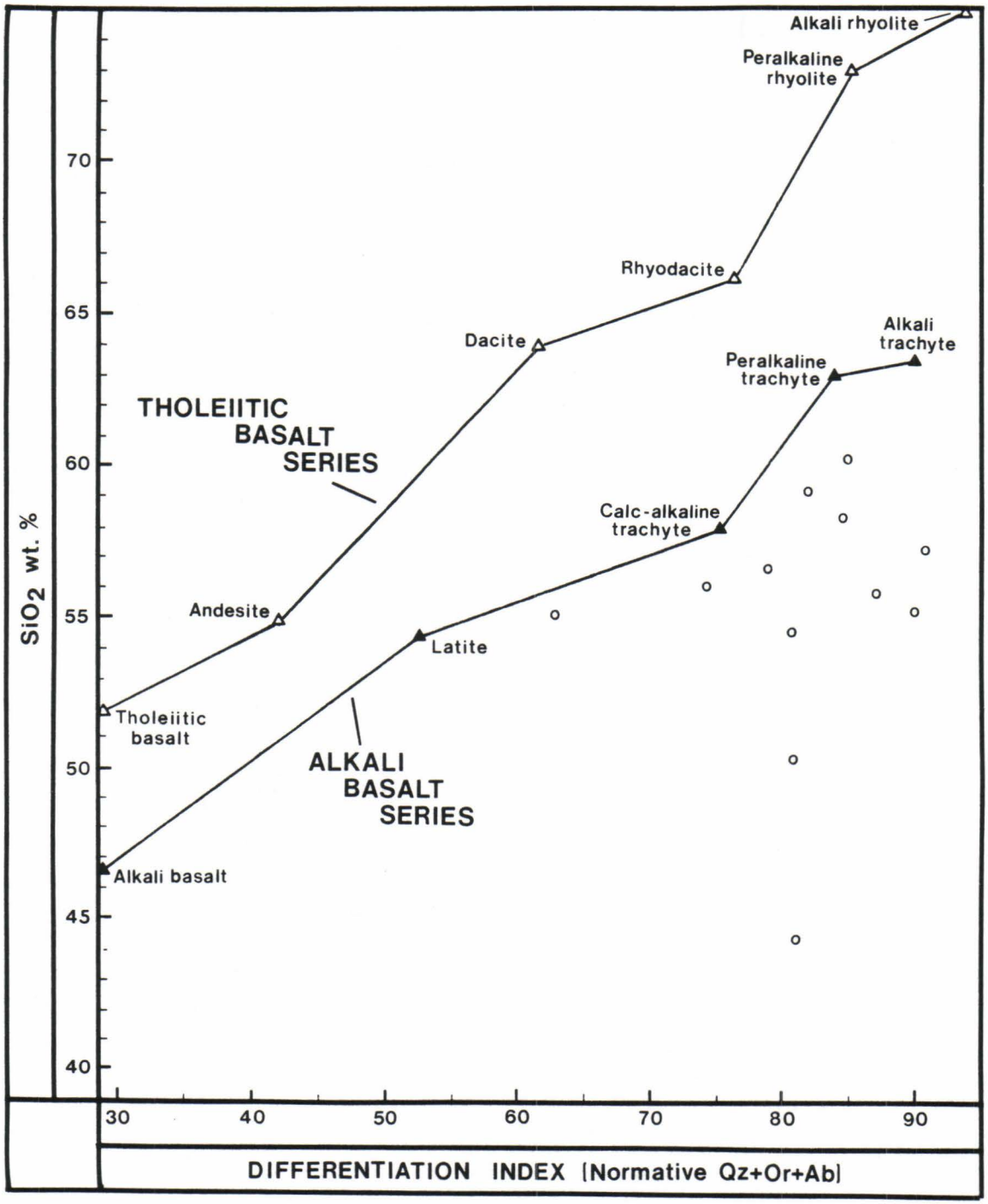
Alkali rhyolite
Peralkaline rhyolite
Rhyodacite
Dacite
Alkali trachyte
Peralkaline trachyte
THOLEIITIC BASALT SERIES
Calc-alkaline trachyte
Andesite
Latite
Tholeiitic basalt
ALKALI BASALT SERIES
Alkali basalt
SiO2 wt. %
70
65
60
55
50
45
40
30
40
50
60
70
80
90
DIFFERENTIATION INDEX (Normative Qz+Or+Ab)

Figure 71. Triangular plot of (Na_2O+K_2O) versus ($FeO+Fe_2O_3$) versus MgO. Samples of unaltered igneous rocks from the southeastern Bear Lodge Moutains plotted as open circles. Average tholeiitic basalt (TB-open triangle) and average alkali basalt (AB-closed triangle) plotted from analyses presented by Nockolds (1954).

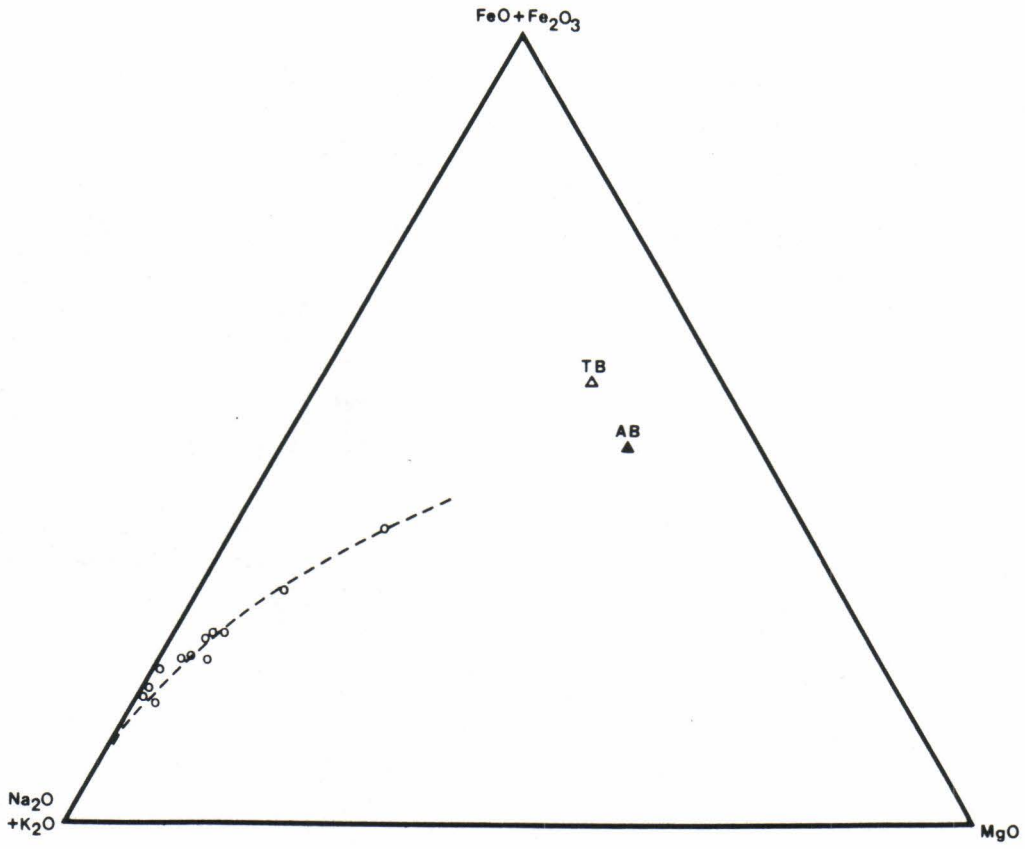
FeO+Fe2O3
TB
AB
Na2O
+K2O
MgO

Figure 72. Larson (1938) variation diagram. Samples of unaltered igneous rocks from the southeastern Bear Lodge Mountains plotted as open circles. Lines best-fitted by least square linear regression technique.

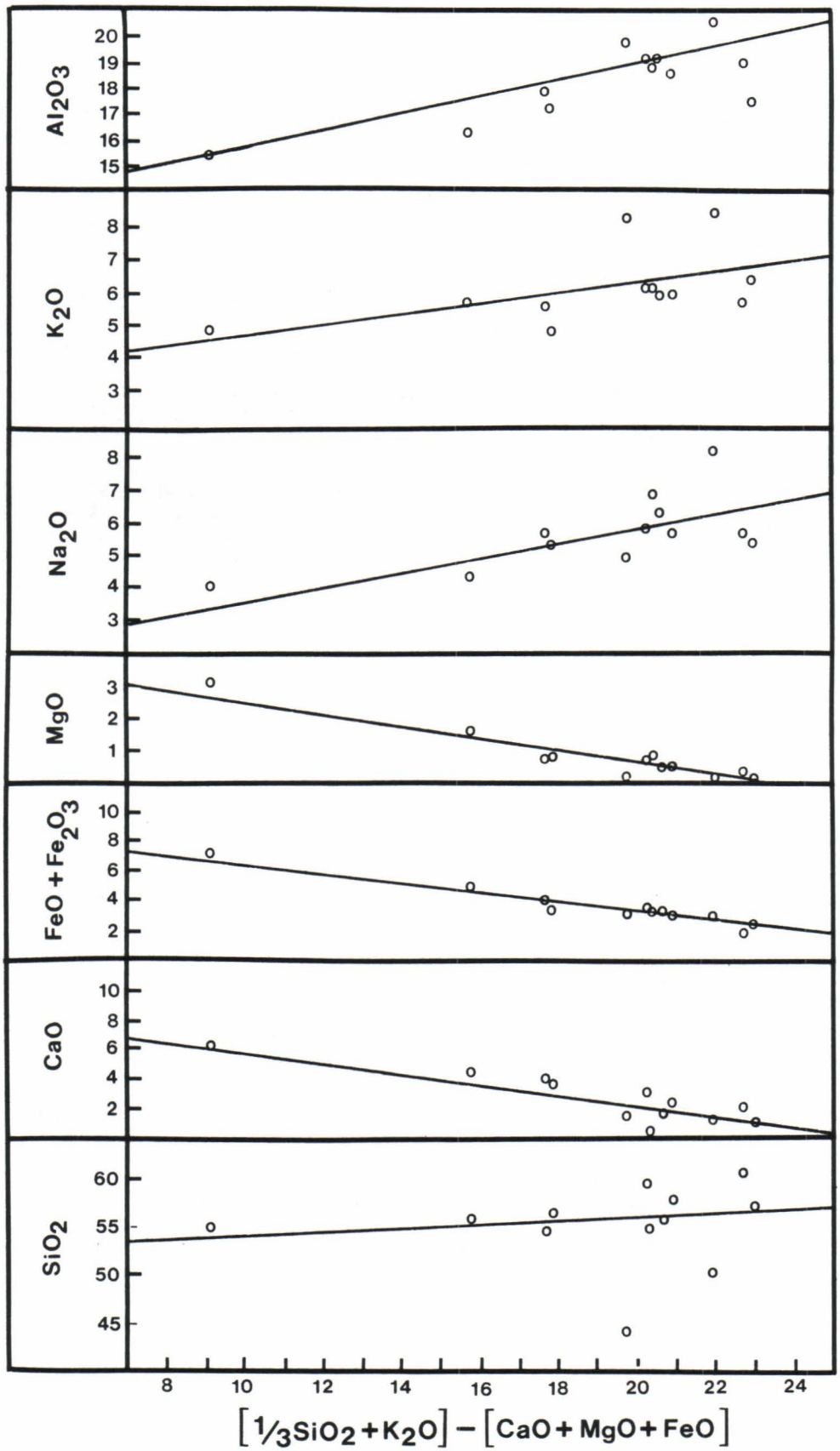
Al2O3
20
19
18
17
16
15
K2O
8
7
6
5
4
3
Na2O
8
7
6
5
4
3
MgO
3
2
1
FeO + Fe2O3
10
8
6
4
2
CaO
10
8
6
4
2
SiO2
60
55
50
45
8
10
12
14
16
18
20
22
24
[1/3SiO2 + K2O] − [CaO + MgO + FeO]

Differentiation by a process of liquid immiscibility is believed to have produced an alkali-rich carbonatitic magma in the Bear Lodge Mountains that was probably similar in composition to, altough more potassic than, the natrocarbonatitic lavas erupted in Tanzania by the volcano Oldoinyo Lengai (Dawson, 1962, 1966). Immiscibility between alkali-rich carbonatitic liquids and CO_2-rich silicate magmas has been confirmed experimentally in a number of systems (Koster van Groos and Wyllie, 1966, 1968, 1973; Wendlandt and Harrison, 1979; Freestone and Hamilton, 1980). The process has also been substantiated in nature. Rankin and LeBas (1974a) report immiscible silicate and carbonate liquids coexisting in fluid inclusions in apatites from ijolite pegmatites of the Wasaki complex of western Kenya. According to to the authors (p. 208) the inclusions represent the "simultaneous entrapping of a portion of a carbonate-rich melt and silicate-rich melt".

Experimental studies by Freestone and Hamilton (1980) have shown that the miscibility gap between an alkali-rich carbonatitic liquid and a coexisting silicate magma expands with increased P_{CO_2} and decreased temperature and that it closes away from Na_2O-rich compositions, indicating that more felsic magmas stand a greater likelihood of exsolving a carbonatitic liquid than more mafic magmas. Thus in the Bear Lodge Mountains the alkali-rich carbonatitic liquid probably separated from a phonolitic or compositionally similar differentiate of the original parent magma. The analcime phonolite porphyries emplaced during the episode of late igneous activity possibly represent the crystallization products of the silicate magma from which the carbonatitic liquids were exsolved.

If immiscible differentiation did produce an alkali-rich

carbonatitic magma in the Bear Lodge Mountains, then the extreme enrichment of cerium and lanthanum in the I-type carbonatites suggests that the light rare-earth elements were preferentially partitioned into the carbonatitic liquid during the process. Experimental studies by Wendlandt and Harrison (1979) have shown that the partion coefficients for light rare-earth elements are in favor of the carbonatitic liquid relative to the silicate liquid by a factor of 2-3 during immiscible differentiation. Thus the rare-earth element enrichment of the I-type carbonatites can be related to two separate events: (1) metasomatic enrichment of light rare-earth elements in the upper mantle source region of the alkali-rich mafic parent magma and (2) partioning of rare-earth elements into the carbonatitic liquid during immiscible differentiation.

The alkali-rich carbonatitic magma is believed to have exsolved an alkali-rich aqueous saline solution, resulting in the potassium-rich fluids responsible for fenitization and also producing an alkali-depleted carbonatitic liquid that later crystallized to form the I-type carbonatites. The same mechanism has been proposed by a number of authors to account for the intimate association between fenites and carbonatites (von Eckermann, 1948; Dawson, 1964; Wooley, 1982; Rubie and Gunter, 1983). The process also has been proposed to account for the common occurrence of alkali-rich aqueous saline fluids in minerals of alkali-depleted intrusive carbonatites (Rankin and LeBas, 1974b; Rankin, 1975, 1977; Nesbitt and Kelly, 1977; Metzger and others, 1977; Aspden, 1980). In the Bear Lodge Mountains the high concentrations of rare-earth elements in both the I-type carbonatites and the potassic fenites suggests a genetic connection between the two varieties of rock and

support the hypothesis that the potassium-rich fluids responsible for fenitization were derived from a carbonatitic liquid.

Although speculative, the petrogenetic model outlined above is consistent with the observed chronology of igneous and metasomatic events for the Bear Lodge Mountains. It also accounts for many of the petrographic and geochemical characteristics of the rocks exposed within the uplift such as the extreme enrichment of rare-earth elements in the I-type carbonatites and potassic fenites. It is hoped that additional isotopic, trace element, and fluid inclusion studies will shed further light on the numerous petrologic problems that are presented by the Eocene rocks of the Bear Lodge Mountains.

CONCLUSIONS

1. The Eocene rocks of the Bear Lodge Mountains record a complex petrologic history of multiple alkalic igneous events, potassic fenitization, carbonatitic magmatism, and hydrothermal alteration.

2. Two of the petrologic events are of potential economic interest. Associated with potassic fenitization are significant deposits of thorium, rare-earth elements, copper, lead, zinc, and gold. Associated with carbonatitic magmatism are significant deposits of thorium, rare-earth elements, copper, lead, and zinc.

3. Two genetically different types of carbonatite, termed I-type and S-type, are distinguished on the basis of rare-earth element and strontium concentrations and on carbon and oxygen isotopic data. I-type carbonatites are of primary igneous origin and formed from mantle-derived CO_2. S-type carbonatites were produced by the fusion of sedimentary limestone by an alkalic silicate magma.

4. I-type carbonatites, which are enriched in rare-earth elements, contain an exotic suite of rare-earth minerals that includes ancylite, burbankite, carbocernaite, a newly recognized rare-earth carbonate, and a newly recognized rare-earth phosphate.

5. The igneous rocks of the Bear Lodge Mountains were probably derived through the differentiation of an alkali-rich parent magma that was generated by partial melting of upper mantle material enriched in potassium, rubidium, iron, titanium, cerium, lanthanum, fluorine, carbon dioxide, water, and other incompatible elements and volatiles. Latitic,

trachytic, and phonolitic differentiates were generated by fractional crystallization and an alkali-rich carbonatitic magma was produced by later immiscible separation, probably from a phonolitic differentiate. Loss of an alkali-rich aqueous liquid from the carbonatitic magma resulted in the potassium-rich fluids responsible for fenitization and also produced an alkali-depleted carbonatitic magma that crystallized to form I-type carbonatites.

APPENDICES

APPENDIX A

ANALYTICAL PROCEDURES

ANALYTICAL PROCEDURES

Modal Analysis

Polished thin sections were modally analyzed on the basis of 500 counts using a standard petrographic microscope. The results are expressed in volume percent. Grid spacings were set at one half average grain size for equigranular rock types and at one half average phenocryst size for inequigranular (porphyritic) rock types as recommended by Chayes (1956). Cryptocrystalline and microcrystalline minerals in porphyritic rock types, unidentifiable by optical methods, were collectively termed "groundmass" and reanalyzed on the basis of 100 counts using an electron microprobe. The accuracy of the results is dependent on the number of counts, the confidence level of the counts, and the volume percent of each mineral constituent (Van der Plas and Tobi, 1965). For 500 counts with a confidence level of 95 percent, a modal percentage of 28-80% varies $\pm$4%; 13-28%, $\pm$3%; 5-13%, $\pm$2%; and 1-5%, $\pm$1%. For 100 counts with a confidence level of 95%, a modal percentage of 28-75% varies $\pm$9%; 20-28%, $\pm$8%; 14-20%, $\pm$7%; 10-14%, $\pm$6%; 7-10%, $\pm$5%; and 5-7%, $\pm$4%.

X-ray Diffraction and X-ray Fluorescence Analyses

Powdered samples for qualitative and quantitative x-ray analysis were prepared as follows:

1. A representative sample (50-200 g) was crushed to less than 2-3mm.
2. The crushed sample was split to approximately 20 g.
3. The 20 g split was ground to less than 20 mesh (0.84 mm) using a SPEX 8000 mixer mill (large vial).
4. Approximately 7 g of sample was extracted from the 20 g split and ground to less than 325 mesh (44 microns)

using a Spex 8000 mixer mill (small vial).

Identification of minerals was facilitated by whole-rock x-ray diffraction analysis. Approximately 0.2 g of silicon powder was mixed with approximately 1 gram of powdered sample and the mixture was backloaded into an aluminum mount using Method B of Hutchinson (1974, p. 145). The silicon powder was added as an internal standard in order to moniter peak positions. Samples were analyzed on a PHILIPS-NORELCO high-angle diffractometer equipped with nickel filter and operated at a tube voltage of 37 Kv and current of 18 mA. Samples were scanned with CuK-alpha radiation at a rate of 1°-2θ minute.

Whole-rock major element chemical analyses were acquired by x-ray fluorescence spectroscopy of pressed pellets. Pellets were prepared using 5.0 g of powdered sample with 3 drops of distilled water added as a binding agent. The mixture was loaded into an aluminum SPEX cap and subjected to a pressure of approximately 4×10^8 N/m^2 (3 tons/in^2) for a period of 1 minute using a SPEX 30-ton hydraulic press. Pressure was gradually released over a 3-4 minute interval and the resulting pellet was removed and placed into an oven at $70^{\circ}C$ for a twelve hour period. The pellets were analyzed on a fully automated RIGAKU/SMAX-E/S wavelength-dispersive x-ray fluorescence spectrometer. Data were reduced using U.S.G.S. standards and the CRISS fundamental alphas software package. Total iron oxides, reported as Fe_2O_3, were converted to FeO and Fe_2O_3 for use in normative calculations by the method of Irving and Barager (1971, p. 526). The results are accurate to within 10% and reproducible to within 5% (Stevenson, 1984, oral communication).

Electron Microanalysis

Mineral analyses were acquired from polished thin sections using a

JEOL 35C scanning electron microprobe equipped with a KEVEX energy-dispersive spectrometer. The JEOL 35C was operated at an accelerating voltage of 15 Kev and beam current of 1000 pa. All of the analyses were made using a 50 second counting time and a beam diameter of 0.2 microns. X-ray spectra were processed using natural and synthetic standards available at the Natural Materials Analytical Laboratory at the University of North Dakota and were fitted by the TRACOR NORTHERN XML program. Matrix corrections were made using the program of Bence and Albee (1968). Replicate analyses of standards are accurate to $\pm$3-4% and reproducible to $\pm$2-3%.

Stable Isotope Analysis

Carbon and oxygen isotopic compositions were determined at the Stable Isotope Laboratory of the Department of Geology and Geophysics at the University of Utah under the supervision of Dr. John Bowman. Calcite grains were handpicked from crushed samples with the aid of a binocular microscope and were crushed to a fine powder with mortar and pestal. Carbon dioxide was extracted from the calcite by reaction with 100% phosphoric acid using the technique outlined by McCrea (1950). The CO_2 was analyzed on a MICROMASS 600D double-collecting mass spectrometer with results reported as δ-values as described by Epstein (1959). For oxygen:

$$\delta O^{18} = \left[\frac{O^{18}/\ O^{16}\ \text{sample}}{O^{18}/\ O^{16}\ \text{std.}} - 1 \right] \times 1000$$

where the standard is standard mean ocean water, abbreviated SMOW (see Clayton and Mayeda, 1963). For carbon:

$$\delta C^{13} = \left[\frac{C^{13}/\ C^{12}\ \text{sample}}{C^{13}/\ C^{12}\ \text{std.}} - 1 \right] \times 1000$$

where the standard is the C^{13}/C^{12} ratio of the Pee Dee belemnite calcite originally analyzed by Urey and others (1951). All results are reproducible to greater than ± 0.1 per mil.

APPENDIX B

MISCELLANEOUS MICROPROBE ANALYSES

TABLE 30

MISCELLANEOUS MICROPROBE ANALYSES

SAMPLE	A.1	A.2	A.3	A.4	A.5	A.6	A.7	A.8
SiO_2	65.41	67.15	53.19	58.52	64.33	47.64	65.22	68.83
Al_2O_3	19.49	20.79	22.55	27.02	22.10	5.42	18.68	20.69
FeO*	0.00	0.16	0.17	0.65	0.35	12.41	0.00	0.57
MgO	0.00	0.00	0.00	0.00	1.09	7.14	0.26	0.00
CaO	0.00	0.95	0.08	7.96	5.63	22.00	0.00	0.34
Na_2O	0.34	7.41	13.17	6.45	6.20	0.97	0.99	11.23
K_2O	15.36	5.35	0.47	0.76	0.67	0.08	14.93	0.87
TiO_2	0.24	0.12	0.00	0.18	0.00	1.61	0.12	0.00
P_2O_5	0.00	0.00	0.00	0.00	0.00	0.29	0.00	0.00
MnO	0.00	0.00	0.00	0.00	0.00	0.44	0.00	0.00
Cl	0.00	0.09	0.00	0.07	0.00	0.00	0.15	0.08
SO_3	0.00	0.00	0.00	0.00	0.00	0.00	0.00	0.00
Total	100.84	102.02	89.63	101.61	100.37	98.00	100.35	102.61

* Total Fe as FeO

Sample key: A.1=Sample 27-217=Sanidine (groundmass)
A.2=Sample 21-109=Anorthoclase (groundmass)
A.3=Sample 27-217=Analcime (groundmass)
A.4=Sample 21-56B=Andesine (phenocryst)
A.5=Sample 27-187=Sanidine (phenocryst)
A.6=Sample 27-187=Salite (phenocryst)
A.7=Sample 27-220=Sanidine (groundmass)
A.8=Sample 21-73A=Albite (groundmass)

A.1-A.6= Minerals of latite and trachyte porphyries
A.7-A.8= Minerals of phonolite and trachyte porphyries

TABLE 30

(continued)

SAMPLE	A.9	B.1	B.2	B.3	B.4	B.5	B.6	B.7
SiO_2	69.06	53.85	65.12	65.85	64.98	66.17	45.73	46.09
Al_2O_3	20.58	25.32	19.27	19.24	19.30	19.27	30.13	27.91
FeO*	0.00	0.00	0.00	0.27	0.62	0.54	0.21	0.20
MgO	0.00	0.00	0.23	0.00	0.00	0.00	0.00	0.00
CaO	0.00	0.00	0.00	0.00	0.00	0.00	0.51	2.91
Na_2O	11.33	13.47	0.84	0.83	1.16	0.95	15.34	12.24
K_2O	0.34	0.11	15.01	15.07	14.36	14.70	0.00	0.00
TiO_2	0.00	0.00	0.13	0.00	0.50	0.17	0.13	0.00
P_2O_5	0.00	0.00	0.00	0.00	0.00	0.00	0.00	0.00
MnO	0.00	0.00	0.20	0.00	0.00	0.00	0.00	0.00
Cl	0.07	0.00	0.11	0.00	0.00	0.06	0.00	0.00
SO_3	0.00	0.00	0.00	0.00	0.00	0.00	0.00	0.00
Total	101.38	92.75	100.91	101.26	100.92	101.86	92.05	89.35

*Total Fe as FeO

Sample key: A.9=Sample 34-316=Albite (groundmass)
B.1=Sample 21-85B=Analcime (groundmass)
B.2=Sample 21-24B=Sanidine (phenocryst)
B.3=Sample WBD-7/310.6=Sanidine
B.4=Sample WBD-13/736.8=Sanidine
B.5=Sample WBD-13/1394.6=Sanidine
B.6=Sample WBD-13/736.8=Natrolite
B.7=Sample WBD-13/1394.6=Natrolite

A.9-B.2= Minerals of phonolite and trachyte porphyries
B.3-B.7= Minerals of natrolite-garnet syenites and malignites

TABLE 30

(continued)

SAMPLE	B.8	B.9	C.1	C.2	C.3	C.4	C.5	C.6
SiO_2	53.97	33.20	39.62	66.93	70.63	66.60	70.38	0.37
Al_2O_3	2.13	2.80	11.95	18.98	20.56	19.09	20.08	0.11
FeO*	26.31	19.62	19.27	0.00	0.00	0.31	0.00	0.79
MgO	0.15	0.88	15.19	0.00	0.00	0.57	0.00	0.00
CaO	1.22	32.66	0.00	0.00	0.00	0.00	0.00	0.00
Na_2O	13.95	0.25	0.39	0.51	11.39	0.00	11.66	0.22
K_2O	0.00	0.00	9.53	15.87	0.79	15.72	0.40	0.14
TiO_2	3.31	7.65	1.18	0.00	0.00	0.00	0.00	97.14
P_2O_5	0.00	0.27	0.26	0.00	0.00	0.29	0.00	0.58
MnO	0.00	0.39	0.49	0.12	0.00	0.00	0.00	0.00
Cl	0.05	0.00	0.00	0.05	0.00	0.06	0.00	0.00
SO_3	0.00	0.00	0.00	0.00	0.00	0.12	0.00	0.00
Total	101.09	97.72	97.88	102.46	103.37	102.76	102.52	99.35

* Total Fe as FeO

Sample key: B.8=Sample WBD-13/736.8=Aegirine
B.9=Sample WBD-13/1339.7=Melanite
C.1=Sample WBD-7/310.6=Biotite
C.2=Sample WBD-12/906.8=Sanidine (groundmass)
C.3=Sample WBD-8/348.2=Albite (groundmass)
C.4=Sample 27-6B=Sanidine (phenocryst)
C.5=Sample WBD-8/348.2=Albite (phenocryst)
C.6=Sample 27-6B=Brookite

B.8-C.1= Minerals of natrolite-garnet syenites and malignites
C.2-C.6= Minerals of alkali trachyte

TABLE 30

(continued)

SAMPLE	C.7	C.8	C.9	D.1	D.2	D.3	D.4	D.5
SiO_2	66.64	66.91	66.61	66.08	66.51	65.25	44.36	3.68
Al_2O_3	19.12	19.60	18.75	19.54	19.28	18.74	38.79	0.00
FeO*	0.37	0.13	0.00	0.31	0.00	0.00	0.66	78.32
MgO	0.00	0.00	0.00	0.00	0.00	0.00	0.24	0.00
CaO	0.00	0.00	0.00	0.00	0.00	0.00	0.00	0.28
Na_2O	1.95	0.00	0.39	0.54	0.00	0.00	0.00	0.41
K_2O	13.22	15.93	15.90	15.23	15.83	15.82	10.20	0.00
TiO_2	0.00	0.20	0.00	0.20	0.10	0.10	0.00	0.00
P_2O_5	0.00	0.00	0.00	0.00	0.00	0.00	0.00	0.43
MnO	0.00	0.00	0.00	0.00	0.00	0.00	0.00	0.00
Cl	0.00	0.00	0.05	0.00	0.00	0.00	0.00	0.00
SO_3	0.00	0.00	0.00	0.00	0.00	0.00	0.00	0.53
Total	101.30	102.77	101.70	101.90	101.72	99.91	94.25	83.65

* Total Fe as FeO

Sample key: C.7=Sample 16-439C=Sanidine (groundmass)
C.8=Sample 27-172A=Sanidine (groundmass)
C.9=Sample 16-439C=Sanidine (phenocryst)
D.1=Sample 21-22B=Sanidine (phenocryst)
D.2=Sample 27-172A=Sanidine (phenocryst)
D.3=Sample WBD-12/804.0=Sanidine (phenocryst)
D.4=Sample 27-172A=Muscovite
D.5=Sample 16-439C=Magnetite

C.7-D.5= Minerals of alkali trachyte porphyry

TABLE 30

(continued)

SAMPLE	D.6	D.7	D.8	D.9	E.1	E.2	E.3	E.4
SiO_2	64.83	66.16	66.14	53.16	52.00	52.46	32.07	35.78
Al_2O_3	19.61	18.99	19.49	25.85	1.07	0.75	1.80	1.96
FeO*	0.00	0.00	0.49	0.13	17.13	28.95	23.61	24.37
MgO	0.00	0.00	0.00	0.00	6.53	0.00	0.36	0.14
CaO	0.00	0.00	0.00	0.72	15.70	3.99	31.65	33.00
Na_2O	1.28	0.75	0.95	11.62	5.22	12.00	0.00	0.23
K_2O	14.49	15.07	14.87	0.32	0.10	0.10	0.00	0.17
TiO_2	0.16	0.21	0.00	0.00	0.00	0.34	7.23	2.98
P_2O_5	0.00	0.00	0.00	0.00	0.36	0.00	0.33	0.00
MnO	0.00	0.00	0.00	0.00	0.97	0.49	0.51	0.70
Cl	0.07	0.07	0.05	0.00	0.00	0.00	0.00	0.00
SO_3	0.11	0.00	0.11	0.00	0.00	0.00	0.00	0.00
Total	100.55	101.25	102.10	91.80	99.09	99.08	97.56	99.33

* Total Fe as FeO

Sample key: D.6=Sample WBD-5/609.5=Sanidine
D.7=Sample WBD-13/848.3=Sanidine
D.8=Sample WBD-13/1651.9=Sanidine
D.9=Sample WBD-13/848.3=Analcime
E.1=Sample WBD-8/1631.0=Aegirine-augite
E.2=Sample WBD-13/848.3=Aegirine
E.3=Sample WBD-5/1545.0=Melanite
E.4=Sample WBD-5/1545.0=Melanite

D.6-E.4= Minerals of alkali melasyenite

TABLE 30

(continued)

SAMPLE	E.5	E.6	E.7	E.8	E.9	F.1	F.2	F.3
SiO_2	39.02	38.39	38.32	30.04	1.37	65.48	65.53	63.62
Al_2O_3	12.34	11.32	10.76	1.38	0.25	18.84	18.54	19.49
FeO*	18.86	22.22	25.93	2.06	91.35	0.24	0.56	0.28
MgO	14.86	12.57	9.48	0.00	0.34	0.00	0.00	0.30
CaO	0.00	0.00	0.00	28.28	0.00	0.00	0.00	0.00
Na_2O	0.23	0.00	0.00	0.32	0.39	0.77	0.29	0.86
K_2O	9.77	9.61	8.80	0.00	0.24	14.84	15.92	14.88
TiO_2	1.60	2.00	2.17	35.93	0.21	0.10	0.00	0.23
P_2O_5	0.00	0.00	0.30	0.25	0.00	0.00	0.00	0.00
MnO	0.87	1.07	1.48	0.00	0.40	0.00	0.00	0.00
Cl	0.00	0.00	0.00	0.00	0.00	0.07	0.11	0.07
SO_3	0.13	0.00	0.00	0.00	0.00	0.00	0.00	0.15
Total	97.68	97.18	97.24	98.26	94.55	100.34	100.95	99.88

* Total Fe as FeO

Sample key: E.5=Sample WBD-5/609.5=Biotite
E.6=Sample WBD-5/1545.0=Biotite
E.7=Sample WBD-13/1651.9=Biotite
E.8=Sample WBD-13/848.3=Sphene
E.9=Sample WBD-5/609.5=Magnetite
F.1=Sample WBD-5/623.8=Sanidine
F.2=Sample WBD-5/1467.5=Sanidine
F.3=Sample WBD-5/1527.6=Sanidine

E.5-E.9= Minerals of alkali melasyenite
F.1-F.3= Minerals of alkali leucosyenite

TABLE 30

(continued)

SAMPLE	F.4	F.5	F.6	F.7	F.8	F.9	G.1	G.2
SiO_2	65.19	64.43	53.54	34.20	30.15	0.59	0.73	0.00
Al_2O_3	18.24	19.29	0.00	2.14	0.11	0.29	0.00	0.00
FeO*	0.27	0.00	19.13	22.24	0.56	88.80	39.08	42.48
MgO	0.00	0.00	5.90	0.43	0.00	0.39	0.00	0.33
CaO	0.00	0.00	9.50	33.07	26.46	1.29	1.10	0.00
Na_2O	0.44	0.70	9.34	0.00	0.94	0.35	0.00	0.00
K_2O	15.59	14.65	0.07	0.11	0.09	0.00	0.00	0.00
TiO_2	0.00	0.47	1.65	7.13	37.51	0.20	51.36	52.09
P_2O_5	0.00	0.00	0.00	0.00	0.00	0.00	0.00	0.00
MnO	0.00	0.00	0.45	0.92	0.00	0.37	8.42	5.99
Cl	0.13	0.10	0.00	0.05	0.00	0.09	0.00	0.00
SO_3	0.00	0.24	0.00	0.00	0.00	0.00	0.00	0.00
Total	99.86	99.88	99.58	100.29	95.82	92.37	100.69	100.89

* Total Fe as FeO

Sample key: F.4=Sample WBD-7/1274.7=Sanidine
F.5=Sample WBD-13/830.5=Sanidine
F.6=Sample WBD-13/830.5=Aegirine
F.7=Sample WBD-5/623.8=Melanite
F.8=Sample WBD-7/1274.7=Sphene
F.9=Sample WBD-5/623.8=Magnetite
G.1=Sample WBD-5/1076.0=Manganian ilmenite
G.2=Sample WBD-5/1467.5=Manganian ilmenite

F.4-G.2= Minerals of alkali leucosyenite

TABLE 30

(continued)

SAMPLE	G.3	G.4	G.5	G.6	G.7	G.8	G.9	H.1
SiO_2	64.59	63.68	60.70	70.60	51.73	54.88	37.82	0.23
Al_2O_3	19.07	18.35	17.79	19.90	24.94	25.46	15.13	0.00
FeO*	0.22	0.24	0.23	0.36	0.63	0.00	14.99	39.15
MgO	0.00	0.00	0.00	0.00	0.00	0.00	14.81	0.17
CaO	0.00	0.00	3.30	0.00	1.43	0.29	0.00	1.17
Na_2O	0.32	0.00	0.50	12.05	11.30	9.94	0.00	0.00
K_2O	15.11	15.18	14.29	0.42	0.28	0.13	9.85	0.07
TiO_2	0.19	0.00	0.14	0.00	0.00	0.00	1.30	57.72
P_2O_5	0.00	0.00	2.71	0.00	0.00	0.00	0.00	0.00
MnO	0.00	0.00	0.00	0.00	0.00	0.21	0.94	1.60
Cl	0.00	0.08	0.00	0.00	0.00	0.00	0.08	0.00
SO_3	0.16	0.00	0.00	0.12	0.00	0.00	0.00	0.00
Total	99.66	97.53	99.66	103.45	90.31	90.91	94.92	100.11

* Total Fe as FeO

Sample key: G.3=Sample BL-4/1175.0=Sanidine
G.4=Sample BL-4/1175.0=Sanidine
G.5=Sample BL-4/1203.6=Sanidine
G.6=Sample BL-4/1203.6=Albite
G.7=Sample BL-4/1175.0=Analcime
G.8=Sample WBD-12/819.8=Analcime
G.9=Sample BL-4/1175.0=Biotite
H.1=Sample BL-4/1175.0=Manganian ilmenite

G.3-H.1= Minerals of pseudoleucite alkali trachyte porphyry

TABLE 30

(continued)

SAMPLE	H.2	H.3	H.4	H.5	H.6	H.7	H.8	H.9
SiO_2	0.00	0.23	68.13	65.15	53.85	54.27	49.23	48.70
Al_2O_3	0.00	0.00	19.10	18.39	27.61	25.14	27.68	28.09
FeO*	46.51	44.09	0.49	0.00	0.25	0.00	0.00	0.25
MgO	0.00	0.00	0.00	0.00	0.00	0.00	0.00	0.00
CaO	0.37	0.00	0.00	0.00	0.31	0.17	0.00	0.00
Na_2O	0.00	0.39	2.53	0.51	8.71	13.57	12.84	16.13
K_2O	0.00	0.00	12.50	14.87	0.00	0.30	0.08	0.05
TiO_2	51.13	50.33	0.00	0.00	0.09	0.00	0.00	0.00
P_2O_5	0.00	0.14	0.00	0.00	0.00	0.00	0.19	0.00
MnO	1.69	2.84	0.00	0.12	0.00	0.13	0.00	0.00
Cl	0.00	0.00	0.04	0.13	0.06	0.00	0.00	0.00
SO_3	0.00	0.00	0.00	0.12	0.14	0.00	0.00	0.00
Total	99.70	98.02	102.79	99.29	91.02	93.58	90.02	93.22

* Total Fe as FeO

Sample key: H.2=Sample BL-4/1175.0=Manganian ilmenite
H.3=Sample WBD-12/819.8=Manganian ilmenite
H.4=Sample 27-126=Sanidine (groundmass)
H.5=Sample 22-377=Sanidine (groundmass)
H.6=Sample 21-43=Analcime (groundmass)
H.7=Sample 27-126=Analcime (groundmass)
H.8=Sample 21-61=Natrolite (groundmass)
H.9=Sample 27-189=Natrolite (groundmass)

H.2-H.3= Minerals of pseudoleucite alkali trachyte porphyry
H.4-H.9= Minerals of analcime phonolite porphyries

TABLE 30

(continued)

SAMPLE	I.1	I.2	I.3	I.4	I.5	I.6
SiO_2	64.94	35.73	48.95	52.20	49.27	0.00
Al_2O_3	17.48	28.02	1.86	1.84	2.41	0.35
FeO*	3.53	0.28	25.50	18.54	19.81	87.16
MgO	0.00	0.00	1.42	6.70	4.82	0.49
CaO	0.00	5.31	13.25	19.70	18.09	0.00
Na_2O	2.30	7.13	6.67	3.40	3.25	0.00
K_2O	13.68	8.91	0.11	0.10	0.08	0.00
TiO_2	0.00	0.00	3.13	0.38	0.48	3.35
P_2O_5	0.00	0.00	0.00	0.00	0.00	0.17
MnO	0.00	0.00	0.81	0.69	0.87	1.17
Cl	0.00	6.15	0.00	0.00	0.00	0.00
SO_3	0.21	0.00	0.00	0.00	0.00	0.00
Total	102.14	91.53	101.70	103.55	99.08	92.69

* Total Fe as FeO

Sample key: I.1=Sample 21-61=Sanidine (phenocryst)
I.2=Sample 21-26A=Sodalite (phenocryst)
I.3=Sample 21-43=Aegirine-augite (phenocryst)
I.4=Sample 27-126=Aegirine-augite (phenocryst)
I.5=Sample 22-377=Aegirine-augite (phenocryst)
I.6=Sample 22-377=Titanian magnetite

I.1-I.6= Minerals of analcime phonolite porphyries

APPENDIX C

MISCELLANEOUS MAJOR ELEMENT CHEMICAL ANALYSES

TABLE 31

MISCELLANEOUS MAJOR ELEMENT CHEMICAL ANALYSES

SAMPLE	A.1	A.2	A.3	A.4	A.5	A.6	A.7	A.8
SiO_2	61.72	55.74	66.55	58.97	60.47	54.78	57.02	59.65
Al_2O_3	17.19	16.65	16.33	17.35	17.15	16.42	17.36	21.09
Fe_2O_3	3.59	6.77	0.58	3.80	4.13	5.47	3.88	1.16
MgO	0.20	0.27	0.23	0.43	0.37	1.56	0.51	0.07
CaO	0.65	0.41	1.10	2.79	0.41	5.62	4.05	0.25
Na_2O	5.36	6.11	4.09	6.05	6.55	4.74	5.58	0.51
K_2O	5.68	4.07	5.71	4.76	3.60	5.85	4.39	12.74
TiO_2	0.63	0.72	0.31	0.71	0.89	0.95	0.56	1.47
P_2O_5	0.18	0.27	0.09	0.25	0.18	0.33	0.11	0.19
MnO	0.13	0.01	0.03	0.12	0.00	0.14	0.20	0.01
Total	95.33	91.02	95.02	95.23	93.75	95.86	93.66	97.14

* Total Fe as Fe_2O_3

Sample key: A.1=Sample 21-47A=Latite/trachyte porphyry
A.2=Sample 27-5A=Latite/trachyte porphyry
A.3=Sample 27-16=Latite/trachyte porphyry (silicified)
A.4=Sample 27-172B=Latite/trachyte porphyry
A.5=Sample 27-192A=Latite/trachyte porphyry
A.6=Sample 27-195A=Latite/trachyte porphyry
A.7=Sample 27-205=Latite/trachyte porphyry
A.8=Sample 15-386=Alkali trachyte

TABLE 31

(continued)

SAMPLE	A.9	B.1	B.2	B.3	B.4	B.5	B.6	B.7
SiO_2	58.32	68.26	58.27	69.31	59.02	59.07	58.42	56.39
Al_2O_3	17.06	11.68	16.45	12.34	19.29	15.65	16.60	15.55
Fe_2O_3	6.89	1.24	8.70	1.26	2.64	3.57	2.60	3.33
MgO	1.10	0.28	1.81	0.05	0.33	0.09	0.06	0.17
CaO	1.48	0.04	0.07	0.04	0.20	0.31	0.50	0.23
Na_2O	3.89	0.61	0.43	0.38	0.37	0.47	0.61	0.63
K_2O	6.16	9.98	13.22	10.63	13.57	13.64	13.40	13.55
TiO_2	0.75	0.07	0.73	0.10	0.81	0.70	0.52	0.48
P_2O_5	0.26	0.04	0.05	0.03	0.17	0.20	0.15	0.15
MnO	0.14	0.05	0.10	0.02	0.01	0.02	0.16	0.21
Total	96.05	92.25	99.83	94.16	96.41	93.72	93.02	90.69

* Total Fe as Fe_2O_3

Sample key: A.9=Sample 16-28=Alkali trachyte
B.1=Sample 16-409B=Alkali trachyte (silicified)
B.2=Sample 16-410=Alkali trachyte
B.3=Sample 16-420=Alkali trachyte (silicified)
B.4=Sample 16-426A=Alkali trachyte
B.5=Sample 21-32=Alkali trachyte
B.6=Sample 21-42=Alkali trachyte
B.7=Sample 21-71=Alkali trachyte

TABLE 31

(continued)

SAMPLE	B.8	B.9	C.1	C.2	C.3	C.4	C.5	C.6
SiO_2	61.98	58.58	54.42	60.66	60.18	67.10	58.21	54.82
Al_2O_3	15.23	16.84	16.41	16.05	17.30	16.28	20.40	19.49
Fe_2O_3	1.15	7.10	8.63	4.44	6.55	1.82	2.63	3.90
MgO	0.08	0.27	0.46	0.08	0.16	0.05	0.30	0.63
CaO	0.25	0.13	1.02	0.35	0.66	0.10	0.09	2.92
Na_2O	0.99	0.97	1.14	0.38	2.61	1.64	0.29	1.00
K_2O	12.25	11.75	10.83	13.77	10.35	10.38	13.81	11.24
TiO_2	0.39	0.90	1.26	0.68	1.17	0.28	0.58	0.70
P_2O_5	0.12	0.38	0.64	0.25	0.40	0.08	0.05	0.15
MnO	0.10	0.01	0.02	0.21	0.19	0.01	0.03	0.21
Total	93.54	96.93	94.83	96.87	99.57	97.74	96.39	95.06

* Total Fe as Fe_2O_3

Sample key: B.8=Sample 21-72=Alkali trachyte
B.9=Sample 21-94=Alkali trachyte
C.1=Sample 21-107B=Alkali trachyte
C.2=Sample 21-112B=Alkali trachyte
C.3=Sample 21-116B=Alkali trachyte
C.4=Sample 22-350=Alkali trachyte (silicified)
C.5=Sample 22-371=Alkali trachyte
C.6=Sample 27-163=Alkali trachyte

TABLE 31

(continued)

SAMPLE	C.7	C.8	C.9	D.1	D.2
SiO_2	66.94	59.65	58.49	58.77	62.60
Al_2O_3	17.69	19.04	15.53	17.26	17.75
Fe_2O_3	2.60	4.91	5.30	4.46	3.53
MgO	0.57	0.50	0.17	0.31	0.23
CaO	0.88	0.32	0.17	0.33	0.09
Na_2O	2.48	2.77	0.37	3.13	0.63
K_2O	6.98	9.53	12.51	9.40	12.08
TiO_2	0.34	0.71	0.39	0.59	0.32
P_2O_5	0.07	0.15	0.52	0.12	0.07
MnO	0.02	0.01	0.01	0.02	0.02
Total	98.57	97.59	93.46	94.39	97.32

* Total Fe as Fe_2O_3

Sample key: C.7=Sample 27-174B=Alkali trachyte (silicified)
C.8=Sample 27-216A=Alkali trachyte
C.9=Sample 27-250=Alkali trachyte
D.1=Sample 34-323=Alkali trachyte
D.2=Sample 34-331=Alkali trachyte

REFERENCES CITED

REFERENCES CITED

Aspden, J. A., 1980, The mineralogy of primary inclusions in apatite crystals extracted from the Alnö ijolite: Lithos, v. 13, p. 263-268.

Baertschi, P., 1957, Messung und Deutung relativer Haufigkeitsvariatonen von ^{18}O and ^{13}C in Karbonatgesteinen und Mineralien: Schweizer Mineralogische und Petrographische Mitt., v. 37, p. 73-152.

Bence, A. E., and Albee, A. L., 1968, Empirical correction factors for the electron microanalysis of silicates and oxides: Journal of Geology, v. 76, p. 302-403.

Boettcher, A. L., and O'Neil, J. R., 1980, Stable isotope, chemical, and petrographic studies of high-pressure amphiboles and micas: evidence for metasomatism in the source regions of alkali basalts and kimberlites: American Journal of Science, v. 280-A, p. 594-621.

Bogoch, R., and Magaritz, M., 1983, Immiscible silicate-carbonate liquids as evidenced from ocellar diabase dykes, southeast Sinai: Contributions to Mineralogy and Petrology, v. 83, p. 227-230.

Brögger, W. C., 1921, Die Eruptivgesteine des Kristianiagebietes. IV. Das Fengebiet in Telemarken, Norwegen: Norske Videns. Skrift. Mat.-Naturv. Kl., 1920, no. 9.

Brown, B. W., 1952, A study of the southern Bear Lodge Mountains intrusive: unpublished M.S. thesis, University of Nebraska, 63 p.

Brown, P. E., 1964, The Songwe scarp carbonatite and associated feldspathization in the Myeba Range, Tanganyika: Quarterly Journal of the Geological Society of London, v. 120, p. 223-240.

Bulakh, A. G., Kondrat'eva, V. V., and Baranova, E. N., 1961, Carbocernaite: American Mineralogist, v. 46, p. 1202.

Chayes, F., 1956, Petrographic modal analysis: New York, John Wiley and Sons, Inc., 113 p.

Chenowith, W. C., 1955, The sedimentary and igneous rocks, structure and mineral deposits of the southeastern Bear Lodge Mountains, Crook County, Wyoming: unpublished M.S. thesis, 220 p.

Clayton, R. N., and Mayeda, T., 1963, The use of bromine pentafluoride in the extraction of oxygen from oxides and silicates for isotopic analysis: Geochimica et Cosmochimica Acta, v. 27, p. 43-52.

Conway, C. M., and Taylor, H. P., 1969, $^{18}O/^{16}O$ and $^{13}C/^{12}C$ ratios of coexisting minerals in the Oka and Magnet Cove carbonatite bodies: Journal of Geology, v. 77, p. 618-626.

Cox, K. G., Hawkesworth, C. J., and O'Nions, R. K., 1976, Isotopic evidence for the derivation of some Roman region volcanics from anomalously enriched mantle: Contributions to Mineralogy and Petrology, v. 56, p. 173-180.

Daly, R. A., 1910, Origin of alkaline rocks: Geological Society of America Bulletin, v. 21, p. 87-118.

-----, 1933, Igneous rocks and the depths of the earth: New York, McGraw Hill, 598 p.

Darton, N. H., 1905a, Sundance Quadrangle, Wyoming-South Dakota, folio 127 of Geologic atlas of the United States: U. S. Geological Survey.

-----, 1905b, Aladdin Quadrangle, Wyoming-South Dakota, folio 128 of Geologic atlas of the United States: U. S. Geological Survey.

Dawson, J. B., 1962, The geology of Oldoinyo Lengai: Bulletin of Volcanology, v. 24, p. 349-387.

-----, 1964, Reactivity of the cations in carbonate magma: Geological Association of Canada Proceedings, v. 15, p. 103-113.

-----, 1966, The kimberlite-carbonatite relationship: International Mineralogical Association, 4th meeting, India, p. 1-4.

Deines, Peter, 1970, The carbon and oxygen isotopic composition of carbonates from the Oka carbonatite complex, Quebec, Canada: Geochimica et Cosmochimica Acta, v. 34, p. 1199-1225.

-----, 1980, The carbon isotopic composition of diamond: relations to diamond shape, color, occurrence, and vapor composition: Geochimica et Cosmochimica Acta, v. 44, p. 943-961.

Deines, Peter, 1973, and Gold, D. P., 1973, The isotopic composition of carbonatite and kimberlite carbonates and their bearing on the composition of deep-seated carbon: Geochimica et Cosmochimica Acta, v. 37, p. 1709-1733.

Dixie, F., Smith, W. C., and Bisset, C. B., 1955, The Chilwa series of southern Nyasaland (rev. ed.): Nyasaland Geological Survey Bulletin, no. 5, 71 p.

Epstein, S., 1959, The variations of the $^{18}O/^{16}O$ ratio in nature and some geologic applications, in Abelson, P. H. ed., Researches in geochemistry: New York, John Wiley and Sons Inc., p. 217-240.

Erickson, R. L., and Blade, L. V., 1963, Geochemistry and petrology of the alkalic igneous complex at Magnet Cove, Arkansas: U. S. Geological Survey Professional Paper 425, 95 p.

Fashbaugh, E. F., 1979, Geology of igneous extrusive and intrusive

rocks in the Sundance area, Crook County, Wyoming: unpublished M.S. thesis, University of North Dakota, 95 p.

Fawley, A. P., and James, T. C., 1955, A pyrochlore (columbium) carbonatite, southern Tanganyika: Economic Geology, v. 50, p. 571-585.

Fischer, F. G. and Meyrowitz, Robert, 1962, Brockite, a new calcium thorium phosphate from the Wet Mountains, Colorado: American Mineralogist, v. 47, p. 1346-1355.

Freestone, I. C., and Hamilton, D. L., 1980, The role of liquid immiscibility in the genesis of carbonatites - an experimental study: Contributions to Mineralogy and Petrology, v. 73, p. 105-117.

Garson, M. S., 1966, in Tuttle, O. F., and Gittens, F., Carbonatites: New York, John Wiley and Sons Inc., p. 33-71.

Gold, D. P., 1963, Average chemical composition of carbonatites: Economic Geology, v.58, p. 988-996.

Gonfiantini, R., and Tongiorgi, E., 1964, Composition isotopique des carbonatites du Kaiserstuhl: EURATOM pub. EUR, 1827, d, e, f, p; p. 193-199.

Gries, J. P., and Tullis, E. L., 1955, Geologic history of the Black Hills, in Black Hills Field Conference: North Dakota Geologic Society Guidebook, p. 32.

Gupta, A. K., and Yagi, Kenzo, 1980, Petrology and genesis of leucite-bearing rocks: New York, Springer-Verlag, p. 4.

Halvorson, D. L., 1980, Geology and petrology of the Devils Tower, Missouri Buttes, and Barlow Canyon area, Crook County, Wyoming: unpublished Ph.D. dissertation, University of North Dakota, 163 p.

Heinrich, W. E., 1966, The geology of carbonatites: New York, Rand McNally, 555 p.

Heinrich, W. E., and Moore, D. G., Jr., 1970, Metasomatic potash feldspar rocks associated with igneous alkalic complexes: Canadian Mineralogist, v. 10, pt. 3, p. 571-584.

Hill, D. J., Izett, G. A., and Naeser, C. W., 1975, Early Tertiary fission track ages of sphene from Devils Tower and Missouri Buttes, Black Hills, northeastern Wyoming: Geological Society of America Abstracts with Programs, Rocky Mountain Section 1975 Annual Meeting, p. 613-614.

Hoefs, Jochen, 1980, Stable isotope geochemistry: New York, Springer Verlag, 208 p.

Hutchinson, C. S., 1974, Laboratory handbook of petrographic techniques: New York, John Wiley and Sons, Inc., 527 p.

Irving, F. N., and Barager, W. R. A., 1971, A guide to the chemical classification of common volcanic rocks: Canadian Journal of Earth Sciences, v. 8, p. 523-548.

Jagger, T. A., Jr., 1901, The laccoliths of the Black Hills: U. S. Geological Survey 21st Annual Report, pt. 3, p. 163-303.

Jenney, W. P., 1876, The mineral wealth, climate and rainfall, and natural resources of the Black Hills of Dakota: U. S. Geologic and Geographicical Survey of the Black Hills, Office of Indian Affairs, p. 5-71.

Karner, F. R., 1981, Geologic relationships in the western centers of the northern Black Hills Cenozoic igneous province, in Rich, E. F., ed., Geology of the Black Hills of South Dakota and Wyoming: Geological Society of America Guidebook, Rocky Mountain Section 1981 Annual Meeting, p. 126-133.

Kirchner, J. G., 1971, The petrography and petrology of the phonolite porphyry intrusions of the northern Black Hills, South Dakota: unpublished Ph.D. dissertation, University of Iowa, 199 p.

Koster van Groos, A. F., and Wyllie, P. J., 1966, Liquid immiscibilty in the system Na_2O-Al_2O_3-SiO_2-CO_2 at pressures to 1kb.: American Journal of Science, v. 264, p. 234-255.

-----, 1968, Liquid immiscibility in the join $NaAlSi_3O_8$-Na_2CO_3-H_2O and its bearing on the genesis of carbonatites: American Journal of Science, v. 266, p. 932-967.

-----, 1973, Liquid immiscibility in the join $NaAlSi_3O_8$-$CaAl_2Si_2O_8$-Na_2CO_3-H_2O: American Journal of Science, v. 273, p. 465-487.

Kukharenko, A. A., and Dontsova, E. I., 1964, A contribution to the problem of the genesis of carbonatites: Economic Geology of the U.S.S.R., v. 1, p. 47-68 (in English).

Larson, E. S., 1938, Some new variation diagrams for groups of igneous rocks: Journal of Geology, v. 46, p. 505-520.

Le Bas, M. J., 1977, Carbonatite-nephelinite volcanism: New York, John Wiley and Sons Inc., 347 p.

Lisenbee, A. L., 1978, Laramide structure of the Black Hills uplift, South Dakota-Wyoming-Montana, in Matthews, Vincent, III, ed., Laramide folding associated with basement block faulting: Geological of America Memoir 151, p. 165-196.

Lorson, R. C., FMC Corporation, Denver, Colorado, oral communication, 1984.

McCrea, J. M., 1950, On the isotopic chemistry of carbonates and a paleotemperature scale: Journal of Chemistry and Physics, v. 18,

p. 849-857.

McDowell, F. W., 1971, K-Ar ages of igneous rocks from the western United States: Isochron/West, no. 2, p. 1-20.

Menzies, Martin, and Murthy, V. R., 1980, Mantle metasomatism as a precursor to the genesis of alkaline magmas: isotopic evidence: American Journal of Science, v. 280-A, p. 622-638.

Metzger, F. W., Kelly, W. C., Nesbitt, B. E., and Essene, E. G., 1977, Scanning electron microscopy of daughter minerals in fluid inclusions: Economic Geology, v. 72, p. 141-152.

Miller, J. A., and Brown, P. E., The age of some carbonatite igneous activity in south-west Tanganyika: Geological Magazine, v. 100, p. 276-279.

Nesbitt, B. E., and Kelly, W. C., 1977, Magmatic and hydrothermal inclusions in carbonatite of the Magnet Cove complex, Arkansas: Contributions to Mineralogy and Petrology, v. 63, p. 271-294.

Newton, Henry, and Jenney, W. P., 1880, Report on the geology and natural resources of the Black Hills of Dakota: U. S. Geographical and Geological Survey (Rocky Mountain Region), 566 p.

Noble, J. A., 1952, Structural features of the Black Hills and adjacent areas developed since Precambrian time: Billings Geological Society, 3rd Annual Field Conference, Guidebook, p. 31-37.

Nockholds, S. R., 1954, Average chemical compositions of some igneous rocks: Geological Society of America Bulletin, v. 65, p. 1007-1032.

O'Toole, F. S., 1981, Petrology of the Cenozoic phonolites and related rocks of the Houston Creek area, Bear Lodge Mountains, Wyoming: unpublished M.S. thesis, University of North Dakota, 112 p.

Palache, Charles, Berman, Harry, and Frondel, Clifford, 1962, Dana's manual of mineralogy: New York, John Wiley and Sons, Inc., 1124 p.

Pecora, W. T., and Kerr, J. H., 1953, Burbankite and calkinsite, two new carbonate minerals from Montana: American Mineralogist, v. 38, p. 1169-1183.

Peterman, Z. E., and Hedge, C. E., 1972, Age of basement rocks from the Williston Basin of North Dakota and surrounding areas: Rocky Mountain Atlas, p. 54.

Rankin, A. H., 1975, Fluid inclusion studies in apatites from carbonatites of the Wasaki area, western Kenya: Lithos, v. 8, p. 123-136.

-----, 1977, Fluid inclusion evidence for the formation conditions of apatite from the Tororo carbonatite complex of eastern Uganda: Mineralogical Magazine, v. 41, p. 155-164.

Rankin, A. H., and Le Bas, M. J., 1974a, Liquid immiscibility between silicate and carbonatite melts in naturally occurring ijolite magma: Nature, v. 250, p. 206-209.

-----, 1974b, Nahcolite ($NaHCO_3$) in inclusions in apatite from some E. African ijolites and carbonatites: Mineralogical Magazine, v. 39, p. 564-570.

Rubie, D. C., and Gunter, W. D., 1983, The role of speciation in alkaline igneous fluids during fenite metasomatism: Contributions to Mineralogy and Petrology, v. 82, p. 165-175.

Shapiro, L. H., 1971a, Structural geology of the Black Hills region and implications for the origins of the uplifts of the Middle Rocky Mountain Province: unpublished Ph.D. dissertation, University of Minnesota, 213 p.

-----, 1971b, Structural geology of the Fanny Peak Linement, Black Hills, Wyoming-South Dakota: Wyoming Geological Association, 23rd Annual Field Conference, Guidebook, p. 61-64.

Sörensen, H., 1974, The alkaline rocks: New York, John Wiley and Sons Inc., 622 p.

Staatz, M. H., 1983, Geology and descriptions of thorium and rare-earth deposits in the southern Bear Lodge Mountains, northeastern Wyoming: U. S. Geological Survey Professional Paper 1049-D, 52 p.

Stevenson, Robert, University of North Dakota Natural Materials Analytical Laboratory, Grand Forks, North Dakota, oral communication.

Streckeisen, A. L., 1967, Classification and nomenclature of igneous rocks: E. Schweizerbartisch Verlagsbuchhandlung, 96 p.

Sun, S. S., and Hanson, G. N., 1975, Evolution of the upper mantle: geochemical evidence from alkali basalt: Geology, v. 3, p. 297-302.

Sutherland, D. S., 1965, Potash trachytes and ultrapotassic rocks associated with the carbonatite complex of Toror Hills, Uganda: Mineralogical Magazine, v. 35, p. 363-378.

Taylor, H. P., 1968, The oxygen isotope geochemistry of igneous rocks: Contributions to Mineralogy and Petrology, v. 19, p. 1-71.

-----, 1971, Oxygen isotope evidence for large-scale interaction between meteoric ground waters and Tertiary granodiorite intrusions, western Cascade range, Oregon: Journal of Geophysical Research, v. 76, p. 7855-7874.

Taylor, H. P., Frechen, Josef, and Degens, E. F., 1967, Oxygen and carbon isotope studies of carbonatites from the Laacher See district, West Germany and the Alnö district, Sweden: Geochimica et Cosmochimica Acta, v. 31, p. 407-430.

Urey, H. C., Lowenstam, H. A., Epstein, S., and McKinney, C. R., 1951, Measurement of paleotemperatures and temperatures of the Upper Cretaceous of England, Denmark, and the southeastern United States: Geological Society of America Bulletin, v. 62, p. 399-416.

Van der Plas, L., and Tobi, A. C., 1965, A chart for judging the reliability of point counting results: American Journal of Science, v. 263, p. 87-90.

von Eckermann, H., 1948, The alkaline district of Alnö Island: Sveriges Geol. Undersok. Ser. Ca., v. 36.

Warren, G. K., 1859, Preliminary report of exploration in Nebraska and Dakota in the years 1855-56-57, in Humphreys, A. A., Annual report of Office of explorations and surveys: U. S. War Department, p. 45-98.

Wendlandt, R. F., and Harrison, W. J., 1979, Rare-earth partitioning between immiscible carbonate and silicate liquids and CO_2 vapor: results and implications for the formation of light rare earth-enriched rocks: Contributions to Mineralogy and Petrology, v. 69, p. 409-413.

White, S. F., 1980, Petrology of the Cenozoic igneous rocks of the Lytle Creek area, Bear Lodge Mountains, Wyoming: unpublished M.S. thesis, University of North Dakota, 69 p.

Wilkinson, Michael, 1982, Petrology and alteration in the core of the Bear Lodge Tertiary intrusive complex, Bear Lodge Mountains, Crook County, Wyoming: unpublished M.S. thesis, University of North Dakota, 127 p.

Wooley, A. R., 1969, Some aspects of fenitization with particular reference to Chilwa Island and Kangankunde, Malawi: Bulletin British Museum (Natural History) Mineralogy, v. 2, no. 4, p. 189-219.

-----, 1973, The pseudoleucite borolanites and associated rocks of the southeastern tract of the Borralan complex, Scotland: Bulletin British Museum (Natural History) Mineralogy, v. 2, no. 6, p. 285-333.

-----, 1982, A discussion of carbonatite evolution and nomenclature, and the generation of sodic and potassic fenites: Mineralogical Magazine, v. 46, p.13-17.

Wyoming Geological Association Guidebook, 1968, Black Hills Area 20th Field Conference, p. 6.

Zartman, R. E., and Stern, T. W., 1967, Isotopic age and geologic relationships of the Little Elk Creek Granite, northern Black Hills, South Dakota, in Geological Survey research 1967: U. S. Geological

Survey Professional Paper 575-D, p. D157-D163.

GEOLOGIC MAP OF THE SOUTHEASTERN BEAR LODGE MOUNTAINS, CROOK COUNTY, WYOMING

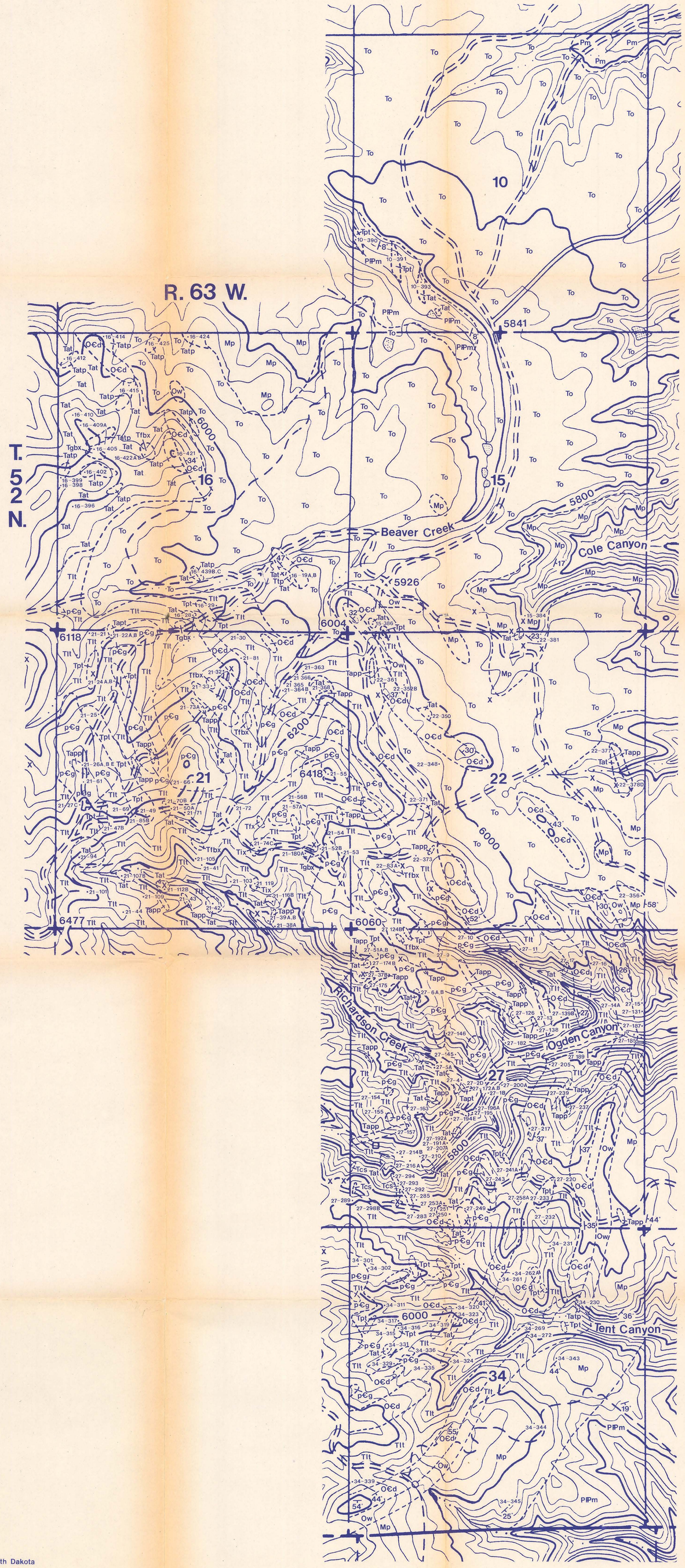

Explanation of mapped units:

To	Ogallala Formation [Pliocene–Miocene]	
Unconformity		
Tapp	Analcime phonolite porphyry	[Eocene]
Tcs	Carbonatite (S-type)	
Tibx	Iron-oxide breccia	
Tfbx	Feldspathic breccia	
Tgbx	Granitic breccia	
Tatp	Alkali trachyte porphyry	
Tat	Alkali trachyte	
Tpt	Phonolite and trachyte porphyries	
Tlt	Latite and trachyte porphyries	
Unconformity		
Pm	Minnekahta Limestone [Permian]	
Unconformity		
Po	Opeche Formation [Permian]	
Unconformity		
PPm	Minnelusa Sandstone [Permian–Pennsylvanian]	
Unconformity		
Mp	Pahasapa Limestone [Mississippian]	
Unconformity		
Ow	Whitewood Limestone [Ordovician]	
Unconformity		
O€d	Deadwood Formation [Ordovician–Cambrian]	
Unconformity		
p€g	Granite [Precambrian]	

Approximate contact

30 Strike and dip of beds

27-150 Sample locality and number

x Prospect pit or small trench

True North 12° Magnetic North

SCALE 1:10,000

1 0 1 km.

Base map from Sundance and Alva Quadrangles, U.S. Geological Survey 1:62,000 topographic maps [1955]

G.A. Jenner
University of North Dakota
Thesis
Plate 1
[1984]